

IDENTIFICATION OF PATZ1 TRANSCRIPTION FACTOR AS A NOVEL
INTERACTING PARTNER AND REGULATOR OF THE p53 TUMOR
SUPPRESSOR PROTEIN

by
NAZLI KESKİN

Submitted to the Graduate School of Engineering and Natural Sciences
in partial fulfillment of
the requirements for the degree of
Doctor of Philosophy

Sabancı University
July 2014

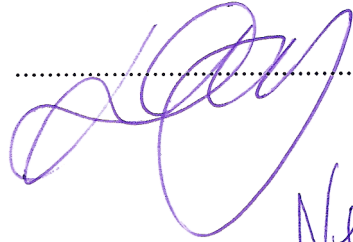
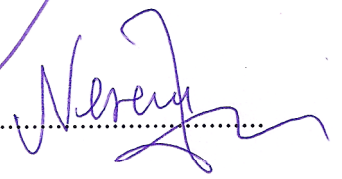
IDENTIFICATION OF PATZ1 TRANSCRIPTION FACTOR AS A NOVEL
INTERACTING PARTNER AND REGULATOR OF THE p53 TUMOR
SUPPRESSOR PROTEIN

APPROVED BY:

Assoc. Prof. Dr. Batu ERMAN
(Thesis Supervisor)

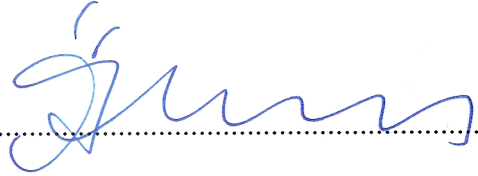

.....

Assoc. Prof. Dr. Devrim GÖZÜAÇIK


.....


Assoc. Prof. Dr. Nesrin ÖZÖREN

Asst. Prof. Dr. Özge AKBULUT


.....

Prof. Dr. Selim ÇETİNER


.....

DATE OF APPROVAL: 23.07.2014

© Nazlı Keskin 2014

ALL RIGHTS RESERVED

ABSTRACT

IDENTIFICATION OF PATZ1 TRANSCRIPTION FACTOR AS A NOVEL INTERACTING PARTNER AND REGULATOR OF THE p53 TUMOR SUPPRESSOR PROTEIN

Nazlı Keskin

Biological Sciences and Bioengineering, PhD. Thesis, 2014

Thesis supervisor: Batu Erman

Keywords: cancer, p53, PATZ1, transcription factor, DNA damage

The tumor suppressor p53 is a stress responsive, sequence specific transcription factor that regulates genes controlling the cell cycle, senescence and apoptosis. Mutation and loss of p53 is the most common genetic event in human cancer resulting in the accumulation of different types of tumors such as testicular carcinoma, soft tissue sarcoma and lymphoma. The focus of this study, the PATZ1 transcription factor, has diverse roles in cancer, development and stem cell biology. Besides being a key transcriptional repressor in lymphocyte development, PATZ1 expression is misregulated in different tumor types such as testicular, colorectal and breast cancers.

Because both proteins are significant modifiers of human cancer, we aimed to link the PATZ1 protein to p53 function using a biochemical approach. In this study, we discovered that both overexpressed and endogenous p53 and PATZ1 proteins interact. We identified a p53 binding region in the C-terminal domain of the PATZ1 protein. We further delineated the interaction region by generating site directed point mutant PATZ1 variants which do not bind p53. The p53 – PATZ1 interaction is functionally significant as neither p53 nor PATZ1 can bind DNA in the presence of the other factor. We examined the cellular responses controlled by p53 in cells overexpressing PATZ1. Treatment with the DNA damage inducing cytotoxic drug doxorubicin activates p53 related pathways. Overexpression of PATZ1 made cells more resistant to death by doxorubicin treatment. This study documents a novel player in the p53 pathway, a suppressor transcription factor, PATZ1.

ÖZET

PATZ1 TRANSKRİPSİYON FAKTÖRÜNÜN TÜMÖR BASKILAYICI p53 PROTEİNİNİN YENİ BİR BAĞLANMA PARTNERİ VE DÜZENLEYİCİSİ OLARAK BELİRLENMESİ

Nazlı Keskin

Biyoloji Bilimleri ve Biyomühendislik, Doktora Tezi, 2014

Tez Danışmanı: Batu Erman

Anahtar Kelimeler: kanser, p53, PATZ1, transkripsiyon faktörü, DNA hasarı

Hücre döngüsünü, hücre yaşlanmasını ve apoptozu kontrol eden genleri düzenleyen tümör baskılayıcı p53, strese tepki veren, sekansa özel bir transkripsiyon faktörüdür. p53'ün mutasyona uğraması ve kaybı insan kanserlerinde en sık görülen genetik olay olup testiküler karsinoma, yumuşak doku sarkoması ve lenfoma gibi farklı tümörlerin oluşumuna neden olur. Bu çalışmanın odağı olan transkripsiyon faktörü PATZ1'in kanser, gelişim ve kök hücre biyolojisinde çok önemli görevleri vardır. Lenfosit gelişiminde önemli bir transkripsiyonel baskılayıcı olmanın yanı sıra, PATZ1 testiküler, kolorektal ve göğüs kanseri gibi farklı tumor çeşitlerinde farklı miktarlarda ifade edilmektedir.

Her iki protein de insan kanserini önemli ölçüde etkilileyici rollere sahip olduğu için biyokimyasal bir yaklaşım kullanarak PATZ1 proteini ile p53'ün fonksiyonları arasında bir ilişki kurmayı amaçladık. Bu çalışmada normalden fazla ve normal miktarda ifade edilen p53 ve PATZ1 proteinlerinin etkileşim içerisinde olduğunu keşfettik. PATZ1 proteininin C terminal bölgesinde p53 için bir bağlanma bölgesi tespit ettik. Bu etkileşim bölgesine has p53'e bağlanmayan nokta mutasyon varyantları yaparak bu bölgeyi daha detaylı olarak tanımladık. p53 – PATZ1 etkileşimi işlevsel olarak da önemlidir çünkü ne p53 ne de PATZ1 diğer faktörün olduğu yerde DNA'ya bağlanabilmektedir. Normal miktardan fazla PATZ1 ifade eden hücrelerde p53 tarafından kontrol edilen hücresel tepkileri inceledik. Hücreleri DNA hasarı oluşturan sitotoksik bir ilaç olan doksorubisin ile muamele etmek p53 ile ilgili olan yolları aktive eder. Normalden fazla PATZ1 ifade edilmesi, hücreleri doksorubisin muamelesi sonucu oluşan ölüme karşı daha dayanıklı yapmıştır. Bu çalışma, baskılayıcı transkripsiyon faktörü PATZ1'i p53 yolağında rol alan yepyeni bir protein olarak sunmaktadır.

To my mother Zülal KESKİN...

ACKNOWLEDGEMENT

First and foremost I would like to thank my supervisor Assoc. Prof. Dr. Batu Erman for his guidance, advice, support and patience during my project. His comments and ideas for every single experiment throughout the whole project gave me the enthusiasm for science. I would like to convey my heartfelt thanks to my comitee members, Assoc. Prof. Dr. Devrim Gözüaık, Assoc. Prof. Dr. Nesrin Özören, Asst. Prof. Dr. Özge Akbulut and Prof. Dr. Selim etiner for their support and ideas for thesis dissertation.

Thanks to my supervisor, my lab collagues, Emre Deniz, Bahar Shamloo, Canan Sayitoęlu, Gülperi Yalın, Yasemin Yozgat and Ahsen Özcan and previous lab members Dr. Ceren Tuncer, Manolya Ün and Jitka Eryılmaz, I have felt the honor of being a member of Erman lab for six years. My dearest friends Emre Deniz, Seil Erbil, Mehmet Üskül, Nur Kocatürk, Gülfem Öztürk, Kumsal Tekirdaę, Yunus Akko, Ezgi Karakaş, Anı Akpınar, Dilek Tekdal, Beyza Vuruşaner and Serra Örey deserve really big thanks for their presence in my all not only good but also hard times.

I owe special thanks to my parents, Zülal and Ali Rıza Keskin, my brothers Zafer and Tanfer Keskin for their continuous and unconditional love. In addition, I am so lucky to have such an understanding and supportive mother. Without her support, help, advice and love, it was impossible for me to overcome everything. Her existence as a co-pilot in my life is the biggest gift for me.

Finally, I would like to thank to The Scientific and Technological Research Council of Turkey, Science TÜBİTAK BİDEB-2211 for the support during my doctoral education.

TABLE OF CONTENTS

1. INTRODUCTION.....	1
1.1 Scientific Background of p53.....	1
1.1.1 p53 in Homeostasis.....	1
1.1.2 p53 Upon Stress Inducing Conditions.....	3
1.1.2.1 Post-translational Modifications of p53 Upon Stress.....	4
1.1.2.2 p53-DNA Interactions.....	5
1.1.2.3 Transcriptional Regulation By p53.....	6
1.1.3 Structure of p53.....	8
1.1.4 Interaction Partners of p53.....	10
1.1.5 Mutations of p53.....	12
1.2 Scientific Background of PATZ1.....	15
1.2.1 Identification of PATZ1.....	15
1.2.2 Structure and Alternative Splice Variants of PATZ1.....	15
1.2.3 Functions of PATZ1.....	17
2. AIM OF THE STUDY.....	19
3. MATERIALS AND METHODS.....	20
3.1 Materials.....	20
3.1.1 Chemicals.....	20
3.1.2 Equipment.....	20
3.1.3 Buffers and Solutions.....	20
3.1.3.1 Bacterial Transformation Buffers and Solutions.....	20
3.1.3.2 Mammalian Cell Culture Buffers and Solutions.....	21
3.1.3.3 Gel Electrophoresis Buffers and Solutions.....	22
3.1.4 Growth Media.....	23
3.1.4.1 Bacterial Growth Media.....	23
3.1.4.2 Tissue Culture Growth Media.....	24
3.1.5 Commercial Molecular Biology Kits.....	24
3.1.6 Enzymes.....	24

3.1.7 Cell Types.....	25
3.1.7.1 Bacterial Cells.....	25
3.1.7.2 Tissue Culture Cell Lines.....	25
3.1.8 Vectors and Primers.....	25
3.1.9 DNA and Protein Molecular Weight Markers.....	27
3.1.10 DNA Sequencing.....	28
3.1.11 Software and Computer Based Programs.....	28
3.2 Methods.....	29
3.2.1 General Molecular Cloning Methods.....	29
3.2.1.1 Bacterial Cell Culture.....	29
3.2.1.2 Vector Construction.....	30
3.2.2 Mammalian Cell Culture.....	32
3.2.2.1 Preparation and Maintenance of Mammalian Cells.....	32
3.2.2.2 Transient Transfection of Adherent Cells with PEI (Polyethylenimine).....	33
3.2.2.3 Cell Lysis, Immunoprecipitation and DNA Pull Down.....	34
3.2.2.4 SDS Gel, Transfer and Western Blot.....	35
3.2.4 Subcellular Localization.....	35
3.2.5 Flow Cytometric Analysis.....	36
3.2.6 Real Time Cell Growth and IC ₅₀ Analysis.....	36
4. RESULTS.....	37
4.1 Subcellular Localization Of p53 and PATZ1 Proteins.....	37
4.2 The Effect Of PATZ1 In The Subcellular Translocation Of p53.....	39
4.3 Interaction of Overexpressed p53 and PATZ1 Proteins.....	41
4.4 Domain Requirements for the p53 – PATZ1 Interaction.....	43
4.5 Amino Acids of PATZ1 Necessary for the p53 – PATZ1 Interaction	45
4.6 DNA Independence of the p53 – PATZ1 Interaction.....	47
4.7 Interaction of Endogenous p53 and PATZ1 Proteins.....	48
4.8 Heterodimerization of PATZ1 and PATZ1Alt Alternative Splice Variants.....	49
4.9 Domain Requirements for the PATZ1 – PATZ1Alt Heterodimerization.	51
4.10 The Interaction of the Δ 40p53 Isoform with PATZ1.....	52
4.11 Construction of a mPATZ1-002-IRES-Cherry Plasmid.....	54
4.12 The Effect of the p53 – PATZ1 Interaction on p53 – DNA Binding in EMSA assays.....	58

4.13 The Effect of the p53 – PATZ1 Interaction on p53 – DNA Binding in Pull Down Assays.....	59
4.13.1 The p53 – PATZ1 Interaction Inhibits p53 – DNA Binding.....	59
4.13.2 PATZ1 Mutants Cannot Inhibit p53 – DNA Binding.....	61
4.14 The Inhibitory Effect of the p53 – PATZ1 Interaction on p53 – DNA Binding on Other p53 Targets.....	63
4.15 The p53 – PATZ1 Interaction Inhibits PATZ1 – DNA Binding.....	65
4.16 The Effect of the p53 – PATZ1 Interaction on Apoptosis.....	67
4.17 The Effect of the p53 – PATZ1 Interaction on Cellular Growth Rate.....	68
5. DISCUSSION AND CONCLUSION.....	70
REFERENCES.....	86
APPENDIX A: Chemicals Used In The Study.....	97
APPENDIX B: Equipment Used In The Study.....	100
APPENDIX C: DNA and Protein Molecular Weight Marker.....	102
APPENDIX D: Plasmids Used In This Project.....	103

LIST OF FIGURES

Figure 1.1 Monoubiquitination and polyubiquitination of p53 by MDM2.....	2
Figure 1.2 Post-translational modifications of p53 upon DNA damage.....	4
Figure 1.3 The binding of p53 to DNA consensus sites.....	6
Figure 1.4 Transcription regulation by p53.....	7
Figure 1.5 Structure of p53.....	8
Figure 1.6 Isoforms of p53.....	9
Figure 1.7 Six hot spots of cancer related mutant p53.....	12
Figure 1.8 Mutant p53 blocks functional p53, p63 and p73 homotetramers by formation of heterotetramer.....	14
Figure 1.9 The structure of PATZ1 protein.....	15
Figure 1.10 Alternative splice variants of PATZ1.....	16
Figure 4.1 Expression patterns of PATZ1 and p53 before and after DNA damage induced by doxorubicin	38
Figure 4.2 Confocal microscopy images p53-GFP transfected HCT116 p53 ^{-/-} cells before and after DNA damage induced by doxorubicin treatment in the presence or absence of HA-PATZ1.....	40
Figure 4.3 FLAG-p53 binds to HA-PATZ1 but not HA-PATZ1Alt.....	42
Figure 4.4 C-terminal tail of PATZ1 is required for binding p53.....	44
Figure 4.5 Aspartic acids in residue 521 and 527 of PATZ1 protein are necessary for p53 – PATZ1 interaction.....	46
Figure 4.6 Interaction of FLAG-p53 and HA-PATZ1 is independent of DNA...	47
Figure 4.7 Endogenous p53 binds to endogenous PATZ1 in HCT116 cells.....	49
Figure 4.8 PATZ1Alt can interact with p53 only in the presence of PATZ1.....	50
Figure 4.9 The BTB domain of PATZ1 and PATZ1Alt proteins was necessary for heterodimerization of the alternative splice variants.....	52
Figure 4.10 $\Delta 40$ p53 isoform of p53 binds to PATZ1 upon doxorubicin treatment in HCT116 cells.....	53
Figure 4.11 PCR amplification and assembly of three fragments for construction of mPATZ1-002 cDNA.....	55

Figure 4.12 Ligation of mPATZ1-002 into the pMIGII-IRES-Cherry plasmid.....	56
Figure 4.13 Conformation digestion of the mPATZ1-002-IRES-Cherry ligation.....	57
Figure 4.14 EMSA assay for p53-DNA binding.....	58
Figure 4.15 p53 – PATZ1 interaction inhibits p53 - DNA interaction.....	60
Figure 4.16 PATZ1 mutants that are incapable of interacting with p53 cannot prevent p53 – DNA interaction.....	62
Figure 4.17 The inhibitory effect of PATZ1 in p53 – DNA interaction is valid for a different p53 binding consensus sequence.....	64
Figure 4.18 p53 – PATZ1 interaction inhibits PATZ1 - DNA interaction.....	66
Figure 4.19 Flow cytometry analysis of stably PATZ1 or PATZ1Alt expressing HCT116 cells before and after DNA damage upon UV treatment...	68
Figure 4.20 Dose response curve and IC50 analysis of stably PATZ1 or mock expressing HCT116 cells after DNA damage induced by Doxorubicin.....	69
Figure 5.1 Homology model of PATZ1.....	71
Figure 5.2 Identification of the putative binding pocket between the 6th and 7th zinc finger motifs of PATZ1 in the homology model.....	72
Figure 5.3 In silico docking study to find an interacting partner for PATZ1.....	73
Figure 5.4 The conserved protein sequence that PATZ1 is predicted to bind....	74
Figure 5.5 p53-PATZ1-PATZ1Alt complex.....	76
Figure 5.6 Conservation of the residue that is important for helper lineage commitment.....	79
Figure 5.7 G2/M dependent phosphorylation motif in the linker domains of PATZ1.....	81
Figure 5.8 TALEN design for PATZ1 knock out cell lines.....	83
Figure 5.9 Model for functional interaction of p53 and PATZ1.....	84
Figure D.1 Map of pCMV-HA plasmid.....	103
Figure D.2 Map of pCMV-HA-PATZ1 plasmid.....	103
Figure D.3 Map of pCMV-HA-PATZ1Alt plasmid.....	104
Figure D.4 Map of pCMV-HA-PATZ1D521Y plasmid.....	104
Figure D.5 Map of pCMV-HA-PATZ1D521Y/D527 plasmid.....	105
Figure D.6 Map of pCMV-Myc plasmid.....	105
Figure D.7 Map of pCMV-Myc-PATZ1 plasmid.....	106

Figure D.8 Map of pCMV-Myc-deltaBTB plasmid.....	106
Figure D.9 Map of pCMV-Myc-BTB plasmid.....	107
Figure D.10 Map of pCMV-Myc-deltaZF plasmid.....	107
Figure D.11 Map of pCMV-FLAG plasmid.....	108
Figure D.12 Map of pCMV-FLAG-p53 plasmid.....	108
Figure D.13 Map of p53-GFP plasmid.....	109

LIST OF TABLES

Table 3.1 Vectors used in this project.....	26
Table 3.2 Primers used in this project.....	27
Table 3.3 Software and computer based programs used in this project.....	28
Table 3.4 Optimized PCR conditions.....	30
Table 3.5 Optimized PCR thermal cycle conditions.....	31
Table 3.6 Components and amounts for restriction enzyme digestion.....	31

LIST OF ABBREVIATIONS

α	Alpha
β	Beta
Δ	Delta
γ	Gamma
σ	Sigma
Amp	Ampicillin
bp	Base pair
BR	Basic Region
BTB	Broad Complex, Tramtrack, and Bric a' brac
CD	Cluster of Differentiation
ChIP	Chromatin Immunoprecipitation
Chl	Chloramphenicol
CIAP	Calf Intestine Alkaline Phosphatase
CMV	Cytomegalovirus
Da	Dalton
DBD	DNA Binding Domain
DM	Double Mutant
DMEM	Dulbecco's Modified Eagle Medium
DMSO	Dimethylsulfoxide
DNA	Deoxyribonucleic Acid
EDTA	Ethylene diamine tetra acetic acid
FACS	Flourescence Activated Cell Sorting
FBS	Fetal Bovine Serum
GFP	Green Flourescent Protein
HCT	Human Colon Carcinoma
IP	Immunoprecipitation
Kan	Kanamycin

LB	Luria Broth
min	Minute
mt	Mutant
Neo	Neomycin
NES	Nuclear Export Sequence
NLS	Nuclear Localization Sequence
OD	Optical Density
ROS	Reactive Oxygen Species
PBS	Phosphate Buffered Saline
PCR	Polymerase Chain Reaction
POZ	Poxviruses and Zinc-Finger
PR	Proline Rich Domain
rpm	Revolution per minute
RNA	Ribonucleic Acid
SDS-PAGE	Sodium Dodecyl Sulfate Polyacrilamide Gel Electrophoresis
SM	Single Mutant
SV40	Simian Virus 40
TBE	Tris Borate EDTA
TET	Tetramerization Domain
wt	Wild Type
ZF	Zinc Finger

1. INTRODUCTION

1.1Scientific Background of p53

1.1.1 p53 in Homeostasis

p53 is a stress responsive, sequence specific transcription factor which has roles in cell cycle arrest, senescence, apoptosis, autophagy and DNA repair. In addition to these, p53 has functional roles in the regulation of metabolic pathways, inhibition of reactive oxygen species (ROS) and angiogenesis ¹⁻³. Under normal circumstances, intracellular p53 protein levels are very low. This is thought to be necessary for cell proliferation and viability ⁴. The mechanism that keeps p53 levels low is mediated by p53 binding proteins that cause p53 ubiquitination and degradation. Mouse double minute 2 (MDM2) which is the first p53 E3 ubiquitin ligase described, binds to p53 and promotes its ubiquitination and degradation ⁵⁻⁸. MDM2 can either monoubiquitinate or polyubiquitinate p53 depending on cellular MDM2-p53 ratios. If MDM2 levels are low in the cell, p53 is monoubiquitinated. MDM2 is then dissociated from p53 and monoubiquitinated p53 is translocated from the nucleus to the cytoplasm due to the open nuclear export sequence of p53. Cytoplasmic MDM2 binds to monoubiquitinated p53 and polyubiquitinates it. After polyubiquitination, p53 undergoes proteasomal degradation in the cytoplasm (figure 1.1A). However, if MDM2 levels are high in the cell, p53 is directly polyubiquitinated in the nucleus. Polyubiquitins block the nuclear export sequence and therefore polyubiquitinated p53 is stuck in the nucleus. Polyubiquitinated p53 then undergoes proteasomal degradation the nucleus (figure 1.1B) ⁹. Therefore, MDM2 is a major protein that controls the protein level of p53 in normal unstressed cells ¹⁰.

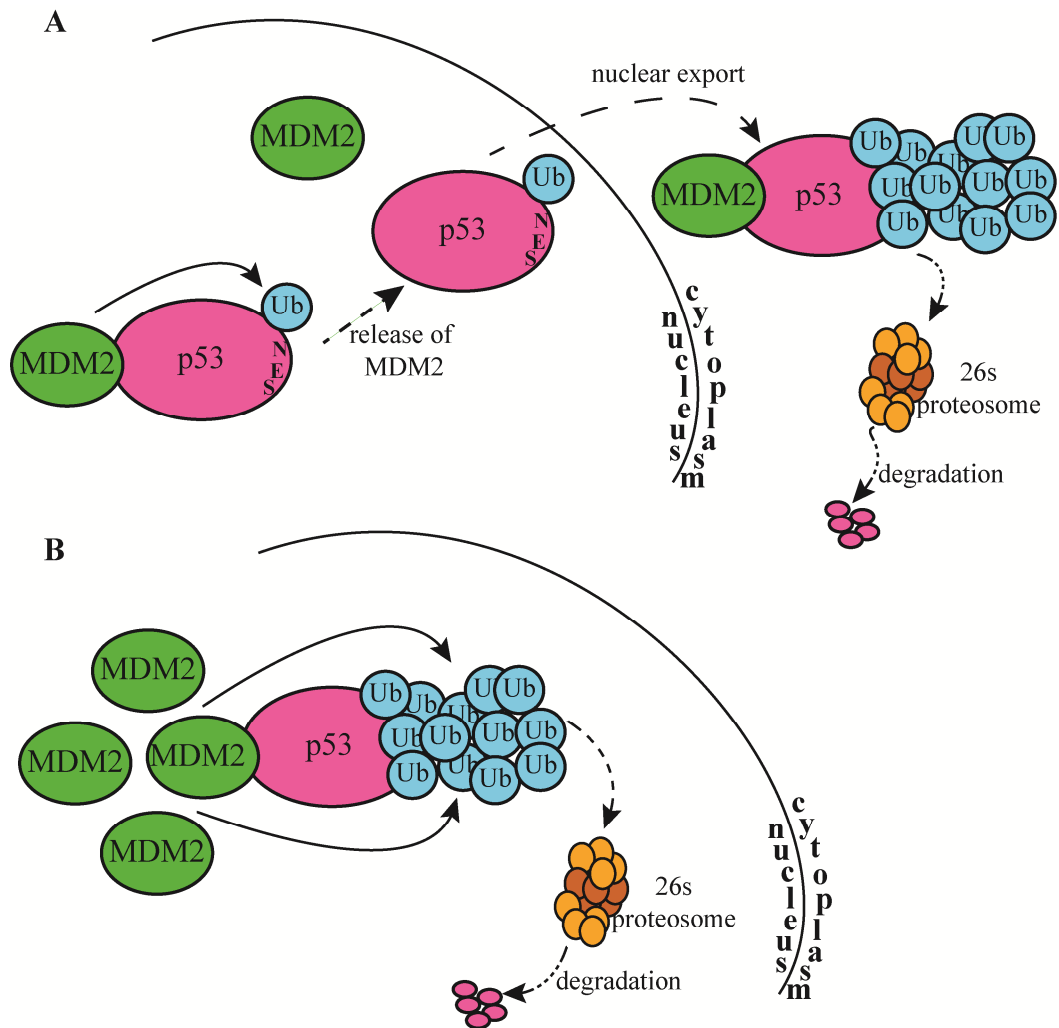


Figure 1.1 Monoubiquitination and polyubiquitination of p53 by MDM2. A) p53 is monoubiquitinated in the nucleus and polyubiquitinated and degraded in the cytoplasm if the MDM2 levels are low in the cell. B) p53 polyubiquitinated and degraded in the nucleus if the MDM2 levels are high in the cell. MDM2 protein is represented as green ellipse, p53 protein is represented as pink ellipse, ubiquitin is represented as blue circle and 26s proteasome is represented as orange and brown circles.

Besides controlling p53 protein levels, MDM2 can also control the transcriptional activity of the p53 protein. MDM2 binds the p53 transactivation domain and inhibits the interaction of p53 with essential transcriptional co-activators such as human positive cofactor (PC4) which is necessary for protein-protein interactions, DNA bending and posttranslational modifications of p53¹¹. MDM2 can also promote the posttranslational modification of p53 by the small protein NEDD8. Neddylation of p53 results in the blockage of its transcriptional activity¹². Therefore, MDM2 not only determines the levels of p53 protein but also inhibits the transcriptional activity of p53 through several mechanisms. MDM4 (also known as MDMX), a close homolog of MDM2 was also identified as an interacting partner of p53¹³. Like MDM2, MDM4 is a ubiquitin

ligase¹⁴. However, unlike MDM2, MDM4 does not ubiquitinate and degrade p53^{15,16}. Although MDM4 does not have a direct role on p53 stabilization, it has been reported that MDM4 can heterodimerize with MDM2 through its C terminal RING domain and stabilize MDM2 by inhibiting its autoubiquitination^{17,18}. Therefore, MDM4 indirectly influences the low levels of p53 in normal cells by inducing MDM2 activity and resulting in p53 degradation. Because the MDM2 – p53 interaction is very important for p53 stabilization, it is a favorite target of therapeutic strategies for cancer. Nonpeptidic small molecules are designed and tested in order to block the MDM2-p53 interaction resulting in the accumulation and activation of p53. There are different classes of these small molecule inhibitors such as spirooxindole, benzodiazepine, terphenyl, quilinol, chalone, sulfonamide and cis-imidazoline compounds. Nutlin 3a which belongs to the cis-imidazoline group of inhibitors is one of the most highly published small molecule inhibitor of the MDM2-p53 interaction. Unlike other drugs, nutlin 3a is nongenotoxic and it induces cell cycle arrest instead of apoptosis¹⁹. In addition to these, doxorubicin which is also known as adriamycin, is also a chemical drug that inhibits MDM2 mediated p53 degradation. Doxorubicin is a genotoxic, DNA damaging agent which causes double strand breaks in the DNA. Upon DNA damage induced by doxorubicin, serine 163 of p53 is phosphorylated by the S6K1 kinase. DNA damage induces the phosphorylation of S6K1 which makes it a direct target of MDM2. Therefore, upon DNA damage both S6K1 and MDM2 are phosphorylated and form a complex which results in the inhibition of the translocation of MDM2 from the cytoplasm to the nucleus. These cellular events prevent MDM2 mediated p53 ubiquitination and proteasomal degradation²⁰. On the other hand, MDM2 is not the only protein that leads to the proteasomal degradation of p53 because p53 is still degraded in Mdm2 null mice²¹. COP1 (constitutively photomorphogenic 1), Pirh2 (p53-Induced RING-H2) and Arf-BP1 (Arf binding protein 1) are recently identified E3 ubiquitin ligases that have p53 ubiquitination and degradation activity, independent from MDM2^{22–24}.

1.1.2 p53 Upon Stress Inducing Conditions

p53 activation starts with the stabilization of p53 induced by ATM/ATR mediated phosphorylation in its N-terminus. As this phosphorylation site overlaps with the MDM2 binding site, phosphorylated p53 dissociates from MDM2, escapes from

ubiquitination and is accumulated in the cell. Accumulation of p53 is the first step in this pathway, followed by sequence specific DNA binding and target gene activation or repression through interactions with the general transcriptional machinery²⁵.

1.1.2.1 Post-translational Modifications of p53 Upon Stress

Under normal or stress conditions, p53 undergoes post-transcriptional modifications such as phosphorylation, ubiquitination, acetylation, methylation, sumoylation, neddylation, glycosylation and ribosylation. As described earlier, the p53 – MDM2 interaction is inhibited due to the N terminal phosphorylation of p53 at Ser15 (mouse Ser18) and Ser 20 (mouse Ser 23) in cells that undergo stress²⁶. This phosphorylation of p53 by the ATM/ATR/DNAPK or Chk1/Chk2 is the initial step of p53 stabilization (figure1.2)²⁷.

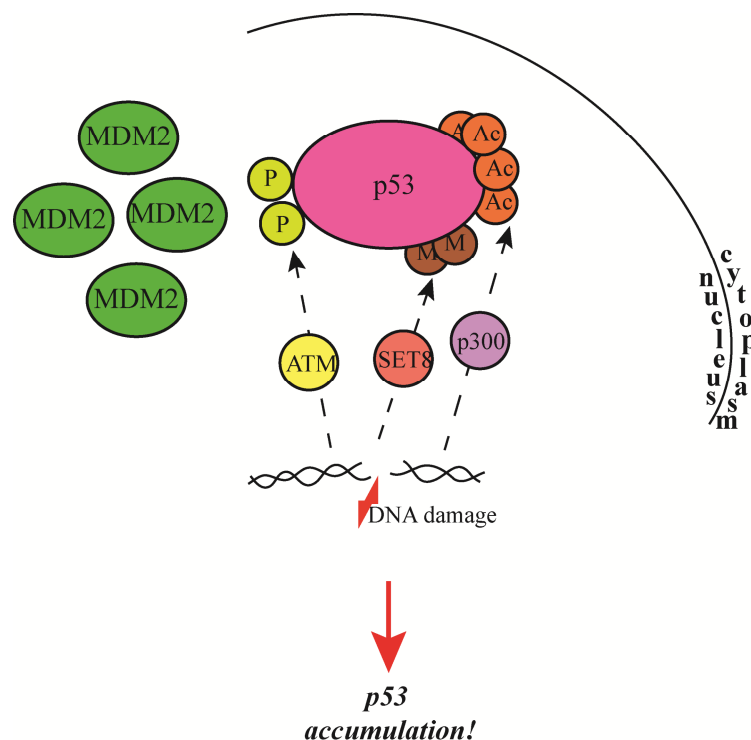


Figure 1.2 Post-translational modifications of p53 upon DNA damage. After DNA damage p53 (represented as pink ellipse) is phosphorylated (represented as green circle) by ATM (represented as yellow circle), acetylated (represented as orange circle) by p300 (represented as purple circle) and methylated (represented as brown circle) by SET8 (represented as red circle). These post-translational modifications result in p53 accumulation

The second important post-translational modification of p53 upon cellular stress is the acetylation of its C terminus by CBP (CREB binding protein)/p300. After CBP/p300 mediated acetylation of six C terminal lysine residues (K370, K371, K372, K381, K382 and K386) which are also the main ubiquitination sites, ubiquitination of p53 is disfavored and its protein levels start to accumulate^{28–30}. Methylation also has a significant role in the transcriptional activation of p53. Especially important is the methylation of p53 lysine 372 by the SET9 methyl-transferase. This modification results in the activation of p53 activity as can be seen by an increase in p21 levels, a major p53 target gene³¹. On the other hand, methylation of lysine 382 by the SET8 and of lysine 370 by the Smyd2 methyl-transferase enzymes result in the suppression of p53 activity^{32,33}.

1.1.2.2 p53-DNA Interactions

p53 is a transcription factor that has a central DNA binding domain. The DNA binding domain of p53 is composed of a beta sandwich with a series of loops and short helices. p53 forms a complex that is composed of four p53 core domains bound to two cognate half sites on DNA, as a dimer of dimers^{34,35}. The consensus p53 binding sequence, is two repeats composed of RRRCWWGYYY, separated by 0-21 bases (where R is a purine, Y a pyrimidine and W either an A or T)³⁶. Each half site binds a p53 dimer and two p53 dimers form tetramers to bind DNA. It is not known if there is a functional significance of the distance between the half sites. In addition to the consensus, there are some exceptional p53 binding sequences such as the (TGYCC)_n site in pig3 micorsatellite response elements, where n indicates the repeat number. p53 can also bind the triplet pairs of pentameric element, RRRCWWGYYY in the aqp3 (aquaporin3, a glycerol and water transporter) locus^{37–40}. Unlike some transcription factors, when p53 binds to DNA, a significant bend in the DNA structure is induced¹¹. The affinity of p53 for its binding site can be influenced by its interaction partners. For example, when c-abl or p53β binds p53 through its tetramerization domain, p53 binds easier to the target response element (figure 1.3)⁴¹.

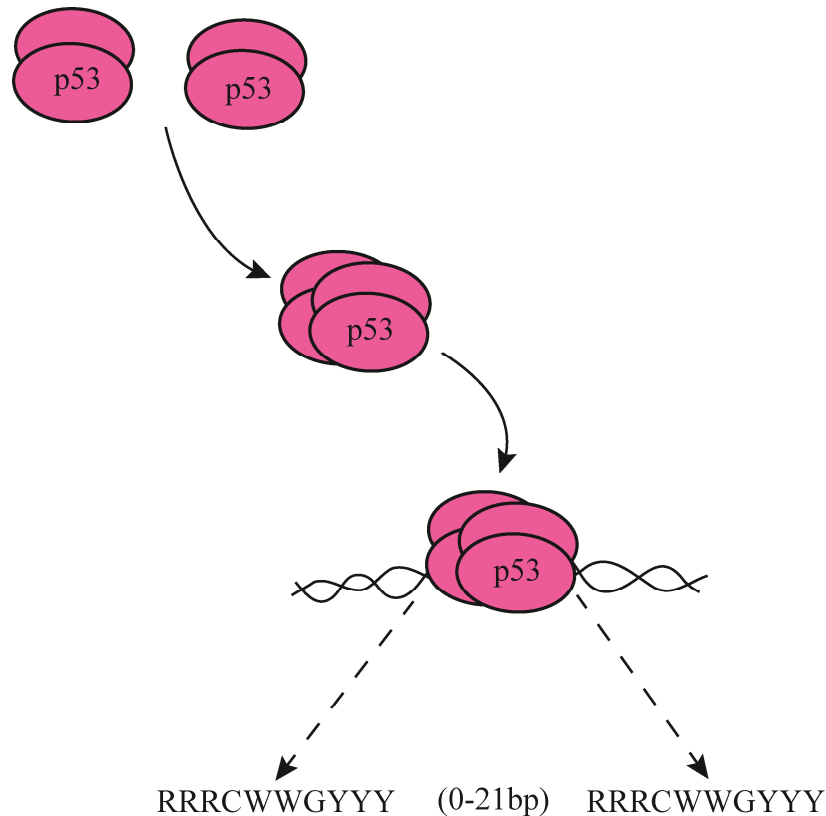


Figure 1.3 The binding of p53 to DNA consensus sites. p53 (represented as pink ellipse) binds to the DNA consensus RRRCWWGYYY where R is a purine, Y a pyrimidine and W either an A or T as a tetramer.

p53 binding site can be located anywhere in the target gene locus. Most p53 binding sites are in the promoters of the target genes. Classical examples of such p53 responsive genes are p21 and Noxa. In genes like Mdm2 and Pcna, the p53 binding site is very close to the transcription start site. In other cases such as the puma and pig3 genes, the p53 binding can be in intronic sequences. Moreover, in genes such as miR-34a exonic regions can even contain functional p53 binding sites⁴².

1.1.2.3. Transcriptional Regulation By p53

DNA damage, telomere erosion, oxidative stress, incomplete mitotic stimulus, ribonucleotide depletion and oncogene activation are some of the factors that transcriptionally activates p53⁴³. p53 has been shown to control various cellular pathways. Activated p53 results in the transcription of p21, the cyclin dependent kinase inhibitor which inhibits cell cycle progression. Other well known p53 targets with p53

response elements are 14-3-3 σ and GADD45. The expression of these proteins also causes cell cycle arrest, like p21. Even very minor increases in p53 protein levels can cause p21 expression and result in G1 arrest in the cell cycle⁴⁴. PAI1 (plasminogen activator inhibitor 1) is also a stress responsive gene, transcriptionally regulated by p53 which promotes senescence^{45,46}. p53 also upregulates NOXA and PUMA gene expression that play a role in the induction of apoptosis. p53 can also increase DRAM levels which control the induction of autophagy. Furthermore, p53 induces TIGAR and SESTRINS which inhibit the production of reactive oxygen species (ROS), promoting cell survival. p53 has also transcription independent cytoplasmic roles linked to mTOR and autophagy². The tumor suppressive function of p53 likely results from a combination of all of these pathways (figure 1.4). In different types of tumors, p53 is the most frequently mutated gene. This finding defines this transcription factor as a tumor suppressor protein^{47–49}. p53 reactivation in cells expressing mutant p53 or in cells lacking p53 expression results in the regression of many different tumor types^{50–52}.

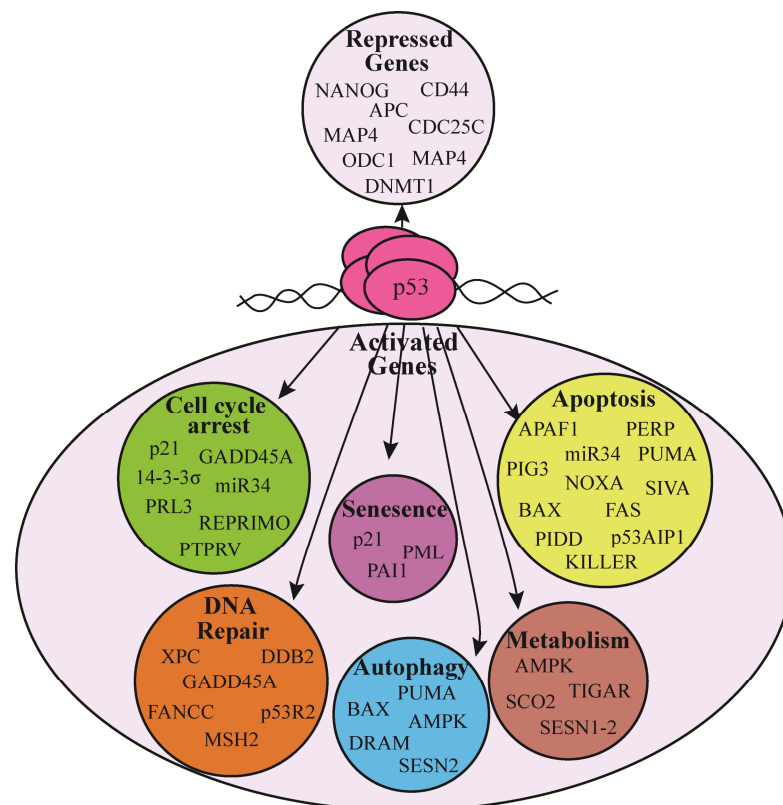


Figure 1.4 Transcription regulation by p53. p53 is a transcriptional activator of cell cycle arrest, senescence, apoptosis, DNA repair, metabolism and autophagy genes. In addition to being a transcriptional activator, p53 is also a transcriptional repressor for a different subset of genes.

1.1.3 Structure of p53

Full length p53 is composed of a loosely structured N-terminal transactivation domain (TAD) that has two sub-domains (TAD-I (residues 1-40) and TAD-II (residues 40-60)), a proline rich region (PR) (residues 63-97), a highly conserved DNA binding domain (DBD) (residues 100-292), a nuclear localization sequence (NLS) (residues 305-322), a tetramerization domain (TET) (residues 326-356), a nuclear export signal within the TET (residues 340-351) and a C terminal basic region (BR) (residues 364-393) (figure 1.5) ^{37,53}.



Figure 1.5 Structure of p53. p53 protein is composed of two transcription activation domains (TAD) such TADI (shown in yellow) and TADII (shown in purple), a proline rich region (PR), shown in green, a DNA binding domain (DBD, shown in pink), a nuclear localization sequence (NLS, shown in blue), a tetramerization domain (TET, shown in orange) and a basic region (BR, shown in turquoise).

In addition to full length p53, some cells express an alternative form ($\Delta 40$ p53) which lacks the N terminal 40 amino acids corresponding to TADI. This isoform results from an alternative translation initiation event. As the alternative form lacks the strong transactivation domain, while retaining the DBD, it may be playing a dominant negative role, binding to DNA without the capability of activating the downstream genes. Another alternative form of p53 results from the activity of an internal promoter found in the 4th intron of the TP53 gene which expresses a truncated version of p53 ($\Delta 133$ p53) which lack the N terminal 133 amino acids. Furthermore, all three forms of p53 (full length p53, $\Delta 40$ p53 and $\Delta 133$ p53) can undergo alternative splicing in the exons encoding their C terminus. There are three known alternative splice events encoding α , β , γ forms. Thus, in total the p53 gene is capable of encoding nine isoforms of the p53 protein: p53 α , p53 β , p53 γ , $\Delta 40$ p53 α , $\Delta 40$ p53 β , $\Delta 40$ p53 γ , $\Delta 133$ p53 α , $\Delta 133$ p53 β and $\Delta 133$ p53 γ (figure 1.6) ⁵³.

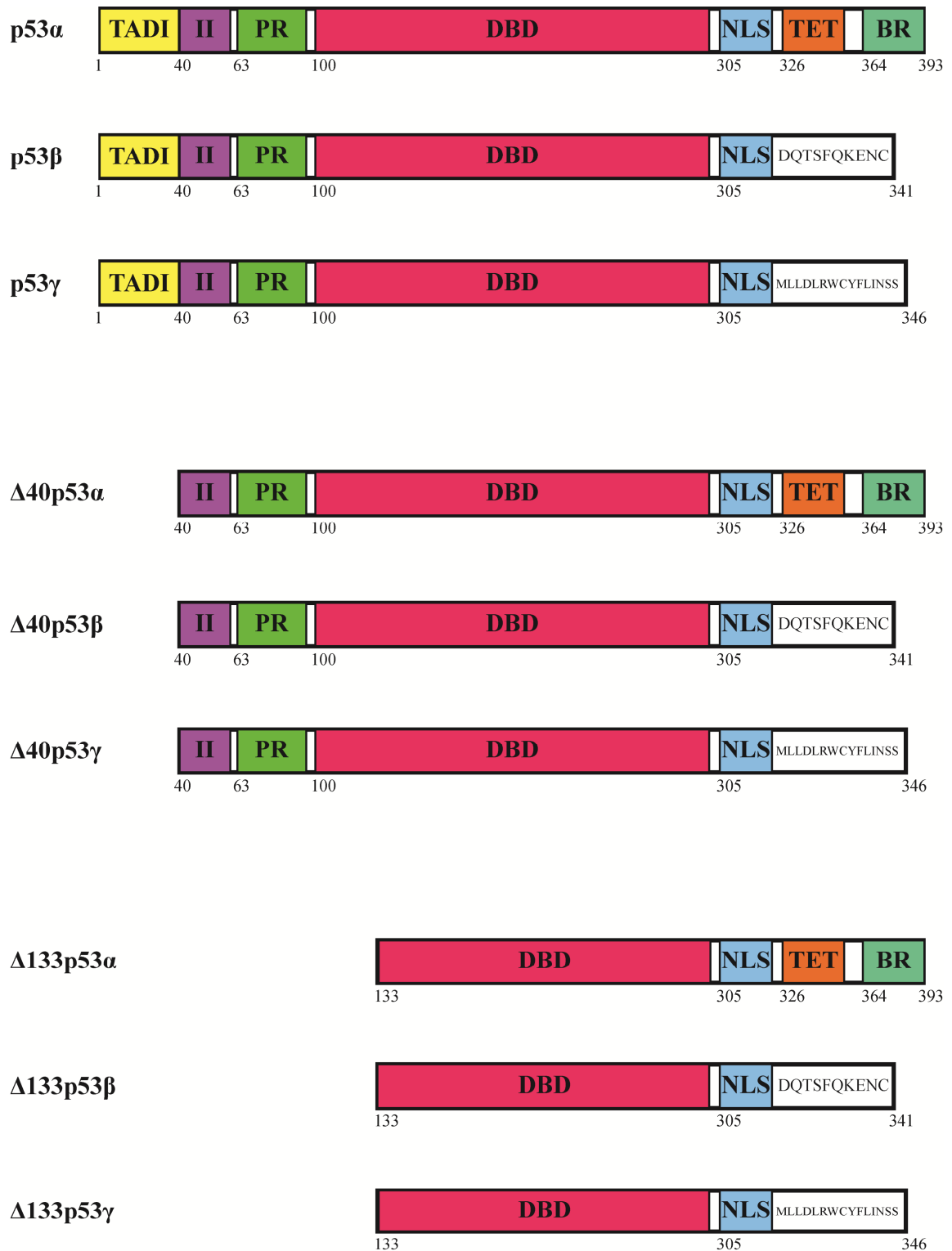


Figure 1.6 Isoforms of p53. There are nine isoforms of the p53 protein: p53 α , p53 β , p53 γ , $\Delta 40$ p53 α , $\Delta 40$ p53 β , $\Delta 40$ p53 γ , $\Delta 133$ p53 α , $\Delta 133$ p53 β and $\Delta 133$ p53 γ . Transactivation domain I (TADI) is shown in yellow, transactivation domain II (TADII) is shown in purple, proline rich domain (PR) is shown in green, DNA binding domain (DBD) is shown in pink, nuclear localization sequence (NLS) is shown in blue, tetramerization domain (TET) is shown in orange and basic region (BR) is shown in turquoise.

Sub-cellular localization studies show that the different p53 isoforms are found in different cellular locations. For instance, although $\Delta 133p53$ and $p53\beta$ are mainly localized in the nucleus, $\Delta 133p53\gamma$ is mainly localized in the cytoplasm and $\Delta 133p53\beta$ and $p53\gamma$ can move between the nucleus and cytoplasm. These difference in the localization suggests that different isoforms of p53 may have different functions⁴¹. For instance, the $p53\beta$ and $\Delta 40p53$ isoforms are highly expressed at the mRNA level in primary melanoma cells, although they are at undetectable levels in normal cells⁵⁴. Also, the $\Delta 133p53$ isoform is shown to inhibit senescence and promote proliferation by binding and inhibiting full length p53⁵⁵.

1.1.4 Interaction Partners of p53

It has been reported that p53 has specific interacting partners which affects its activity. Among p53 interacting proteins, there are general transcription factors, protein kinases, protein acetylases/deacetylases, ubiquitin ligases, p53 regulatory proteins, viral proteins, p53 family members, replication and repair proteins⁵⁶. Among these, p53 interacts with transcription factors such as TBP (TATA-binding protein) and TAFII31 (TBP associated factorII31) and transcriptional co-activators such as p300/CBP through its N-terminal transactivation domain which results in the activity of on its response elements^{57–62}.

Another group of interacting partners of p53 consists of the proteins that make post-translational modifications on p53. The interaction of p53 with protein kinases such as casein kinase 2, HIPK2 (Homeodomain Interacting Protein Kinase 2) and JNK1 (C-Jun N-terminal kinase 1) results in the phosphorylation of p53^{63–66}. For other post-translational modifications, p53 has interacting partners which are protein acetylases such as p300/CBP and PCAF (p300/CBP-Associated Factor), protein deacetylases such as HDAC1 (Histone Deacetylase 1) and Sir2 α and protein deacetylase adaptors such as Sin3a^{61,62,67–72}. Moreover, there are also other interacting partners of p53 which results in other post translational modifications that affect its stability such as ubiquitination and deubiquitination. In addition to MDM2 which was described earlier, E6AP is a ubiquitin ligase and HAUSP (Herpesvirus-Associated Ubiquitin-Specific

Protease) is a ubiquitin protease that interacts with p53 and results in the stability or instability, respectively ⁷³⁻⁷⁵.

p53 regulatory proteins are the most important group of p53 interacting proteins due to their effects on p53 function. One of the regulating interacting partners of p53 is 53BP1. The p53 - 53BP1 interaction, induces p53 to cause cell cycle arrest ⁷⁶. 53BP2 is another p53 interactor that works as a co-activator of p53 resulting in cell cycle arrest ⁷⁷. One protein family that has interactions with p53 is the ASPP (Apoptosis Stimulating Protein of p53) family which has an antiapoptotic mediator, iASPP and two proapoptotic mediators, ASPP1 and ASPP2. When iASPP binds p53, it inhibits transcriptional activation by p53 ⁷⁸. On the other hand, the interaction between p53 and ASPP1 and ASPP2 results in the apoptotic function of p53 through binding to the PUMA (p53 Upregulated Modulator of Apoptosis), PIG3 (p53-Inducible Gene 3) and BAX (BCL2-Associated X Protein) proapoptotic response elements ⁷⁹. 14-3-3σ is another interacting partner of p53 which regulates p53 in a positive manner and leads p53 to induce G2/M cell cycle arrest ⁸⁰. The balance between apoptosis and autophagy upon cell stress is affected by another p53 interacting partner, HMGB1 (High Mobility Group Protein B1). HMGB1 normally makes a complex with Beclin1 which has important roles in autophagy. The presence of HMGB1 promotes the formation of p53-HMGB1 complexes and decreases the formation of p53-Beclin1 complexes regulating the balance between apoptosis and autophagy ^{81,82}.

One of the reasons for the preference of p53 to choose bind promoters of cell cycle arrest genes is due to HZF (Hematopoietic Zinc Finger Protein) which is a binding partner of p53. In the presence of HZF, p53 mediated cell cycle arrest is promoted, whereas in the absence of HZF, p53 mediated apoptosis is promoted ⁸³. Conversely, APAK (ATM And p53-Associated KZNF Protein) is another p53 interactor which changes p53 activity to promote apoptosis through changing the target specificity of p53 ⁸⁴. hCAS/CSE1L (Chromosome Segregation 1 Like) also regulates the selection of p53 response elements by binding and modifying the target specificity of p53 ⁸⁵. Redox sensitive proteins HIF1α (Hypoxia Inducible Factor 1α) and REF-1 are also bound to p53. The interaction between p53 and HIF1α stabilizes p53 whereas REF-1 – p53 interaction enhances p53 transcriptional activity ^{86,87}. A final group of proteins that bind to and modify p53 function are viral proteins. AdE1B55kD, EBV ENBA-5, HBV X,

HPV E6 and SV40 bind to p53 and either interact or modify its function to promote viral infection^{88–96}. This large list of interacting proteins modifies the activity of p53 towards the different pathways it controls.

1.1.5 Mutations of p53

In cancer cells the tumor suppressor proteins are commonly inactivated due to deletion or truncation. However most of cancer associated p53 mutations are only single base pair substitutions or missense mutations that do not affect the expression of the full length protein but only change one single amino acid. Mutation frequencies of different amino acids demonstrate that there are six hot spots that undergo mutations significantly more frequently than the others. These six hot spots are in the conserved DNA binding domain (residues 175, 245, 248, 249, 273 and 282) (figure 1.7)^{35,97–99}.



Figure 1.7 Six hot spots of cancer related mutant p53. The six hot spot mutation spots (residues 175, 245, 248, 249, 273 and 282, shown with stars) of p53 are conserved in the DNA binding domain (DBD, shown in pink).

Many of these missense mutations result in the increase of the half-life of the p53 protein¹⁰⁰. Mutant forms of p53 have a dominant negative effect on wild type p53 by forming wild type/mutant co-tetramers^{101–103}. In human tumor cells, even if a single allele of p53 is mutated, loss of heterozygosity results in the loss of the remaining wild type p53 allele. According to the ‘gain of function hypothesis’, mutation of p53 does not simply mean p53 function loss. Instead, due to the strong selection to remove the wild type p53, mutant p53 seems to have gained new functions in tumorigenesis. Similar to wild type p53 (wt p53), mutant p53 (mt p53) has interacting partners for inducing different pathways¹⁰¹. For instance, MRE11 (Mitotic Recombination 11) is a interacting partner that cannot bind the wild type p53 but it interacts with the two p53 mutants: R248W and R273H¹⁰⁴. Of course there are some proteins that are common

interacting partners of wt p53 and mt p53. PML (Promyelocytic Leukemia) protein is one example. The interaction with PML protein transcriptionally activates not only wt p53 but also its mutant versions. However, p53 mediated transcriptional activation in two cases have different results. The PML – wt p53 interaction results in tumor suppression whereas PML – mt p53 interaction results in oncogenic activity¹⁰⁵. Another common interactor of wt p53 and mt p53 is the PIN1 (Peptidyl-Prolyl Cis-Trans Isomerase NIMA-Interacting 1) protein. Although the interaction of wt p53 and PIN1 results in direction of p53 towards p21 promoter which finally results in cell cycle arrest, the interaction of mt p53 and PIN1 results in the aggressiveness of breast cancer cells which indicates cell cycle is promoted rather than arrested¹⁰⁶. In addition to these, mt p53 can form different combinations of complexes with other p53 family members such as p63 and p73. Normally p63 and p73 can make homotetramers or heterotetramers with each other. However, neither p63 nor p73 makes heterotetramers with wt p53. On the other hand, mt p53 interacts with p63 and p73 and can form heterotetramers^{107–111}. Mt p53 inhibits the transcriptional activation of p63 and p73 by making heterotetramers with them. Heterotetramers of neither p63 – mt p53 nor p73 – mt p53 are incapable of activating normal p53 target genes involved in tumor suppression, senescence and genomic stability (figure 1.8)^{112,113}.

Similar to wt p53, mt p53 is a transcription factor and can transcriptionally activate genes that have roles in tumorigenesis^{100,101,114}. Although wt p53 and mt p53 share an intact transactivation domain, it makes wt p53 a tumor suppressor but mt p53 an oncogenic protein^{115–119}. MYC, CXCL1 (Chemokine (C-X-C Motif) Ligand 1) and MAP2K3 (Mitogen Activated Protein Kinase Kinase3) which can promote proliferation of cancer cells, are some examples of genes that can be activated by mt p53^{116,120,121}. Moreover, mt p53 transcriptionally activates genes that inhibit cell death, such as BclxL (B-cell Lymphoma-extra large Protein), EGR1 (Early Growth Response Protein 1) and MDR1 (Multi drug transporter protein 1)^{121–123}. In addition to these, limitless replication causing TERT (Telomerase Reverse Transcriptase) is shown to be upregulated by mt p53¹²⁴. All of these results are point to the unique oncogenic functions of mt p53.

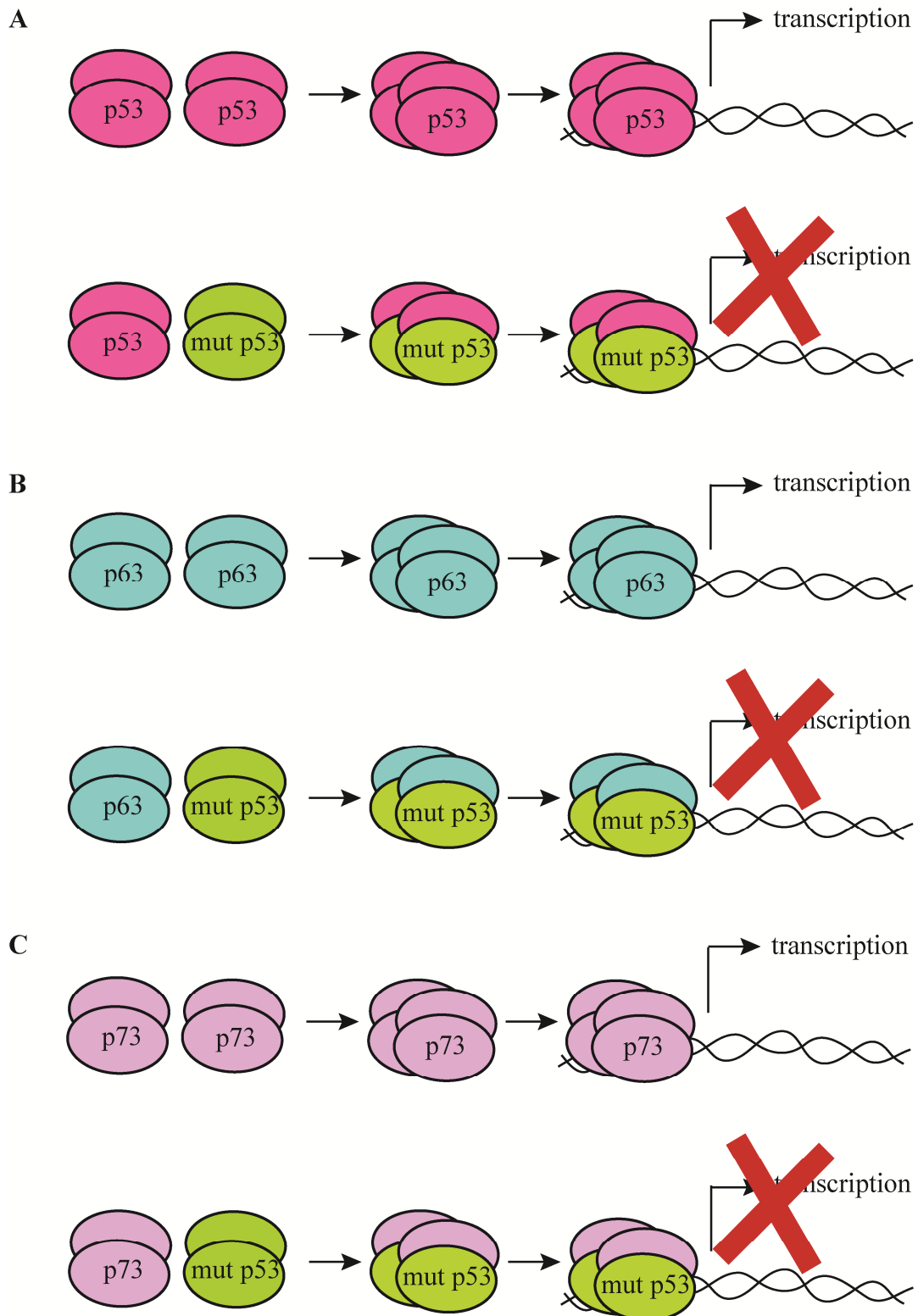


Figure 1.8 Mutant p53 blocks functional p53, p63 and p73 homotetramers by formation of heterotetramer. Heterotetramers of neither p63 (represented as turquoise ellipse) – mutant p53 (represented as green ellipse) nor p73 (represented as purple ellipse) – mutant p53 are incapable of activating normal p53 (represented as pink ellipse) target genes involved in tumor suppression, senescence and genomic stability.

1.2 Scientific Background of PATZ1

1.2.1 Identification of PATZ1

PATZ1 (POZ/BTB and AT-hook-containing zinc finger protein 1) which is also known as MAZR (MAZ-related factor), ZSG (zinc finger sarcoma gene) and ZNF278 (zinc finger protein 278) is first identified as a transcription factor and an interacting partner of the B cell and neuronal transcriptional repressor BACH2 (BTB and CNC Homology 1, Basic Leucine Zipper Transcription Factor 2)¹²⁵. Although being a transcription factor, N terminal part of PATZ1 does not show any transcriptional activity unlike other common transcriptional activators¹²⁵. PATZ1 mRNA levels are significantly high in the thymus, fetal liver and bone marrow. PATZ1^{-/-} mice are born at a severely reduced Mendelian ratio, are much smaller compared to the wild type littermates and are infertile^{125,126}.

1.2.2 Structure and Alternative Splice Variants of PATZ1

PATZ1 is a member of the transcription factor family of proteins that share an N terminal BTB/POZ (Broad Complex, Tramtrack, and Bric a' brac / Poxviruses and Zinc-finger (POZ) and Kruppel domain for protein-protein interaction which are involved in transcriptional regulation, chromatin structures and cytoskeleton organization and a C-terminal zinc finger motif containing DNA binding domain^{125,127}. PATZ1 is a transcription factor that is composed of a N terminal BTB/POZ domain, two AT-hook domains and a DNA binding domain consisting of C2H2 type zinc finger motifs (figure 1.9)^{125,128,129}.



Figure 1.9 Structure of PATZ1 protein. PATZ1 is composed of a BTB domain (shown in pink, two AT-hook domains (shown in purple) and a DNA binding domain consisting of zinc finger motifs (shown in yellow).

There are four alternative splice variants of the PATZ1 protein which are PATZ1-001, PATZ1-002, PATZ1-003 and PATZ1-004. The isoforms of the PATZ1 protein share the same N terminal BTB/POZ domain and AT-hook domains but have different numbers of zinc finger domains in the DNA binding domain (figure 1.10). The most highly expressed alternative splice variants are PATZ1-004 and PATZ1-002.

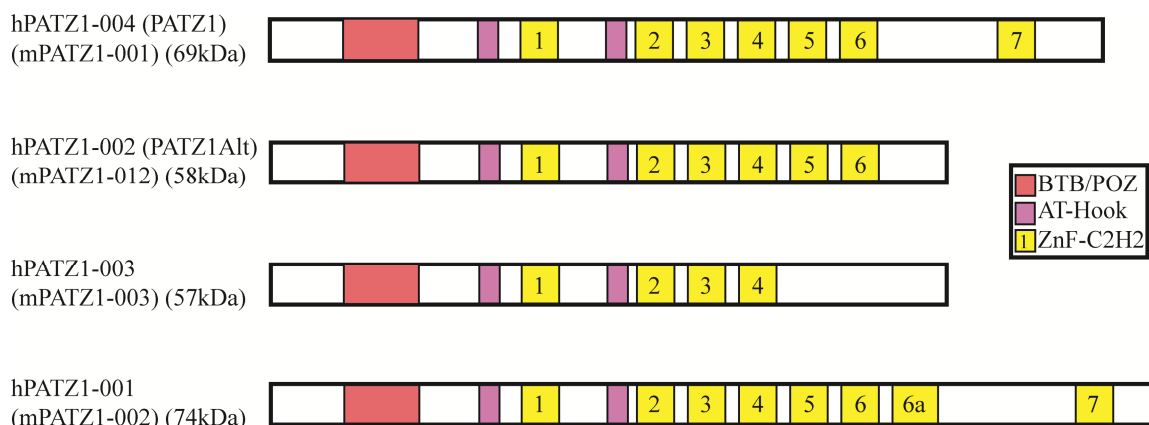


Figure 1.10 Alternative splice variants of PATZ1. There are four alternative splice isoforms of the PATZ1 protein: hPATZ1-004 (PATZ1, mPATZ1-001), hPATZ1-002 (PATZ1Alt, mPATZ1-012), hPATZ1-003 (mPATZ1-003) and hPATZ1-001 (mPATZ1-002). The BTB/POZ domain is shown in pink, the AT-hook domain is shown in purple and the zinc finger domains are shown in yellow.

The N terminal BTB/POZ domain is mainly known as an interaction motif among proteins resulting in different roles in cytoskeleton dynamics, targeting proteins for ubiquitination, ion channel assembly and regulation of transcription¹³⁰. The AT-hook domain is another important part of PATZ1 involved in the DNA binding of PATZ1 protein. The AT-hook motif has a conserved palindromic, core sequence of proline-arginine-glycine-arginine-proline¹³¹. Besides the AT-hook domains, the major part of PATZ1 – DNA interaction is maintained by the zinc finger motifs. All the zinc finger motifs of PATZ1 protein are C2H2 type in which the zinc ion is coordinated by two cysteine and two histidine residues. In addition to the DNA binding, the zinc finger motifs contribute to the three dimensional conformation of the PATZ1 protein.

1.2.3 Functions of PATZ1

PATZ1 was first identified as a transcriptional repressor of BACH2 which is specific to B cells ¹²⁵. Later it was reported that PATZ1 interacts with BCL6 and negatively modulates its expression. Consistently, Patz1 knockdown mice showed up-regulation of BCL6 expression and BCL6-dependent B cell neoplasias ¹³². In addition to the role in B cells, PATZ1 was shown to have an important role in cell fate determination of T lymphocytes in the thymus. As thymocytes decide to become either CD4 positive or CD8 positive lymphocytes, PATZ1 plays a critical role by transcriptionally repressing the Cd8 gene ¹³³. PATZ1 is an important member of a transcription network that decides the CD4/CD8 lineage fate in double positive thymocytes ¹²⁶. However, other publications show that the function of PATZ1 is not restricted to B and T lymphocytes. Chromatin immunoprecipitation (ChIP) sequencing experiments revealed that there are more than 5000 binding sites of PATZ1 in the mouse genome ¹³⁴. PATZ1 transcriptionally represses the androgen receptor, activates mast cell protease 6 and either activates or represses c-Myc in a context dependent manner ^{125,128,135,136}.

Moreover, PATZ1 was shown to repress neuronal developmental genes ¹³⁴. Patz1 gene expression is evident in actively proliferating neuroblasts. However, more mature neurons, the expression of Patz1 gene becomes more restricted. Upon Patz1 gene disruption, embryos have severe defects in the central nervous system and in the cardiac outflow tract. Thus, PATZ1 has critical roles in embryonic development ¹³⁷. PATZ1 is also shown to be an important regulator of pluripotency in embryonic stem cells. PATZ1 expression levels are much higher in pluripotent mouse ICM than in the non-pluripotent trophectoderm ¹³⁸. Moreover, transcription factors such as Oct4, Nanog, Sox2, Klf4, and c-Myc that are related with the pluripotency of embryonic stem cells can bind the PATZ1 genomic region ^{139,140}. PATZ1 is reported to have also a role on the regulation of mast cells through interacting with the mi transcription factor (MITF) that has roles in mast cell differentiation and survival ^{136,141,142}. Mast cells have a role in hypersensitivity reactions such as allergic asthma, allergic rhinitis and systemic

anaphylaxis^{143,144}. Still another report claims that Patz1 knock down results in the upregulation of apoptotic genes and downregulation of cell cycle and cellular metabolism genes¹³⁴. In human umbilical vascular endothelial cells (HUVECs), PATZ1 expression levels decrease during cellular senescence. Patz1 knock down results in the acceleration of cellular senescence in young HUVECs whereas PATZ1 overexpression reverses the phenotypes of senescence in old HUVECs. Moreover, PATZ1 induced senescence is associated with ROS-mediated p53 dependent DNA damage responses¹⁴⁵.

Several studies report links between Patz1 gene expression and cancer development. The Patz1 gene is rearranged and deleted in small round cell carcinoma¹²⁹. Furthermore, in human colorectal, breast and testicular tumors, PATZ1 mRNA is upregulated^{146–148}. The Patz1 gene maps on the FRA22B fragile site which results in loss of heterozygosity in several solid tumors and thus has a role in carcinogenesis¹⁴⁹. When PATZ1 is silenced by siRNA, the growth of colorectal cancer cells is blocked¹⁴⁶. Also, silencing of PATZ1 resulted in induction of apoptosis in gliomas¹⁵⁰. Even though the mechanism is not known, in testicular tumors, the PATZ1 protein is localized to the cytoplasm instead of the nucleus where PATZ1 is normally localized^{148,151}.

2. AIM OF THE STUDY

p53 mutations that allow cells to escape from death are the most common genetic event in human cancer. p53 is identified as a tumor suppressor protein because the deficiency of p53 results in the accumulation of different types of tumors such as carcinomas, osteocarcinomas testicular tumors, soft tissue sarcomas and lymphomas in mice. The aim of this project is to find a new interacting partner of p53 that can modify its role. One of the candidates that may have a regulatory role on p53 was a transcriptional repressor called PATZ1. Besides from its function during B and T cell development, PATZ1 protein is also involved in human colorectal, breast and testicular tumors. In the first part of the project we aimed to identify and characterize the interaction of p53 and PATZ1 proteins from different perspectives. We planned to overexpress p53 and PATZ1 proteins and confirm their interaction. By using N terminal and C terminal truncations of PATZ1, we wanted to find the domain required for this interaction. Furthermore, we aimed to find the amino acids necessary for the p53 – PATZ1 interaction by introducing site directed mutations in the required domain of PATZ1. For further characterization, we also planned to determine if the interaction between p53 and PATZ1 DNA dependent or not by treating with DNA damaging agents. In addition to these, we aimed to confirm the interaction in endogenous conditions and find if another isoform of p53 or PATZ1 is involved in the interaction. In the second part of the study, we wanted to investigate if there is a role of this interaction on p53 function. Thus, we planned to find out the effect of PATZ1 overexpression on the sub-cellular translocation of p53 from cytoplasm to nucleus and induction of apoptosis upon DNA damage. Finally, we aimed to reveal the effect of the formation of p53 – PATZ1 complex on p53 – DNA and PATZ1 – DNA interactions. Thus, in this project our aim was to investigate the functional interaction of p53 and PATZ1 which may have roles in tumor formation and cancer development.

3. MATERIALS AND METHODS

3.1 Materials

3.1.1 Chemicals

All the chemicals used in this project are listed in the Appendix A.

3.1.2 Equipment

All the equipment used in this project are listed in the Appendix B.

3.1.3 Buffers and Solutions

Standard buffers and solutions used in the project were prepared according to the protocols in Sambrook et al ., 2001.

3.1.3.1 Bacterial Transformation Buffers and Solutions

Calcium Chloride (CaCl₂) Solution: 60mM CaCl₂ (diluted from 1M stock), 15% Glycerol, 10mM PIPES at pH 7.00 were mixed and the solution prepared was autoclaved at 121 °C for 15 min and stored at 4 °C.

3.1.3.2 Mammalian Cell Culture Buffers and Solutions

Phosphate-buffered saline (PBS): 1 tablet of PBS (Sigma, P4417) was dissolved in 200mL ddH₂O.

Polyethylenimine (PEI): 100 mg PEI was dissolved in 90mL of ddH₂O. pH was adjusted to 7.00 with 5 M NaOH and the solution was completed to 100mL with ddH₂O. The buffer was filter-sterilized, stored at -20 °C.

Trypan blue dye (0.4% w/v): 40µg of trypan blue was dissolved in 10mL PBS

Hypotonic Lysis Buffer: The solution was prepared with a final concentration of 10mM HEPES-KOH pH 7.9, 2mM MgCl₂, 0.1mM EDTA, 10mM KCl, 0.5% NP-40. 1 tablet protease inhibitor (complete mini EDTA free)/10mL buffer was mixed prior to using.

Hypertonic Lysis Buffer: The solution was prepared with a final concentration of 50mM HEPES-KOH pH 7.9, 2mM MgCl₂, 0.1mM EDTA, 50mM KCl, 400mM NaCl, 10% glycerol. 1 tablet protease inhibitor (complete mini EDTA free)/10mL buffer was mixed prior to using.

Immunoprecipitation (IP) Buffer: The solution was prepared with a final concentration of 50mM HEPES-KOH pH 7.9, 5mM MgCl₂, 100mM KCl, 0.1% NP-40, 10% glycerol. 1 tablet protease inhibitor (complete mini EDTA free)/10mL buffer was mixed prior to using.

3X Laemli Buffer: The solution was prepared with a final concentration of 175 mM Tris pH 6.8, 30% glycerol, 3% SDS and 15% β-mercaptoethanol.

20X Oligo Annealing Buffer: The solution was prepared with a final concentration of 200mM Tris-HCl pH 8.0, 1M NaCl, 40mM MgCl₂, 10mM EDTA.

2X Bead – DNA Binding Buffer: The solution was prepared with a final concentration of 10mM Tris-HCl pH 7.5, 2M NaCl and 1mM EDTA.

5X Protein – DNA Binding Buffer: The solution was prepared with a final concentration of 50mM Tris-HCl pH 7.5, 250mM NaCl, 2.5mM EDTA, 2.5mM DTT, 20% glycerol, 5mM MgCl₂, 0.5µg/µL polydI/dC, 0.5µg/µL BSA.

1X PBS-Tween20 (PBS-T) Solution: 0.5mL of Tween20 was dissolved in 1L of 1X PBS.

Blocking Buffer: 0.5g milk powder was dissolved 10mL 1XPBST.

3.1.3.3 Gel Electrophoresis Buffers and Solutions

Agarose gel: For 1% w/v agarose gel preparation, 1 g of agarose was dissolved in 100 mL 0.5X TBE buffer by heating. 0.01% (v/v) ethidium bromide was added to the solution.

10X Tris-Borate-EDTA (TBE) Buffer: 104g tris base, 55g boric acid and 40mL 0.5M EDTA at pH 8.0 were dissolved in 1L of ddH₂O.

10X Tris – Glycine Buffer: 40g tris base and 144g glycine were dissolved in 900mL ddH₂O. pH was adjusted to 8.3 with 37% HCl and the solution was completed to 1L with ddH₂O.

1X Running Buffer: 100mL 10X Tris – Glycine Buffer and 5mL 20% SDS solution were mixed and completed to 1L with ddH₂O.

1X Transfer Buffer: 100mL 10X Tris – Glycine Buffer, 200mL methanol and 1.8mL 20% SDS were mixed and completed to 1L with ddH₂O.

SDS Separating Gel (10%): For 10mL gel; 2.5mL Tris 1.5M at pH 8.8, 4mL ddH₂O, 3.34mL Acryl: Bisacryl (30%), 100μL 10% SDS, 100μL 10% APS, and 10μL TEMED were mixed.

SDS Stacking Gel (4%): For 5mL gel; 1.25mL Tris 0.5 M at pH 6.8, 2.70mL H₂O, 1mL Acryl: Bisacryl (30%), 50μL 10% SDS, 15μL 10% APS, and 7.5μL TEMED were mixed.

3.1.4 Growth Media

3.1.4.1 Bacterial Growth Media

Luria Broth from BD was used for liquid culture of bacteria. 20 g of LB Broth was dissolved in 1 L of distilled water and autoclaved at 121°C for 15 min. For selection, ampicillin with a final concentration of 100μg/mL, kanamycin with a final concentration of 50μg/mL and chloramphenicol with a final concentration of 12.5μg/mL were added to the liquid medium after autoclave.

LB agar from BD was used for preparation of solid medium for the growth of bacteria. 40g of LB agar were dissolved in 1L distilled water and autoclaved at 121°C for 15 min. For selection, ampicillin with a final concentration of 100μg/mL, kanamycin with a final concentration of 50μg/mL and chloramphenicol with a final concentration of 12.5μg/mL were added to the medium after cooling down to 50°C. Antibiotic added medium was poured onto sterile Petri dishes (~ 20 mL/plate). Sterile solid agar plates were kept at 4°C.

3.1.4.2 Tissue Culture Growth Media

Growth Media For Adherent cell lines: HCT116 and HCT116 p53^{-/-} cell lines were grown in filter-sterilized DMEM that was supplemented with 10% heat-inactivated fetal bovine serum, 2mM L-Glutamine, 100 unit/mL penicillin and 100 unit/mL streptomycin.

Freezing Medium: All the cell lines were frozen in medium containing DMSO added into fetal bovine serum (FBS) at a final concentration of 10% (v/v) and stored at 4°C.

3.1.5 Commercial Molecular Biology Kits

- QIAGEN Plasmid Midi Kit, 12145, QIAGEN, Germany
- Qiaquick Gel Extraction Kit, 28706, QIAGEN, Germany
- Qiaquick PCR Purification Kit, 28106, QIAGEN, Germany

3.1.6 Enzymes

All the restriction enzymes and their corresponding 10X reaction buffers, DNA modifying enzymes and polymerases used in this study were from New England Biolabs (NEB).

3.1.7 Cell Types

3.1.7.1 Bacterial Cells

E. coli DH-5 α (F- endA1 glnV44 thi-1 relA1 gyrA96 deoR nupG lacZdeltaM15 hsdR17) competent cells were used for bacterial transformation of plasmids.

3.1.7.2 Tissue Culture Cell Lines

Human colon carcinoma cell lines HCT116 that has wild type p53 and HCT116 p53^{-/-} cells that lacks p53 were used in this study.

3.1.8 Vectors and Primers

Vectors and primers used in this project are listed in Table 3.1 and Table 3.2

Vector Name	Use	E.coli Resistance Marker
pcDNA-GFP	Transfection Control Vector	Amp
pCMV-HA	Mammalian Expression Vector with N Terminal HA Tag	Amp
pCMV-HA-PATZ1	Mammalian Expression Vector Encodes of HA-PATZ1	Amp
pCMV-HA-PATZ1Alt	Mammalian Expression Vector Encodes of HA-PATZ1Alt	Amp
pCMV-HA-PATZ1D521Y	Mammalian Expression Vector Encodes of HA-PATZ1 D521Y Single Mutant	Amp
pCMV-HA-PATZ1D521Y/D527Y	Mammalian Expression Vector Encodes of HA-PATZ1 D521Y/D527Y Double Mutant	Amp
pCMV-FLAG	Mammalian Expression Vector with N Terminal FLAG Tag	Amp
pCMV-FLAG-p53	Mammalian Expression Vector Encodes of FLAG-PATZ1	Amp
pCMV-Myc	Mammalian Expression Vector with N Terminal Myc Tag	Amp
pCMV-Myc-PATZ1	Mammalian Expression Vector Encodes of Myc-PATZ1	Amp
pCMV-Myc-deltaZF	Mammalian Expression Vector Encodes of Myc-PATZ1 Δ ZF Truncation	Amp
pCMV-Myc-deltaBTB	Mammalian Expression Vector Encodes of Myc-PATZ1 Δ BTB Truncation	Amp
pCMV-Myc-BTB	Mammalian Expression Vector Encodes of Myc-PATZ1 BTB Only Truncation	Amp

Table 3.1 Vectors used in this project

Primer Name	Sequence	Use
p53_GADD45_fwd	(Biotin)GAACATGTCTAAGCATGCTG	Pull down
p53_GADD45_rev	(Biotin)CAGCATTCTTAGACATGTTC	Pull down
p53_pg13_fwd	(Biotin)CCAGGCAAGTCCAGGCAGG	Pull down
p53_pg13_rev	(Biotin)CCTGCCTGGACTTGCCTGG	Pull down
MAZRtop	(Biotin)AGGTGTGCTGCCCCCAGGTCC ACCCGCAGGAGGAGAGGGGGCT	Pull down
MAZRbot	(Biotin)AGCCCCCTCTCCTCCTGCGGG TGGACCTGGGGGCAGCACACCT	Pull down
HAMAZRfwd	CTAGAATTCCCCACCATGTACCCAT ACGATGTTCCAGATTACGCTATGGA GCGGGTCAACGACGCTTC	Cloning of mPATZ1-002- IRES-Cherry
MAZRrev	CTAGAATTCCGACGGGACACAGCAT GTCTCAC	Cloning of mPATZ1-002- IRES-Cherry
patz1-001/002Rev	TAGGAGGCAGAGGAGAAACCTCGGT TACAGATGCTACAGAAGT	Cloning of mPATZ1-002- IRES-Cherry
patz1-002 For	CTTCTGTAGCATCTGTAACCGAGGTT TCTCCTCTGCCTCCTACTTAAAG	Cloning of mPATZ1-002- IRES-Cherry
patz1-002 Rev	TGATGTGAGCATTCTGGCCTTCTTT GTTGCCATAGGTCCTGGCG	Cloning of mPATZ1-002- IRES-Cherry
patz1-002/001For	CCAGGACCTATGGCAACAAAGAAG GCCAGAAATGCTCAC	Cloning of mPATZ1-002- IRES-Cherry

Table 3.2 Primers used in this project

3.1.9 DNA and Protein Molecular Weight Markers

DNA and protein molecular weight markers used in this project are listed in Appendix C.

3.1.10 DNA Sequencing

Sequencing service was commercially provided by McLab, CA, USA.
(<http://www.mclab.com/home.php>)

3.1.11 Software and Computer Based Programs

The software and computer based programs used in this project are listed in Table 3.3

Program Name	Website/Company	Use
CLC Main Workbench	QIAGEN	Vector maps, primer design, restriction analysis, alignments
FlowJo 7.6.1	Tree Star Inc.	View and analyze flow cytometry data
Finch TV 1.4.0	Geospiza Inc.	View and analyze sequencing results
ZEN 2009 Light Edition	Carl Zeiss Inc.	View and analyze confocal microscope data
Quantity One	Bio-Rad	View and analyze DNA gel images
Ensembl Genome Browser	http://www.ensembl.org	View and analyze genomic sequences

Table 3.3 Software and computer based programs used in this project

3.2 Methods

3.2.1 General Molecular Cloning Methods

3.2.1.1 Bacterial Cell Culture

Bacterial Culture Growth: *E.coli* DH5 α strain was grown overnight (16h) at 37°C shaking at 250 rpm in Luria Broth (LB). For the glycerol stock preparation of bacterial cells, glycerol was added to the overnight grown bacterial cultures to a final concentration of 10%. Cells were frozen first in liquid nitrogen and stored at -80°C. Bacterial strains were either streaked or spread were on LB agar petri dishes overnight at 37°C. All growth medium were prepared with or without selective antibiotics prior to any application.

Preparation of Chemically Competent Bacterial Cells: *E.coli* DH5 α competent cells were prepared starting from a single colony previously streaked on LB agar without any selective antibiotics. This colony was inoculated in 50mL LB without any selective antibiotics in a 200mL flask and grown overnight at 37°C, 250 rpm. The next day, 4mL from the overnight culture was diluted in 400mL LB medium in a 2L flask and incubated at 37°C, 250 rpm until the optical density at 590nm reached 0.375. The culture was then transferred into 50mL falcon tubes (8 tubes in total) and incubated on ice for 10 minutes prior to centrifugation at 1600g for 10min at 4°C. After centrifugation, cell pellets were resuspended in 10mL (for each falcon tube) ice-cold CaCl₂ solution and centrifuged at 1100g for 5 min at 4°C. The cell pellets were resuspended in 10mL (for each falcon tube) ice-cold CaCl₂ solution again and incubated on ice for 30min. Following a final centrifugation at 1100g for 10 min at 4°C, the pellet was resuspended in 2mL (for each falcon tube) ice-cold CaCl₂ solution and dispensed into 200 μ L aliquots into pre-chilled 1.5mL eppendorf tubes. Aliquotted competent cells

were frozen immediately in liquid nitrogen and then stored at -80°C. The transformation efficiency of the competent cells was tested routinely between 10⁷-10⁸ colonies/μg DNA by pUC19 plasmid transformation.

Chemical Transformation of Bacterial Cells: Chemically competent DH5α *E.coli* were thawed from -80°C to 4°C and 100pg of DNA was added before the cells were completely thawed. The cells were then incubated on ice for 30 min. After the incubation on ice, the cells were heat shocked for 90 seconds at 42°C and transferred back onto ice for 60 seconds. 800μL of sterile LB without any antibiotics was added on the cells and this culture was incubated for 45 min at 37°C for the recovery of the cells. After 45 min, the cells were spread with 4mm glass beads on the LB agar plate containing appropriate antibiotic for selection. The plate was incubated overnight at 37°C.

Plasmid DNA Isolation: Plasmid DNA isolation was performed with alkaline lysis protocols. The concentration and purity of the DNA isolated were determined by using a UV-spectrophotometer or nanodrop. Measurements for DNA concentration and purity were done at an optical density of 260nm by using quartz cuvettes.

3.2.1.2 Vector Construction

Polymerase Chain Reaction (PCR) Amplification:

Optimized PCR conditions are shown in Table 3.4

PCR Reaction	Volume Used	Final Concentration
Template DNA	1-10μL	4pg/μL – 4ng/μL
10X Pfu Polymerase Buffer with MgCl ₂	2.5μL	1X
dNTP mix (10mM)	0.5μL	0.2mM
Forward Primer (10μM)	2μL	0.8μM
Reverse Primer (10μM)	2μL	0.8μM
Pfu Polymerase (2.5U/μL)	0.5μL	0.025U/μL
ddH ₂ O	Up to 25μL	
Total	25μL	

Table 3.4 Optimized PCR conditions

Optimized PCR thermal cycle conditions are shown in Table 3.5

Step	Temperature (°C)	Time (min)
Initial Denaturation	95	4
Denaturation	95	1
Annealing	56	1
Extension	72	2
Final Extension	72	10
Hold	4	∞

} 30
cycles

Table 3.5 Optimized PCR thermal cycle conditions

Restriction Enzyme Digestion:

Components and the amounts for restriction enzyme digestion are shown in Table 3.6

Components	Used Amount
Plasmid DNA	1μg-10μg
Restriction enzyme (10U/μL)	1.5μL
Compatible Buffer (10X)	1.5μL
ddH ₂ O	Up to 15μL
Total	15μL

Table 3.6 Components and amounts for restriction enzyme digestion

Restriction enzyme digestion reactions were set by the mixture of ddH₂O, DNA, the enzyme and the compatible buffer in a 1.5mL eppendorf tube and incubated at the optimum temperature for 2 hours. For diagnostic digestions 1μg of DNA was used. 10μg or more DNA was digested for gel extraction and cloning purposes. If the DNA was a digested vector that would be used in the ligation, the 5' overhang of the linear plasmid was dephosphorylated by calf intestinal alkaline phosphatase, CIAP (Fermentas).

Agarose Gel Electrophoresis: PCR products, digestion products and DNA samples were observed on 1% agarose gels. Gels were prepared by dissolving 1g of agarose in 100mL 0.5X TBE. The mixture was heated in a microwave until the agarose

was completely dissolved (typically 2 minutes). The solution was then cooled down and ethidium bromide with a final concentration of 0.001v/v was added. After mixing, the gel was poured onto the gel casting tray and let to cool down to room temperature and solidify. When the gel was in solid form, the DNA samples which were previously mixed with 6X DNA loading dye reaching to a final concentration of 1X were loaded into the wells. 0.5X TBE was used as a running buffer. Agarose gels were run at 100V for 80 min and the bands were observed under UV in a BIO-RAD gel imager.

DNA Extraction From Agarose Gel: DNA samples were extracted with Qiagen Gel Extraction Kits according to the manufacturers protocols.

Ligation: The ligation reaction mixtures were composed of insert either digested or amplified by PCR and digested thereafter, digested vector, T4 ligation buffer (NEB), T4 DNA ligase (NEB) and ddH₂O. Ligation reactions contained 1:3, 1:5 or 1:10 vector:insert molar ratio using 100ng of vector. For ligations, vectors which were dephosphorylated by using calf intestine alkaline phosphatase, CIAP (Fermentas) after digestion, in order to avoid self ligation. Also for each ligation, a separate ligation reaction mixture without insert was always used as a negative control. Ligation reactions were incubated at 16°C for 16 hours. The mixture was then transformed into chemically competent bacterial cells.

3.2.2 Mammalian Cell Culture

3.2.2.1 Preparation and Maintenance of Mammalian Cells

Maintenance of Adherent Cells: Adherent cells used in this project were HCT116 and HCT116 p53^{-/-} cells. These cell lines were grown in filter-sterilized DMEM that was supplemented with 10% heat-inactivated fetal bovine serum, 2mM L-Glutamine, 100unit/mL penicillin and 100unit/mL streptomycin in 10mm tissue culture plates in a 37°C, 5%CO₂ incubator. When the plate reached to 70-80% confluency, cells were split into a pre-warmed, fresh medium with a ratio of 1:10. Adherent cells were trypsinized before splitting.

Trypsinization: Adherent cells were trypsinized to detach the cells both from the plate and from each other. After removing the old medium, plate was washed with serum free DMEM to remove the serum which would inactivate the trypsin enzyme. 2mL of trypsin solution was added on the plate and incubated until the cells were detached from the plate (approximately 2 minutes) at 37°C. 8 mL of fresh medium containing serum was then added to the trypsin on the plate surface and cells were harvested to a 15 mL falcon tube. After centrifugation at 1000 rpm for 5 minutes, the medium was removed and cells were resuspended in pre-warmed fresh DMEM that was supplemented with 10% heat-inactivated fetal bovine serum, 2mM L-Glutamine, 100unit/mL penicillin and 100unit/mL streptomycin for further incubation.

Cell Freezing: 10^6 cells were centrifuged at 1000 rpm for 5 minutes and the medium was removed. The cells were then resuspended in 1 mL ice-cold freezing medium containing DMSO added into fetal bovine serum (FBS) at a final concentration of 10% (v/v) and were put in cryovials. They were stored at -80°C in a cryobox for 24-48 hours and were then transferred to liquid nitrogen tank.

Cell Thawing: Frozen cells in the cryovials were resuspended in 10mL complete growth medium in a 15mL falcon tube. The cells were then centrifuged at 1000 rpm for 5 minutes. After removing the supernatant, the cells were resuspended in 10mL pre-warmed fresh complete medium and transferred to either plates or flasks.

3.2.2.2 Transient Transfection of Adherent Cells with PEI (Polyethylenimine)

Adherent cells used in this project were HCT116 and HCT116 p53^{-/-}. Transient transfection of these cell lines were done by using the PEI method. One day before transfection 4×10^6 cells were split onto 10-cm plates. On the transfection day, 10µg DNA was diluted in 1mL ddH₂O followed by 30µgPEI addition. The mixture was vortexed immediately and incubated for 15 minutes at room temperature. After incubation, the mix was added dropwise on the cells.

3.2.2.3 Cell Lysis, Immunoprecipitation and DNA Pull Down

48 hours after transfection of expression plasmids, 20×10^6 cells were trypsinized and harvested in a 15mL falcon tube. After centrifugation at 1000 rpm for 5 minutes, the cells were washed with 1XPBS and transferred to a 1.5mL eppendorf tube. Another centrifugation at 1000 rpm for 5 minutes was done to remove the PBS and the cells were then resuspended in 1000 μ L hypotonic lysis buffer. The cells were incubated with the hypotonic lysis buffer suspension on ice for 10 minutes and then centrifuged at 13,200 rpm for 10 minutes. Cytoplasmic lysate (the supernatant after centrifugation) was transferred to a clean 1.5mL eppendorf tube. The pellet was dounce homogenized by 10 strokes in 150 μ L hypertonic lysis buffer for nuclear extraction. The suspension was incubated on ice for 15 minutes and then centrifuged at 13,200 rpm for 10 minutes. Nuclear lysate (the supernatant after centrifugation) was transferred to a clean 1.5mL eppendorf tube. Cytoplasmic and nuclear lysates were stored at -80°C for western blot experiments, however if there was an immunoprecipitation experiment going on, then the lysates were used fresh. For immunoprecipitation, nuclear lysates were diluted at a 1:2 ratio in IP buffer. The dilution was incubated with anti-FLAG or anti-HA antibody conjugated sepharose beads or anti-p53 antibody conjugated magnetic beads at 4°C overnight, washed several times in ice-cold wash buffer. Finally, beads were boiled at 95°C in 1X Laemni Buffer for 10 minutes leading the protein samples transfer from beads to the buffer. After centrifugation, the samples were loaded onto SDS-PAGE gels.

For DNA pull down, biotinylated oligos were diluted with annealing buffer up to a concentration of 1X. The mixture was placed in a water bath at 100°C for 5 minutes and then the heater was shut off and the mixture was allowed to cool down slowly to room temperature in the water bath. Streptavidin coupled magnetic beads were conjugated with the annealed biotinylated double stranded probes in 1X Bead-DNA binding buffer at room temperature for 15 minutes. Nuclear lysates were incubated with the streptavidin beads conjugated with biotinylated probes in 1X Protein – DNA binding buffer at room temperature for 30 minutes. Protein contents of the bead conjugates were eluted in 1X Laemni Buffer.

3.2.3.4 SDS Gel, Transfer and Western-Blot

The SDS gels used in this project had a 10% separating part and a 4% stacking part and their contents were explained in section 3.1.3.1. After the samples were loaded, the SDS gels were run with 1X running buffer at constant voltage 80V for 1.5-2 hours using a BIORAD MiniProtean Tetra Cell. After running, the gels were transferred to 0.45µm PVDF membranes (Thermo Scientific) in 1X transfer buffer at constant current 250mA for 105 minutes at 4°C using a BIORAD Mini Trans-blot wet electrophoretic transfer cells. Membranes were then blocked in 10mL blocking buffer at room temperature for 1 hour with constant shaking. Primary antibody incubations were performed overnight at 4°C and secondary antibody incubations were performed for 1 hour at room temperature. Membranes were washed with PBS-T buffer 3 times for 10 minutes after blockings, primary antibody incubations and secondary antibody incubations. After the final washing step, the membranes were incubated with an enhanced chemiluminescent substrate (Supersignal west pico chemiluminescent substrate, Thermo Scientific lot number JL126474) for 4 minutes at room temperature in the dark room for HRP detection. Membranes were then transferred to cassettes and exposed to X-Ray Films (Fuji), developed and fixed in the dark room.

3.2.4 Subcellular Localization

Prior to the transfection of cells with PEI, coverslips were attached to the surface of six-well plates and cells were seeded those cover slips. Transfection of the DNA into the cells was performed according to the protocol explained in section 3.2.3.3. 48 hours after from transfection, the medium was removed and the cover slips were washed with 1XPBS twice. 4% paraformaldehyde (PFA) was then added to the plates and cells were incubated for 30 minutes in dark at room temperature for fixation of the cells to the cover slips. Then, the covers slips were washed with 1XPBS twice and incubated in 1µg/mL DAPI (4',6-Diamidine-2'-phenylindole dihydrochloride) solution for 5 minutes in dark at room temperature. Covers slips were washed with 1XPBS two times again. 15µL ProLong Gold Antifade (Invitrogen) mounting medium was added on the

slides and the cover slips were inverted and seated on the slides. After the cover slips were fixed, the cells were visualized with the fluorescence microscope with GFP, dsRED and DAPI filters and Plan-Apochromat 63x/1.40 Oil DIC M27 objective.

3.2.5 Flow Cytometric Analysis

10^6 cells were used for each flow cytometric analysis. After centrifugation of the cells, the supernatant was removed and the cells were washed with PBS for two times. In order to exclude dead cells and detect the apoptotic cells, the cells were incubated with SytoxRED and AnnexinV-FITC at room temperature for 15 minutes in dark. The flow cytometric analysis of the cells was performed by using a BD FACSCanto flow cytometer. AnnexinV-FITC was excited by the 488 nm argon laser and fluorescence was detected with FITC 530/30nm band pass filter.

3.2.6 Real Time Cell Growth and IC₅₀ Analysis

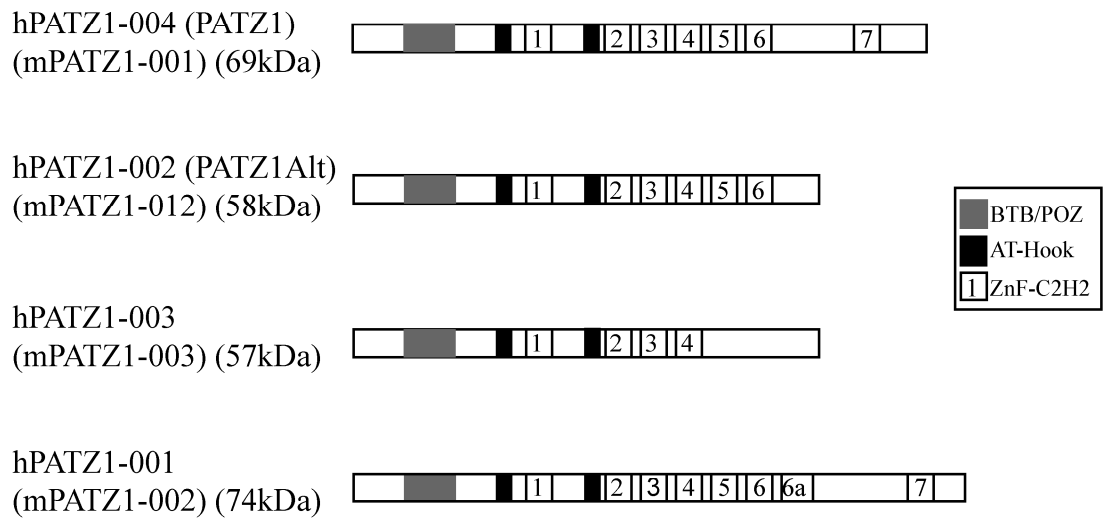
Cell proliferation was measured continuously with an RTCA DP system (ACEA Biosciences, San Diego), by seeding 10 000 cells in each well of an E-Plate VIEW 16 tissue culture plates (10 000 cells/150 μ L) on the XCelligence station in 5%CO₂ and 37°C incubator. 24 hours after seeding, doxorubicin was added in 50 μ L with a final concentration of 1000 nM, 330 nM, 110nM, 37nM, 12nM and 4nM in different wells. Cell index measurements were taken from the beginning (20 minutes after the seeding) and every 15 minutes for up to 120 hours. Medium only wells were also included in the monitoring as a negative control of the experiment. The experiments were performed as triplicates. The results were analyzed by RTCA 2.0 software.

4. RESULTS

4.1 Subcellular Localization of p53 and PATZ1 Proteins

In order to find the subcellular localization of p53 and PATZ1 proteins, we extracted the cytoplasm and the nucleus of human colon carcinoma cell line, HCT116 wild type or p53^{-/-} cells. We treated the cells with DNA damaging, genotoxic drug doxorubicin. 8 hours after treatment we performed cytoplasmic and nuclear lysis and the lysates separated on acrylamide gels were immunoblotted with anti-PATZ1 and anti-p53 antibodies in a western blot experiment. As shown in figure 4.1B cytoplasmic and nuclear lysate fractions from HCT116 WT or HCT116 p53^{-/-} cells treated (or not) with 1 μ M doxorubicin for 8 hours revealed the presence of PATZ1 and PATZ1Alt variants in the nuclear fraction (top row). Same lysates blotted with anti-p53 (bottom row) revealed low levels of p53 before DNA damage (lanes 1, 5) and induced levels after DNA damage induced by doxorubicin treatment (lanes 2, 6) both in the cytoplasmic and nuclear fraction. In figure 4.1B, it is clearly seen that PATZ1 is a nuclear protein while p53 is present both in the cytoplasm and nucleus. Although, doxorubicin treatment dramatically increased the levels of cellular p53 both in cytoplasm and nucleus, the localization of the PATZ1 and PATZ1Alt transcription factors were predominantly nuclear, independent of doxorubicin treatment.

A



B

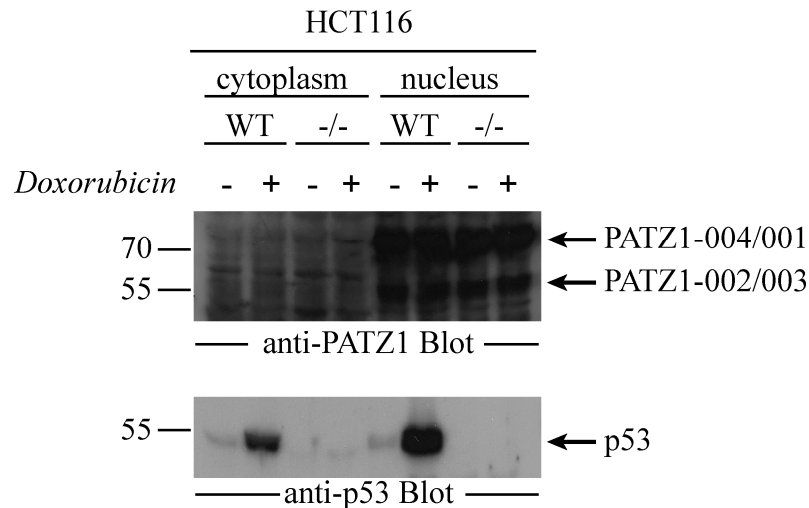


Figure 4.1 Expression patterns of PATZ1 and p53 before and after DNA damage induced by doxorubicin. A) Schematic representation of PATZ1 and its alternatively spliced variants. Grey boxes represent the protein-protein interaction BTB/POZ domain, black boxes represent the DNA binding AT-hook domains and numbered boxes represent the zinc finger motifs. The name and expected molecular size of the PATZ1 isoforms are indicated on the left. B) Cytoplasmic and nuclear fractionation of HCT116WT and p53^{-/-} cells before and after DNA damage for p53 and PATZ1 expression.

4.2 The Effect Of PATZ1 In The Subcellular Translocation Of p53

In normal unstressed cells, endogenous p53 was localized both in the cytoplasm and in the nucleus which is shown in figure 4.1. We wanted to test the effect of doxorubicin treatment on p53 localization and the effect of PATZ1 protein if there would be a change in the localization of p53. Therefore, we transfected HCT116 p53^{-/-} cells with a p53-GFP fusion plasmid (map is shown in appendix figure D.13) alone or with HA-PATZ1. 40 hours after transfection, we treated the transfected cells with doxorubicin for 8 hours. In figure 4.2, DAPI reveals the nucleus of the cells and GFP fluorescence shows the localization of the p53-GFP fusion protein. In the absence of DNA damage, p53-GFP fusion protein is mostly in the cytoplasm. Upon DNA damage induced by doxorubicin, all the p53-GFP fusion protein translocates to the nucleus. However, HA-PATZ1 overexpression did not have any significant effect on p53-GFP localization in either doxorubicin treatment or no treatment conditions.

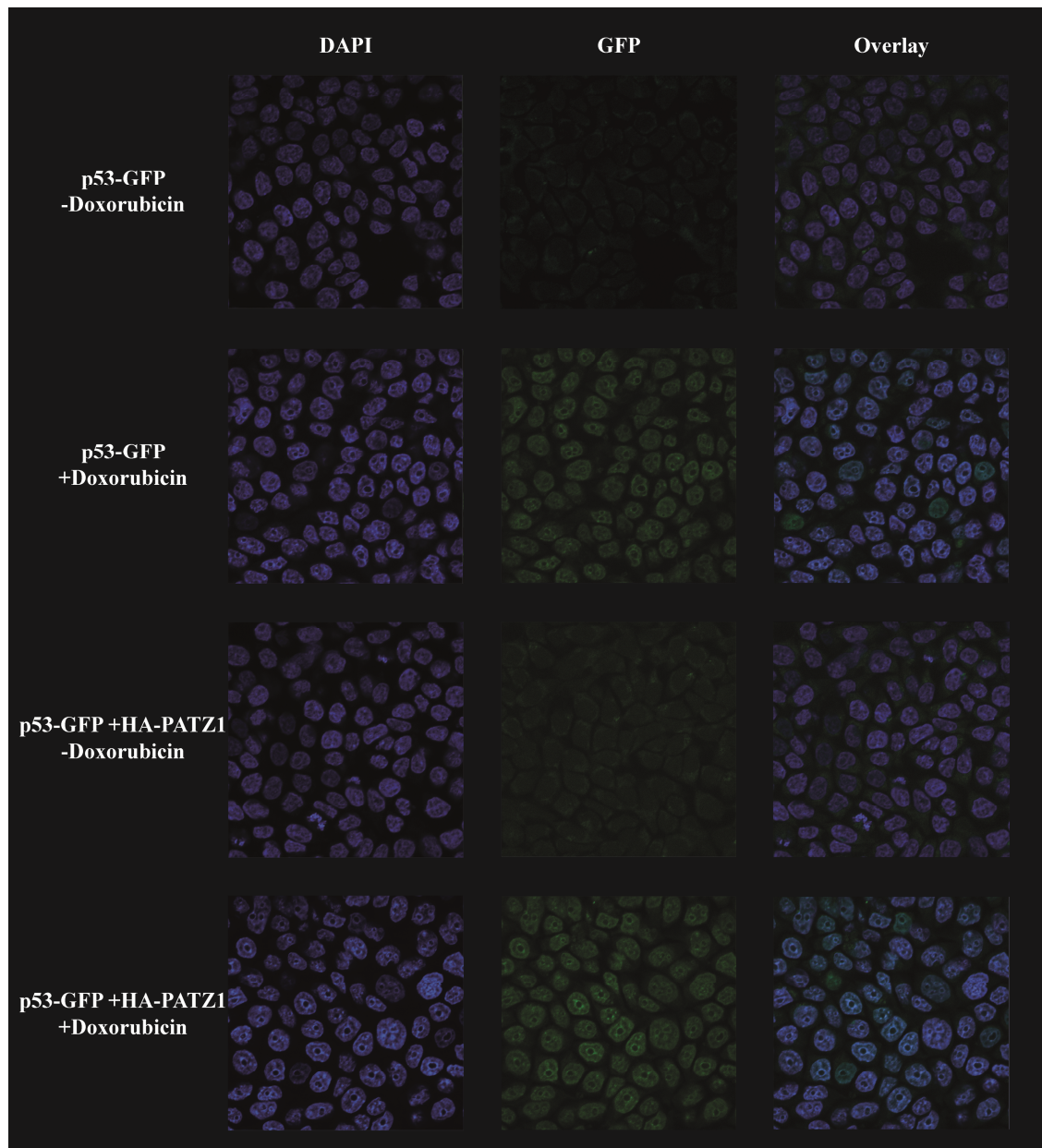


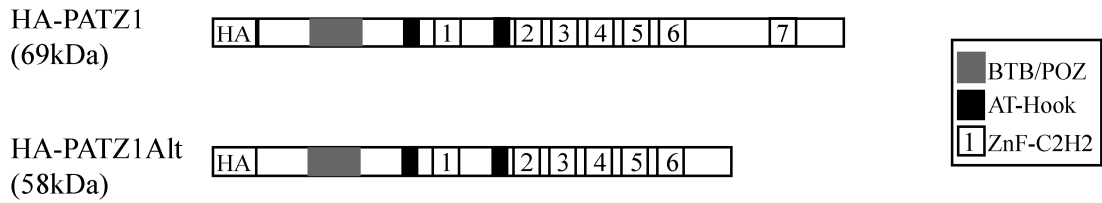
Figure 4.2 Confocal microscopy images p53-GFP transfected HCT116 p53^{-/-} cells before and after DNA damage induced by doxorubicin treatment in the presence or absence of HA-PATZ1. DAPI staining shows the nucleus of the cells, GFP shows the overexpressed p53-GFP protein. The images are taken with Zeiss LSM710 Confocal Microscope with 63X magnification.

4.3 The Interaction of Overexpressed p53 and PATZ1 Proteins

A recent study reported the association of p53 with PATZ1 in HEK293 cells¹⁵². In order to confirm the physical interaction of p53 and PATZ1 proteins in other cells, we overexpressed FLAG epitope tagged p53 protein and HA epitope tagged PATZ1 or PATZ1Alt protein isoforms in HCT116 p53^{-/-} cells which lack endogenous p53. To overexpress epitope tagged proteins, we transfected HCT116 p53^{-/-} cells with plasmids encoding FLAG-p53 (pCMV-FLAG-p53, shown in appendix figure D.12) and HA-PATZ1 (pCMV-HA-PATZ1 shown in appendix figure D.2) or HA-PATZ1Alt (pCMV-HA-PATZ1Alt shown in appendix figure D.3). 48 hours after transfection, cells were lysed and lysates were immunoprecipitated with anti-FLAG antibody conjugated sepharose beads. Immunoprecipitates or whole cell lysates were separated on acrylamide gels and were immunoblotted with anti-HA-HRP antibodies in a western blot experiment.

The schematic representation of HA epitope tagged PATZ1 and PATZ1Alt alternative splice variants are shown in figure 4.3A. The only difference between the PATZ1 and PATZ1Alt protein is after the 6th zinc finger motif in their DNA binding domains. In this experiment anti-FLAG immunoprecipitation of the lysates brought down all proteins associated with FLAG epitope tagged p53 and anti-HA western blotting revealed the presence of PATZ1 in these immunoprecipitates. In figure 4.3B, anti-FLAG immunoprecipitation followed by anti-HA western blot shows the presence of HA-PATZ1 (lane 1) but not HA-PATZ1Alt (lane2) in transfected HCT116 p53^{-/-} cells. Binding is specific as no co-immunoprecipitation is evident in lysates lacking HA-PATZ1 (lane 5) or FLAG-p53 (lane 3). Lysates of transfected cells show that HA-PATZ1 and HA-PATZ1Alt (middle row) and FLAG-p53 (bottom row) are expressed at equal levels in transfected cells.

A



B

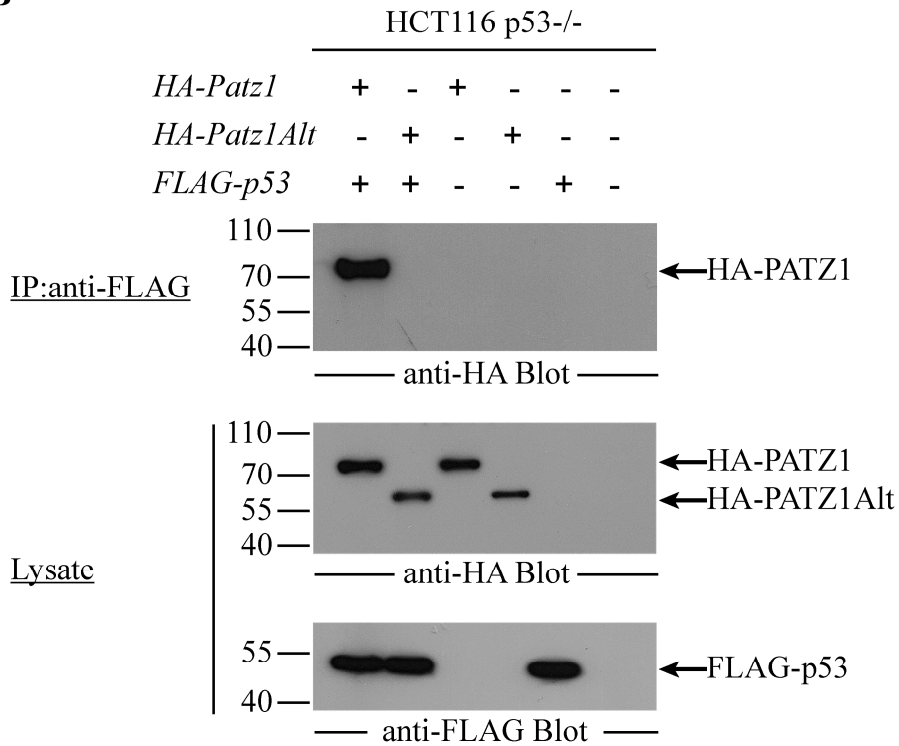


Figure 4.3 FLAG-p53 binds to HA-PATZ1 but not HA-PATZ1Alt. A) Schematic representation of HA-PATZ1 and HA-PATZ1Alt variants. Grey boxes represent the protein-protein interaction BTB/POZ domain, black boxes represent the DNA binding AT hook domains and numbered boxes represent the zinc finger motifs. N-terminal epitope tags are indicated by boxes with HA. The name and expected molecular size of the PATZ1 and PATZ1Alt variants are indicated on the left. B) Anti-FLAG immunoprecipitation and anti-HA western blot to show FLAG-p53 – HA-PATZ1 interaction.

4.4 Domain Requirements for the p53 – PATZ1 Interaction

PATZ1 and PATZ1Alt isoforms share exactly the same N terminal BTB domain but differ after the 6th zinc finger motif in their DNA binding domain. Because p53 could not be immunoprecipitated with PATZ1Alt, we hypothesized that p53 binds to the C terminal region of PATZ1. To test this hypothesis, we created various constructs that encode different truncated forms of the Myc epitope tagged PATZ1 protein shown in figure 4.2A. These truncation mutants encode all of the protein except the C terminal zinc finger domain (Δ ZF), only the N terminal BTB domain (BTB) or all of the protein except for the N terminal BTB domain (Δ BTB). We transfected HCT116 p53^{-/-} cells with plasmids encoding FLAG-p53 (pCMV-FLAG-p53, shown in appendix figure D.12) and Myc-PATZ1 (pcDNA-Myc-PATZ1 shown in appendix figure D.7) or Myc- Δ BTB (pcDNA-Myc-deltaBTB shown in appendix figure D.8) or Myc-BTB (pcDNA-Myc-BTB shown in appendix figure D.9) or Myc- Δ ZF (pcDNA-Myc-deltaZF shown in appendix figure D.10). 48 hours after transfection, we lysed the cells and immunoprecipitated with anti-Myc antibody conjugated sepharose beads. We separated immunoprecipitates or whole cell lysates on acrylamide gels and immunoblotted with anti-FLAG-HRP antibodies in a western blot experiment.

Anti-Myc immunoprecipitation followed by anti-FLAG western blot shows that FLAG-p53 interacts with Myc-PATZ1 (lane 1) and Myc- Δ BTB (lane 3) but not Myc-BTB (lane 2) or Myc- Δ ZF (lane 4) (top row). Binding is specific as no co-immunoprecipitation is evident in lysates lacking FLAG-p53 (lanes 6-9). Lysates of transfected cells show that FLAG-p53 (middle row) and Myc-PATZ1 and its truncations (bottom row) are expressed at equal levels in transfected cells. The interaction of FLAG-p53 with Myc- Δ BTB lacking the N terminal BTB domain and the absence of an interaction with Myc-BTB and Myc- Δ ZF lacking the C terminal DNA binding domain indicate that the C terminal domain of PATZ1 is necessary for the interaction between p53 and PATZ1 proteins.

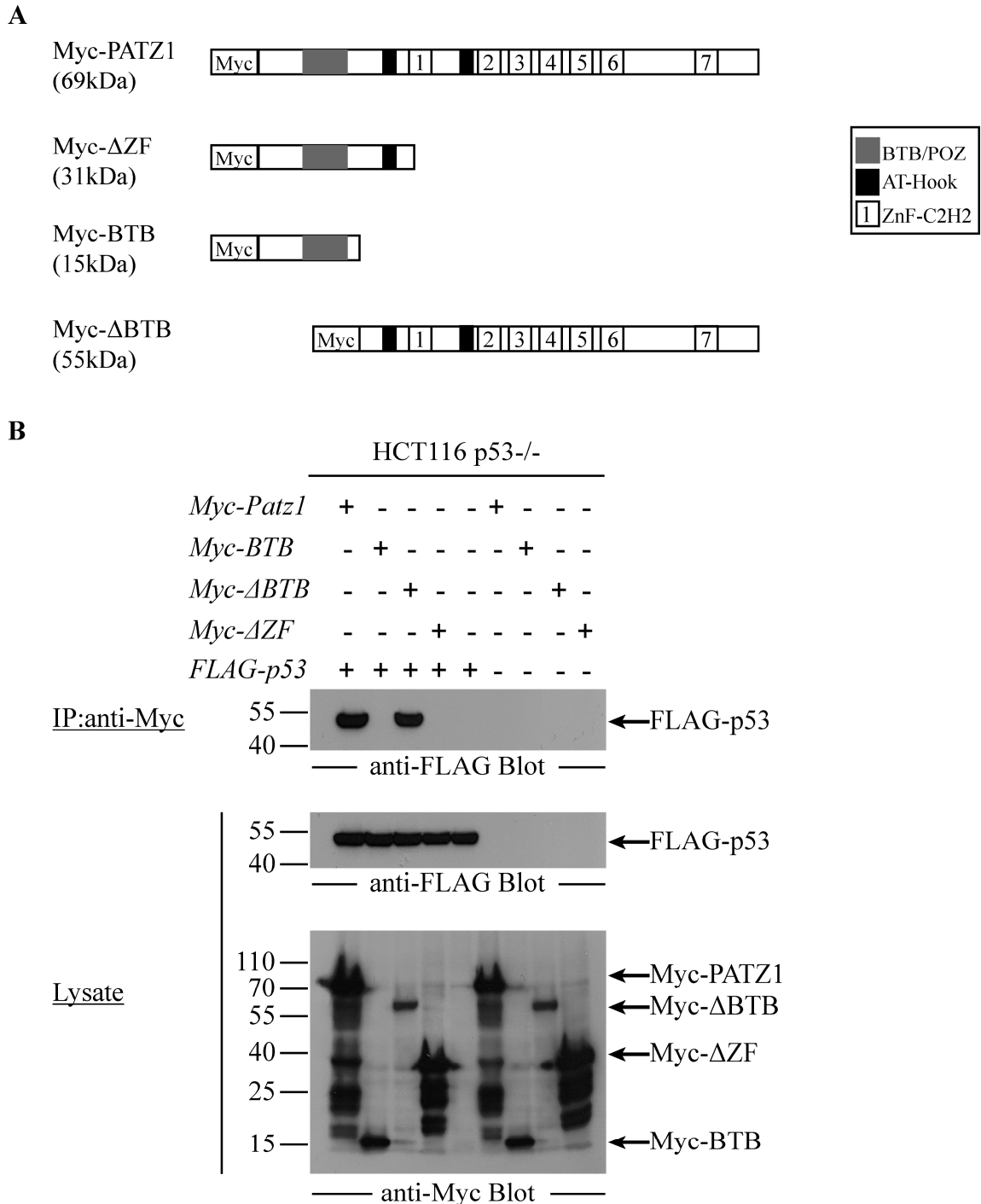


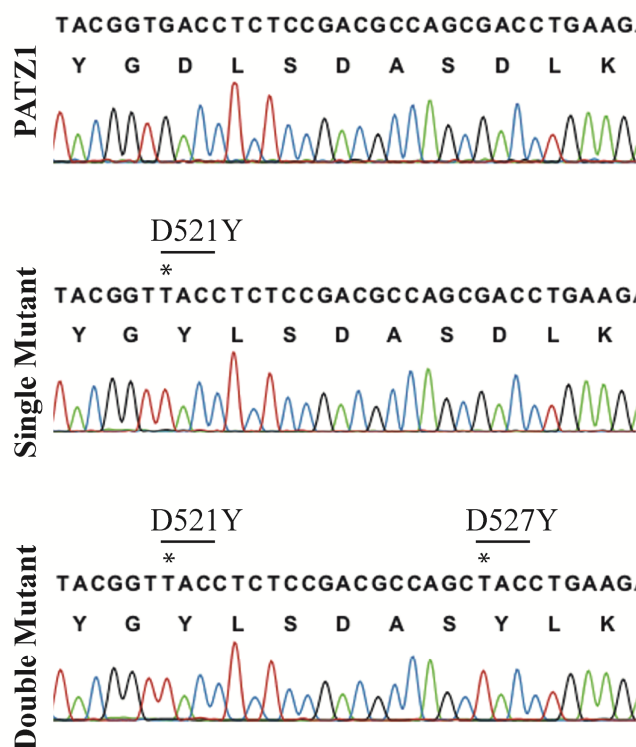
Figure 4.4 C-terminal tail of PATZ1 is required for binding p53. A) Schematic representation of Myc-PATZ1, Myc-ΔZF, Myc-BTB and Myc-ΔBTB truncation forms. Grey boxes represent the protein-protein interaction BTB/POZ domain, black boxes represent the DNA binding AT hook domains and numbered boxes represent the zinc finger motifs. N-terminal epitope tags are indicated by boxes with Myc. The name and expected molecular size of the full length PATZ1 and truncated proteins are indicated on the left. B) Anti-Myc immunoprecipitation and anti-HA western blot to show the interaction between FLAG-p53 – and Myc-PATZ1 or Myc epitope tagged truncations.

4.5 Amino Acids of PATZ1 Necessary for the p53 – PATZ1 Interaction

In order to narrow down the p53 – PATZ1 interaction region to a domain between the 6th and 7th zinc finger motifs of the PATZ1 protein, we aligned the sequences of this region from PATZ1 proteins of several species. This region which is necessary for the p53 – PATZ1 interaction is highly conserved among many species. We observed that most of the amino acids in this region are bulky and negatively charged. Therefore, we hypothesized that, the negatively charged amino acids form an interaction region for p53 and PATZ1. To test this hypothesis, we generated site directed mutants that substitute the bulky negatively charged amino acids with bulky non-charged amino acids. We surmised that if our hypothesis was correct, the non-charged mutant PATZ1, would not be able to interact with p53. To identify the critical negatively charged amino acids that have a role in this interaction, we created single (D521Y) and double (D521Y/D527Y) site directed mutant versions of the HA-Patz1 cDNA shown in figure 4.5A. We transfected HCT116p53^{-/-} cells with FLAG-p53 and HA-PATZ1 or HA-PATZ1D521Y Single Mutant (SM) or HA-PATZ1D521Y/D527Y Double Mutant (DM) cDNAs (shown in appendix figure D.13, D.2, D.4, D.5, respectively). 48 hours after transfection, transfected cells were lysed and lysates were immunoprecipitated with anti-FLAG sepharose beads. Immunoprecipitates and lysates separated on acrylamide gels were immunoblotted with anti-HA-HRP antibody in a western blot experiment. In this experiment anti-FLAG immunoprecipitation of the lysates brings down all proteins associated with the FLAG epitope tagged p53. Anti-HA western blotting reveals if HA-PATZ1WT or its mutant derivatives are present in these immunoprecipitates. In figure 4.5B, we show that the negatively charged amino acids encoded by codon 521 and 527 of PATZ1 were necessary for the p53 – PATZ1 interaction. In this experiment, anti-FLAG immunoprecipitations from lysates of transfected cells revealed the presence of WT HA-PATZ1 (lane1), albeit only reduced (40%) levels of single mutant HA-PATZ1(D521Y) (lane2) and undetectable double mutant HA-PATZ1(D521Y/D527Y) (lane3). Binding is specific as no co-immunoprecipitation is evident in lysates lacking FLAG-p53 (lanes 5-8). Lysates of transfected cells show that HA-PATZ1 and its

mutants (middle row) and FLAG-p53 (bottom row) are expressed at equal levels in transfected cells.

A



B

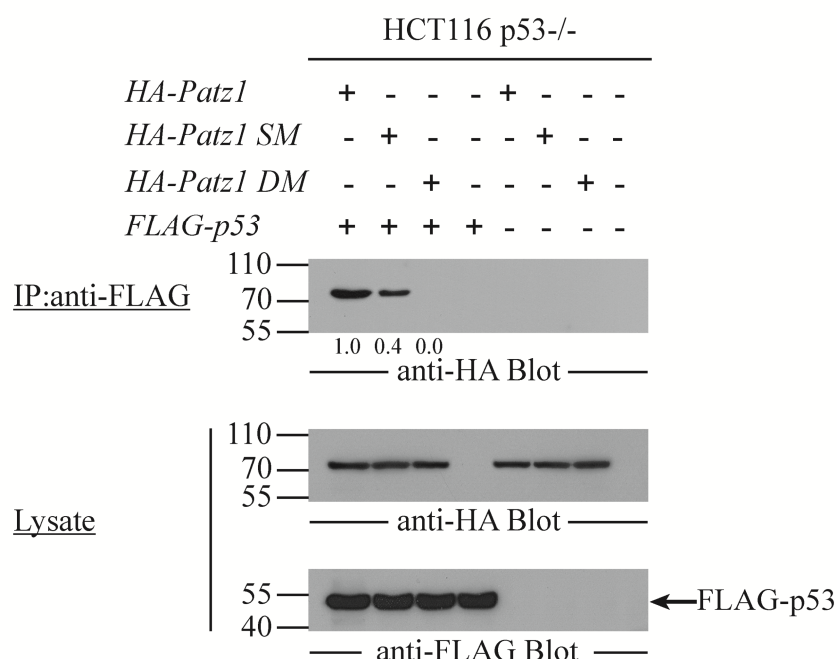


Figure 4.5 Aspartic acids in residue 521 and 527 of PATZ1 protein are necessary for p53 – PATZ1 interaction. A) Sequencing histogram analysis of the HA-Patz1 wild type and mutant constructs. Sequencing histograms indicate the WT codons in Patz1 (top row), the D521Y encoding mutation in single mutant (HA-PATZ SM) (middle row) and the D521Y and D527Y encoding mutations in double mutant (HA-PATZ DM) (bottom row) encoding constructs. B) Anti-FLAG immunoprecipitation and anti-HA western blot to show the interaction between FLAG-p53 – and HA-PATZ1 or mutants.

4.6 DNA Independence of the p53 – PATZ1 Interaction

To investigate the requirements for the interaction between p53 and PATZ1 in detail, we next assessed if this interaction depended on the presence of DNA. We repeated our immunoprecipitations in the presence of two different chemical agents. The first chemical doxorubicin damages DNA *in vivo* and the second, ethidium bromide intercalates into DNA *in vitro*. We transfected HCT116 p53^{-/-} cells with FLAG-p53 and HA-PATZ1 cDNAs. 40 hours after transfection, we treated cells with doxorubicin for 8 hours and lysed the cells and performed anti-HA immunoprecipitation followed by anti-FLAG-HRP western blotting. Figure 4.6 top row, lane 3, demonstrates that the p53 – PATZ1 interaction was stable in cells undergoing DNA damage, as anti-HA immunoprecipitates from cells treated with doxorubicin continued to reveal the presence of FLAG-p53. Next, we treated anti-HA immunoprecipitates from FLAG-p53 and HA-PATZ1 co-transfected HCT116 p53^{-/-} cells with ethidium bromide. Compared to the immunoprecipitated FLAG-p53 from non-treated anti-HA immunoprecipitates, equal amounts were evident in the ethidium bromide treated samples (lane 4). We conclude that the interaction between p53 and PATZ1 is independent of DNA.

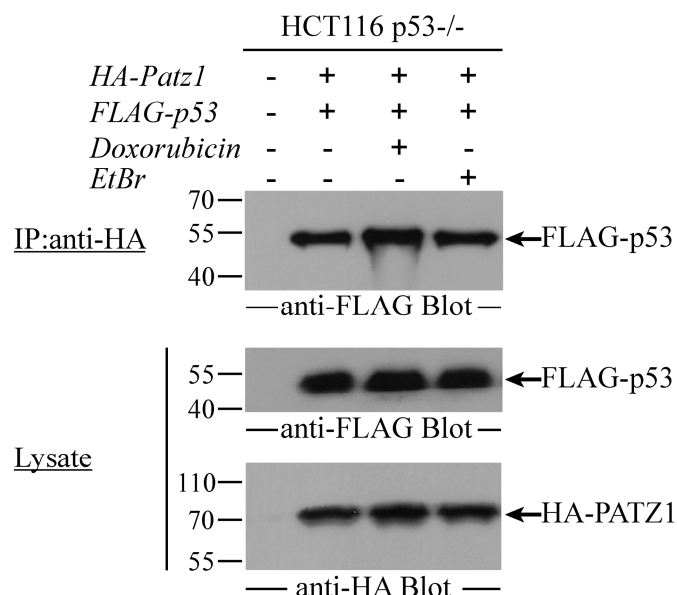


Figure 4.6 Interaction of FLAG-p53 and HA-PATZ1 is independent of DNA. Anti-FLAG immunoprecipitation and anti-HA western blot to show FLAG-p53 – HA-PATZ1 interaction still exists in the presence of doxorubicin and ethidium bromide.

4.7 The Interaction of Endogenous p53 and PATZ1 Proteins

After revealing the nuclear expression of PATZ1 and its alternatively spliced variants, we wanted to confirm the interaction of endogenous p53 and PATZ1 in HCT116 WT cells and also used HCT116p53^{-/-} cells lacking endogenous p53 as a negative control. To this end, we either treated the cells with doxorubicin for 8 hours or left the cells untreated. After treatment, we performed nuclear extraction and immunoprecipitation with anti-p53 antibody conjugated protein A magnetic beads. Immunoprecipitates and nuclear lysates separated on acrylamide gels were immunoblotted with anti-PATZ1 and anti-p53 antibodies in a western blot experiment.

In this experiment anti-p53 immunoprecipitation of the nuclear lysates brings down all proteins associated with the endogenous p53. Anti-PATZ1 western blotting reveals if PATZ1 is present in these immunoprecipitates. In figure 4.7, we showed that anti-p53 immunoprecipitation followed by anti-PATZ1 antibody blotting revealed the presence of PATZ1 and PATZ1Alt in complex with p53, in the absence (lane 1) or presence of doxorubicin treatment (lane 2) from HCT116 WT cells (top row). Binding was specific as immunoprecipitates from HCT116 p53^{-/-} cells (lane 3, 4) did not reveal the presence of PATZ1 or PATZ1Alt. Anti-p53 immunoprecipitation followed by anti-p53 antibody blotting revealed that doxorubicin treatment induced p53 expression, as expected (lane 1,2, middle row). Nuclear lysates of transfected cells showed that PATZ1 and PATZ1Alt proteins were expressed at equal levels (bottom row).

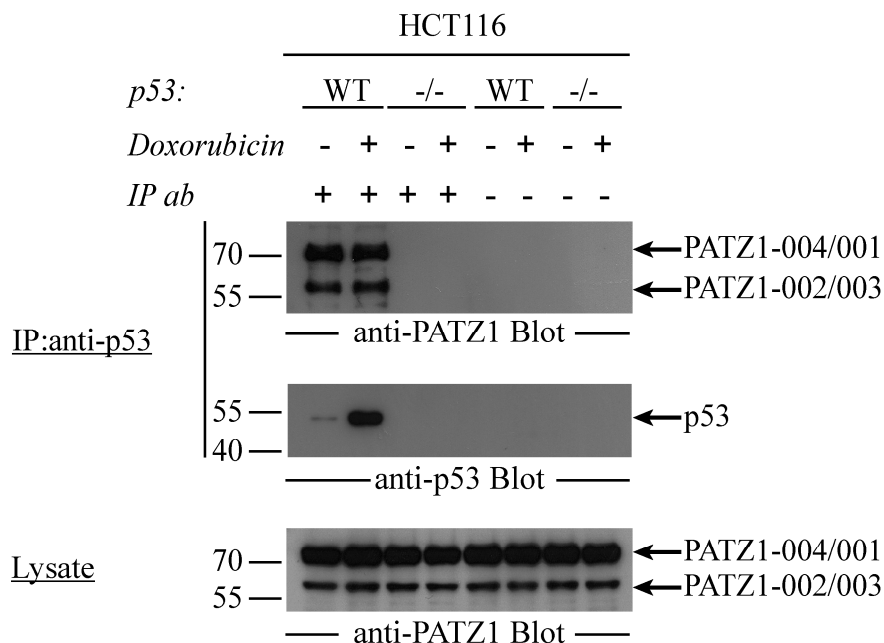


Figure 4.7 Endogenous p53 binds to endogenous PATZ1 in HCT116 cells. Anti-p53 immunoprecipitation and anti-PATZ1 western blot to show endogenous p53 and PATZ1 proteins interact.

4.8 Heterodimerization of PATZ1 and PATZ1Alt Alternative Splice Variants

We found that endogenous p53 and PATZ1 proteins interacted like overexpressed p53 and PATZ1. However, we were surprised to see the endogenous PATZ1Alt isoform in p53 immunoprecipitates, because overexpressed PATZ1Alt had failed to interact with p53. It was previously shown that PATZ1 could form homodimers (Koboashi et al., 2000). Therefore, we hypothesized that PATZ1 could also form heterodimers with PATZ1Alt and this complex would bind to p53. If the hypothesis was correct, PATZ1Alt and p53 could be in the same complex although they did not have a direct interaction. PATZ1 would be protein that would interact with both PATZ1Alt and p53 at the same time and form a complex which would bring PATZ1Alt and p53 together without a direct interaction.

In order to test this hypothesis, we transfected HCT116 p53^{-/-} cells with Myc-Patz1, HA-Patz1Alt and FLAG-p53 cDNAs. 48 hours after transfection, the cells were lysed and nuclear lysates were immunoprecipitated with anti-HA sepharose beads.

Immunoprecipitates and lysates were separated on acrylamide gels and were immunoblotted with anti-Myc-HRP and anti-FLAG-HRP antibodies in a western blot experiment. In figure 4.8, we show that anti-HA immunoprecipitation followed by anti-Myc antibody blotting revealed the presence of Myc-PATZ1 and HA-PATZ1Alt complex (lane 1,3 top row). On the other hand, anti-HA immunoprecipitation followed by anti-FLAG antibody blotting revealed the presence of HA-PATZ1Alt and FLAG-p53 complex only in the presence of Myc-PATZ1 (lane 1 second row). Nuclear lysates of transfected HCT116 p53^{-/-} cells blotted with anti-Myc, anti-HA and anti-FLAG antibodies showed that Myc-PATZ1, HA-PATZ1Alt and FLAG-p53 proteins were expressed at equal levels (bottom three rows). Thus, this experiment reveals the reason behind the difference of overexpressed and endogenous PATZ1Alt isoform binding to p53. PATZ1Alt could heterodimerize with full length PATZ1 protein and indirectly be co-immunoprecipitated with p53 in a three molecule complex.

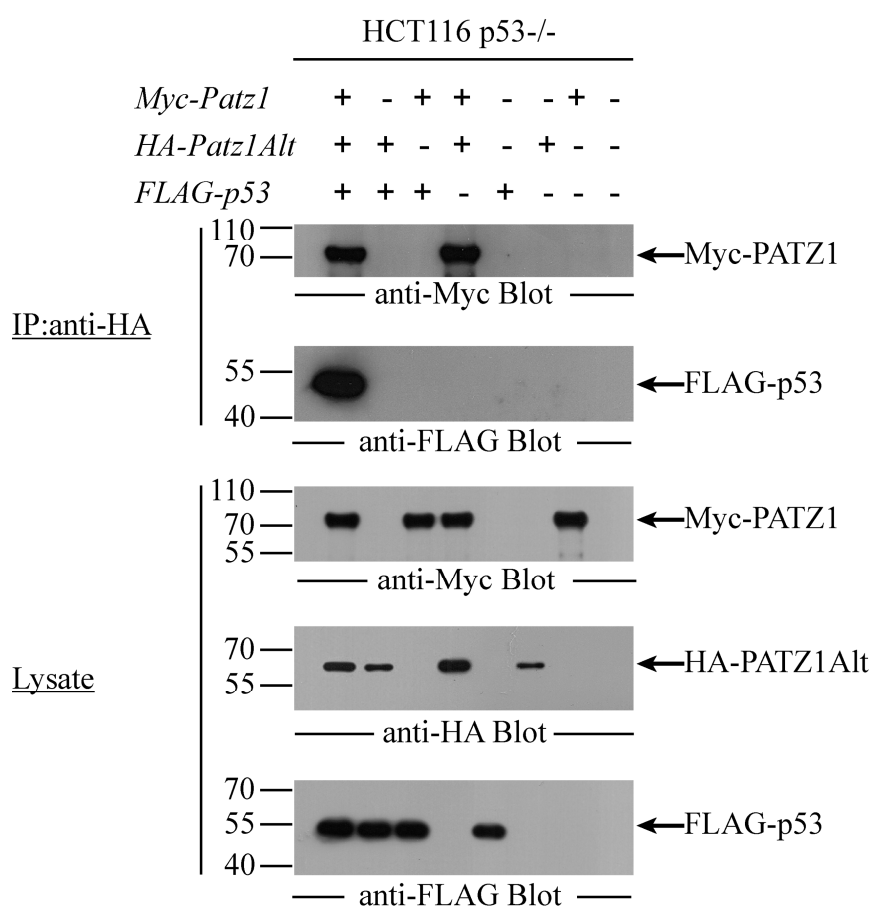


Figure 4.8 PATZ1Alt can interact with p53 only in the presence of PATZ1. Anti-HA immunoprecipitation - anti-Myc western blot to show Myc-PATZ1 and HA-PATZ1Alt heterodimerize and anti-HA immunoprecipitation – anti-FLAG western blot to show the interaction of HA-PATZ1Alt with FLAG-p53 only in the presence of Myc-PATZ1

4.9 Domain Requirements for the PATZ1 – PATZ1Alt Heterodimerization

As we found out that PATZ1 and PATZ1Alt alternatively spliced variants could heterodimerize, we wanted to further characterize this heterodimerization by identifying the domain requirements for the heterodimer between the PATZ1 and PATZ1Alt isoforms. Therefore, we co-transfected HCT116 cells with HA-Patz1Alt and Myc-Patz1 full length or Myc epitope tagged truncations (Myc- Δ BTB, Myc-BTB and Myc- Δ ZF). The schematic representation of the Myc epitope tagged full length protein and the truncations were shown in Figure 4.4. 48 hours after transfection, the cells were lysed and nuclear lysates were immunoprecipitated with anti-Myc sepharose beads. Immunoprecipitates and nuclear lysates were separated on acrylamide gels and were immunoblotted with anti-HA-HRP antibody in a western blot experiment. In this experiment anti-Myc immunoprecipitation of the nuclear lysates brings down all proteins associated with the HA-PATZ1Alt. In figure 4.9, we identified that anti-Myc immunoprecipitation followed by anti-HA antibody blotting revealed the presence of the Myc-PATZ1 and HA-PATZ1Alt complex only in cells expressing BTB containing Myc-PATZ1 proteins (lane 1,2 and 4, top row). Myc- Δ BTB could not bind to HA-PATZ1Alt (lane 3, top row). Lysates of transfected HCT116 cells blotted with anti-HA and anti-Myc antibodies showed that full length PATZ1, truncation variants of PATZ1 and PATZ1Alt proteins were expressed at equal levels (bottom two rows).

As we have shown that anti-Myc immunoprecipitates from nuclear lysates of transfected cells revealed the presence of all truncated PATZ1 variants except the truncation lacking the BTB domain and in fact, the BTB domain by itself was sufficient to heterodimerize with the PATZ1Alt protein, we concluded that the BTB domain of PATZ1 and PATZ1Alt proteins is the region necessary for heterodimerization of these variants.

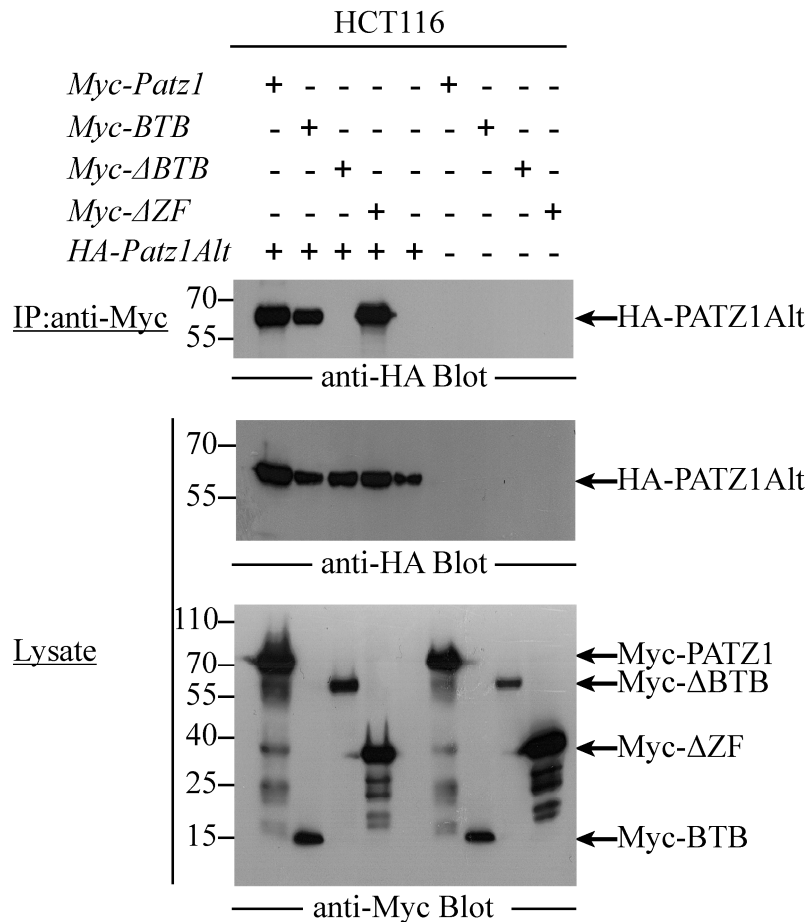


Figure 4.9 The BTB domain of PATZ1 and PATZ1Alt proteins is necessary for heterodimerization of the alternative splice variants. Anti-Myc immunoprecipitation and anti-HA western blot to show the interaction of HA-PATZ1Alt and Myc-PATZ1 is lost when the BTB domain of PATZ1 is truncated.

4.10 The Interaction of the Δ40p53 Isoform with PATZ1

In order to assess if other isoforms of p53 can also interact with PATZ1, we repeated the endogenous anti-p53 immunoprecipitation followed by anti-PATZ1 western blot using a different p53 antibody that can detect the Δ40p53 isoform in addition to the full length p53 protein. Therefore, we treated HCT116 WT and p53^{-/-} cells with Doxorubicin for 8 hours. After treatment, we performed nuclear extraction and immunoprecipitation with protein A magnetic beads which are conjugated with a different p53 antibody that can detect the other p53 isoforms. Immunoprecipitates and nuclear lysates separated on acrylamide gels were immunoblotted with anti-PATZ1 and

anti-p53 antibodies in a western blot experiment. In this experiment anti-p53 immunoprecipitation of the nuclear lysates brings down all proteins associated with the endogenous p53 and its isoforms. Anti-PATZ1 western blotting reveals if PATZ1 is present in these immunoprecipitates. In figure 4.10, we show that anti-p53 immunoprecipitation followed by anti-PATZ1 antibody blotting revealed the presence of PATZ1 and PATZ1Alt in complex with p53, in the absence (lane 1) or presence of doxorubicin treatment (lane 2) from HCT116 WT cells (top row). Anti-p53 immunoprecipitation followed by anti-p53 antibody blotting revealed that doxorubicin treatment induced p53 expression, as expected (lane 1,2, middle row). On the other hand $\Delta 40$ p53 is expressed much higher levels in HCT116 p53^{-/-} cells than in HCT116WT cells (lane1,3, middle row). Unlike p53, the protein levels of $\Delta 40$ p53 are not affected by DNA damage induced by doxorubicin. (lane 3,4, middle row). Anti-p53 immunoprecipitation followed by anti-PATZ1 antibody blotting revealed the presence of PATZ1 and PATZ1Alt in complex with $\Delta 40$ p53, only in the presence of doxorubicin treatment from HCT116 p53^{-/-} cells (lane4, top row). Nuclear lysates of transfected cells showed that PATZ1 and PATZ1Alt proteins were expressed at equal levels (bottom row). Therefore, we concluded that in addition to full length p53, the $\Delta 40$ p53 isoform which lacks the first 40 amino acids, can bind to PATZ1. Although the p53 – PATZ1 interaction was seen in either absence or presence of the DNA damaging agent, doxorubicin, the $\Delta 40$ p53 isoform – PATZ1 interaction was evident only upon doxorubicin treatment.

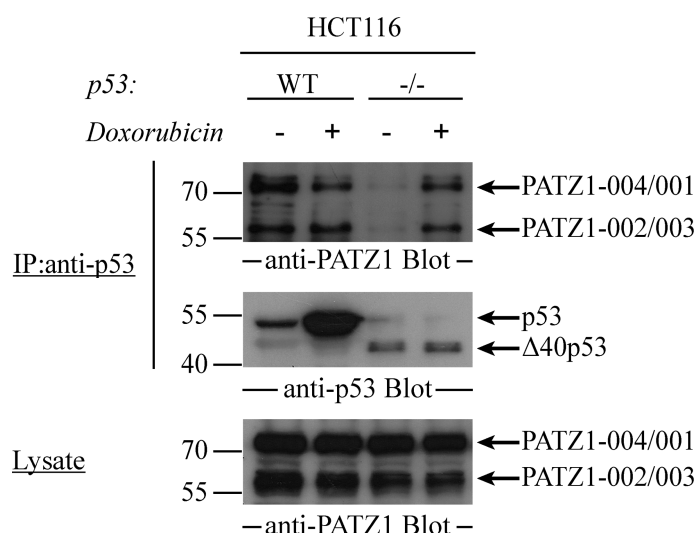


Figure 4.10 $\Delta 40$ p53 isoform of p53 binds to PATZ1 upon doxorubicin treatment in HCT116 cells. Anti-p53 immunoprecipitation and anti-PATZ1 western blot to show the interaction of endogenous PATZ1 and p53 or $\Delta 40$ p53 isoform in the presence or absence of doxorubicin.

4.11 Construction of a mPATZ1-002-IRES-Cherry Plasmid

PATZ1 protein has 4 alternative splice variants with a molecular weight of 69kDa [PATZ1 (hPATZ1-004/mPATZ1-001)], 58kDa [PATZ1Alt (hPATZ1-002/mPATZ1-012)], 74kDa [hPATZ1-001/mPATZ1-002] and 57kDa [hPATZ1-003/mPATZ1-003]. It is not possible to differentiate between the 57 and 58 kDa alternative splice variants by SDS-PAGE. Although it is also difficult to discriminate between the 74 and 69kDa proteins, we decided to generate a cDNA expression construct for the 74kDa hPATZ1-001/mPATZ1-002 variant to compare its properties to the 69kDa hPATZ1-004/mPATZ1-001 cDNA expression construct. The mPATZ1 cDNA is encoded in the HA-PATZ1 plasmid shown in appendix figure D.2. The 5' and 3' cDNA sequences of the PATZ1 and 74kDa mPATZ1-002 variants are exactly the same. However, the 74kDa mPATZ1-002 variant has an additional zinc finger motif, 6a between the 6th and 7th zinc finger motifs. Hence, we decided to amplify the 5' and 3' regions of the mPATZ1-002 cDNA from the HA-PATZ1 plasmid and the 6a zinc finger motif from the genomic DNA of RLM11 cells which are mouse CD4 single positive T lymphocytes expressing PATZ1. Therefore, we planned to have three amplified PCR constructs: F1 (5' cDNA sequence upto zinc finger 6a), F2 (sequence of zinc finger 6a) and F3 (from zinc finger 6a to the end of the 3' cDNA sequence). These fragments have overlapping regions in order to assemble and form the complete mPATZ1-002 cDNA sequence.

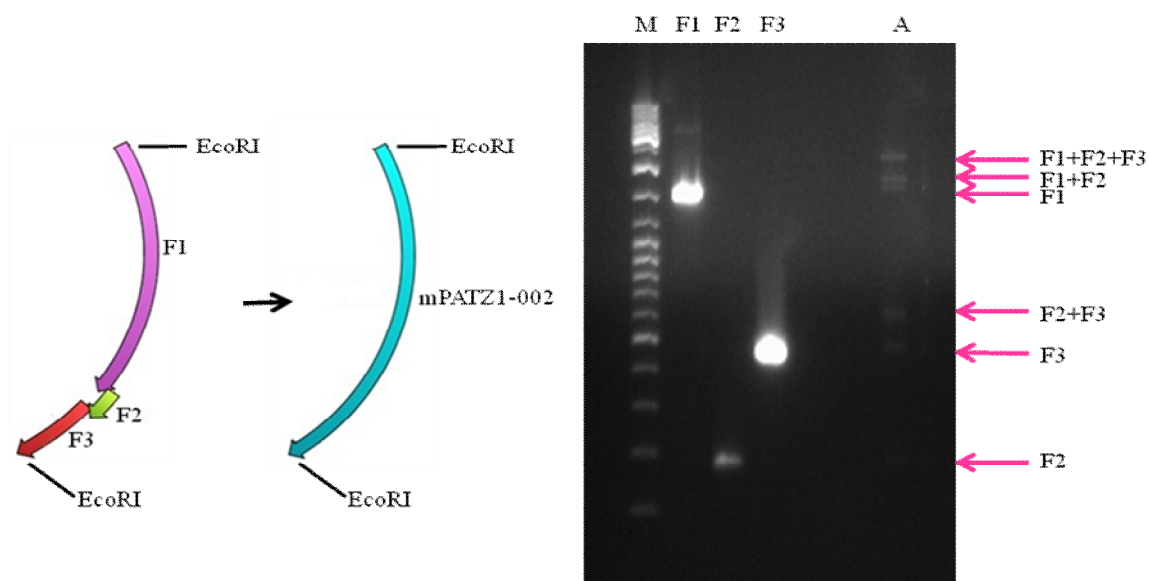


Figure 4.11 PCR amplification and assembly of three fragments for construction of mPATZ1-002 cDNA. M symbolizes DNA marker, F1 symbolizes fragment 1, F2 symbolizes fragment 2, F3 symbolizes fragment 3 and A symbolizes assembly of the three fragments.

After individually PCR amplifying the three fragments, we assembled them to construct the complete cDNA sequence of mPATZ1-002 and reamplified these fragments. We cloned the mPATZ1-002 construct into the pMIGII-IRES-Cherry mammalian expression plasmid through the single EcoRI restriction site. The mPATZ1-002 cDNA was flanked with EcoRI sites at the both ends during PCR. After purification steps followed by EcoRI restriction digestion of the vector, pMIGII-IRES-Cherry and the insert, mPATZ1-002, we performed a ligation and obtained the mPATZ1-002-IRES Cherry expression plasmid.

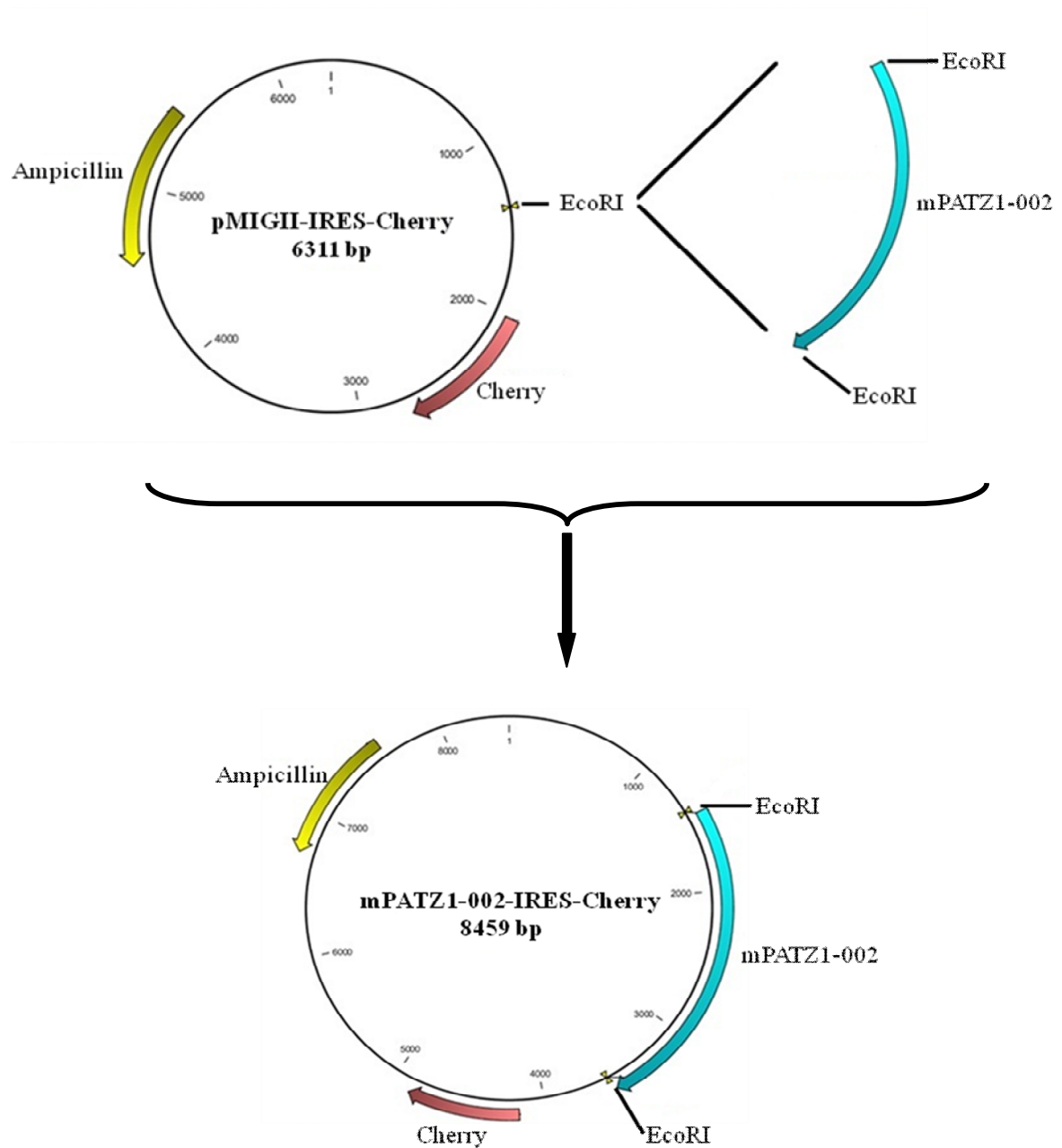


Figure 4.12 Ligation of mPATZ1-002 into the pMIGII-IRES-Cherry plasmid. Schematic representation of cloning of the mPATZ1-002 into pMIG-II IRES-Cherry plasmid.

We extracted DNA from the colonies containing ligated plasmid and confirmed the ligation by restriction digestion. Due to having **EcoRI** at the both ends of the sequence, mPATZ1-002 could be inserted either in the correct or wrong orientation. Therefore, we decided to use the **XhoI** restriction site for the confirmation digestion because both the vector and the insert have only one **XhoI** site each and **XhoI** site in the insert is very close to the end of the insert. Therefore, the band sizes after **XhoI**

restriction site would not only confirm the success of the ligation but also its orientation. If the ligation is in the correct orientation we expect to see 750 and 7709bp bands whereas if it is in the reverse orientation we expect to see 1337 and 7322bp bands. We screened 20 colonies after the ligation and 5 of them were in the correct orientation (colony 2,6,10,18 and 20).

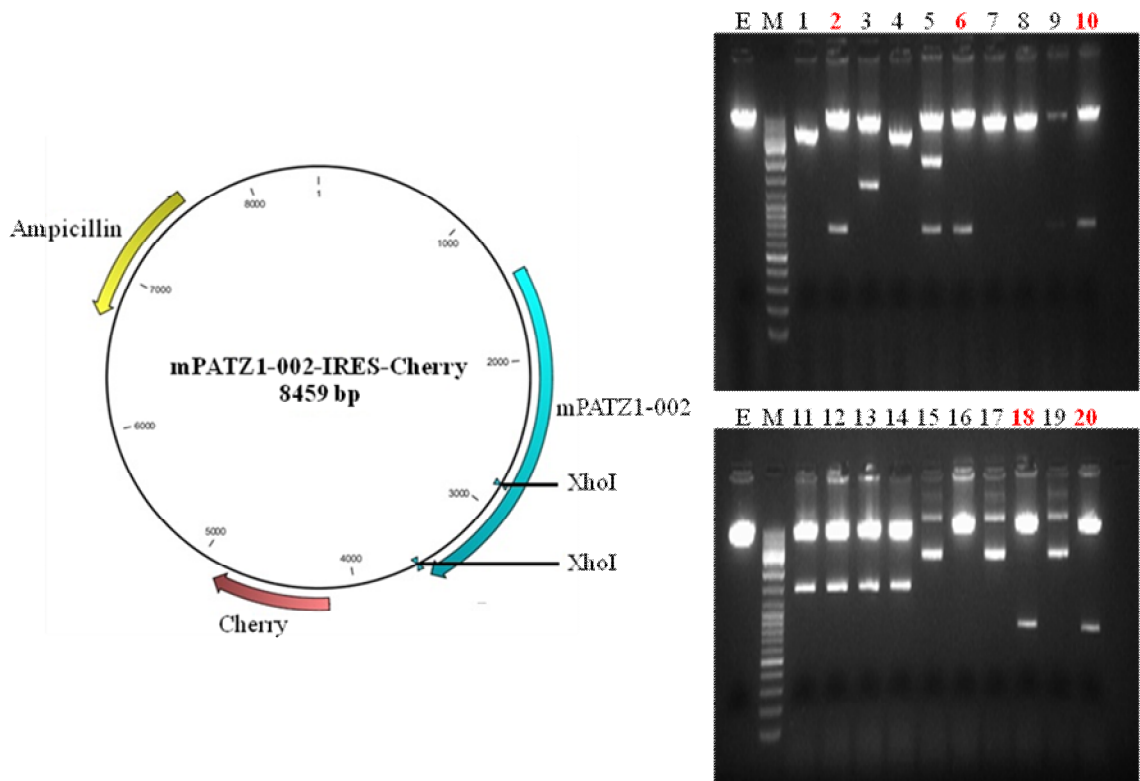


Figure 4.13 Conformation digestion of the mPATZ1-002-IRES-Cherry ligation. The ligation is confirmed with Xho I restriction digestion. Upon XhoI restriction digestion, colonies that have the empty vector should generate a linearized 8459 bp band, colonies that have the insert in the correct orientation should generate two bands of 750 and 7709bp and colonies that have the insert in the wrong orientation should generate two bands of 1337 and 7322bp.

4.12 The Effect of the p53 – PATZ1 Interaction on p53 – DNA Binding in EMSA Assays

Both p53 and PATZ1 are transcription factors which interact with DNA using their DNA binding domains. In order to further analyze the p53 and PATZ1 interaction, we wanted to examine the effect of this interaction on the ability of p53 DNA binding. For this purpose, we performed electro mobility shift assays (EMSA) with a consensus p53 binding site and overexpressed FLAG epitope tagged p53 protein. We transfected HCT116 p53^{-/-} cells with FLAG-p53 with or without HA-Patz1 cDNA. 48 hours after transfection, we lysed the cells and incubated the nuclear lysates with biotinylated p53 probes in the presence or absence of non-biotinylated (cold) probes. The incubated samples were then loaded onto non-denaturing acrylamide DNA gels and immunoblotted with Streptavidin-HRP antibodies. In figure 4.14, the free biotinylated probe (lane 1) was shifted after the FLAG-p53 binding (lane2). This binding was specific because the addition of 200 fold excess non-biotinylated cold probe reduced the shift of biotinylated probe which resulted in more free biotinylated probe (lane3). However, we could not observe any significant changes in the FLAG-p53 – biotinylated probe interaction in the presence of HA-PATZ1 (lane 4).

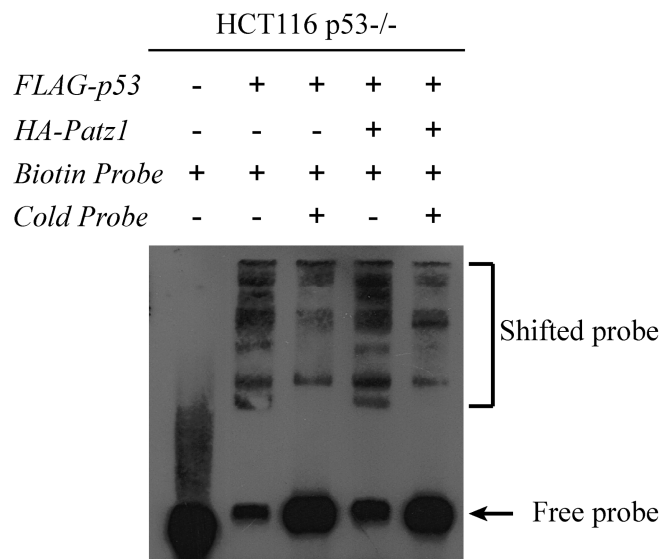


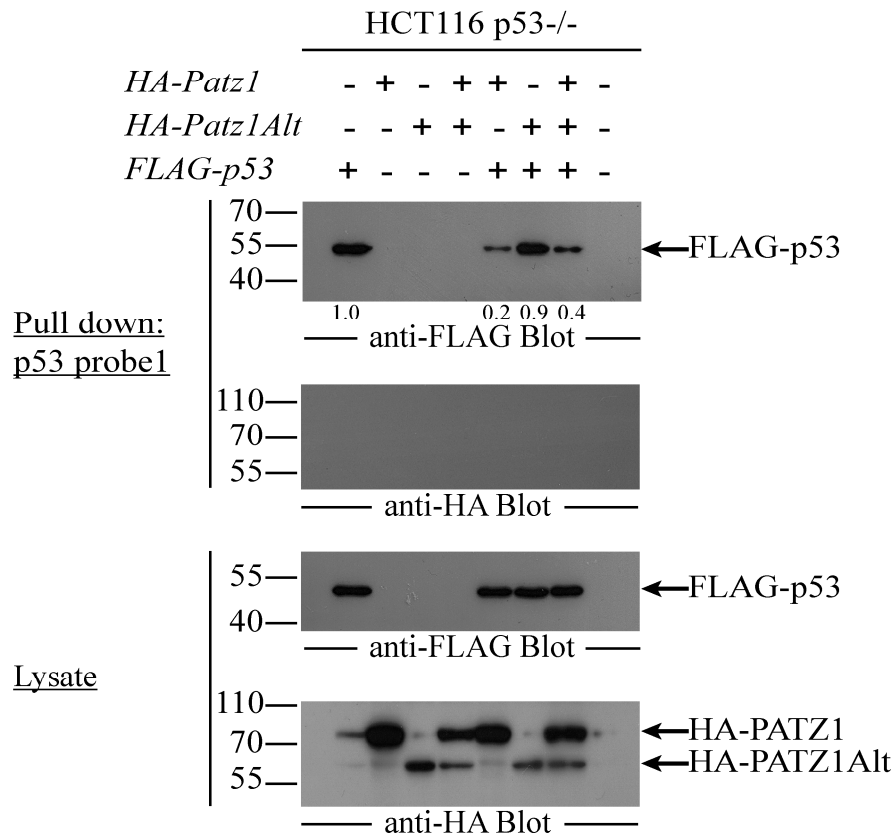
Figure 4.14 EMSA assay for p53-DNA binding. Electro mobility shift assay is performed with a consensus p53 binding site and overexpressed FLAG epitope tagged p53 protein. Free probes and shifted probes are indicated on the right.

4.13 The Effect of the p53 – PATZ1 Interaction on p53 – DNA Binding in Pull Down Assays

4.13.1 The p53 – PATZ1 Interaction Inhibits p53 – DNA Binding

In EMSA experiments we observed multiple shifted bands which may be obscuring the effect of PATZ1 on p53 DNA binding. These multiple bands result from impurities in the nuclear lysates. Also, it is known that palindrome p53 sequences in EMSA probes could generate higher order DNA structures which could bind multiple p53 proteins¹⁵³. Therefore, we changed our strategy to find the PATZ1 effect on p53-DNA binding. We performed a DNA pull down experiment followed by western blotting which would specifically show the DNA bound form of p53. In this experiment, we overexpressed FLAG-p53 in HCT116 p53^{-/-} cells in the presence or absence of HA-PATZ1 or HA-PATZ1Alt. 48 hours after transfection, we lysed the cells and incubated the nuclear lysate with biotinylated p53 probes. After incubation, the biotinylated probes were captured with streptavidin magnetic beads and anti-FLAG western blot was performed. In figure 4.15A, we demonstrate that PATZ1 inhibited p53 binding to its consensus site. In the absence of PATZ1, p53 could bind to probe 5 fold more (top row, lane 1 and 5). In addition to this, we did not observe any significant changes in p53-DNA binding in the presence of PATZ1Alt which could not bind to p53 (top row, lane 6). Neither HA-PATZ1 nor HA-PATZ1Alt were bound to p53 probes in this experiment (second row). Lysates of transfected cells show that FLAG-p53 (third row) and HA-PATZ1 and HA-PATZ1Alt (bottom row) are expressed at equal levels in transfected cells. Therefore, we concluded that when p53 and PATZ1 were forming a complex together, p53 could not bind to its probe as efficiently as when it was alone. In figure 4.15B, the quantification of the amount of DNA bound p53 from 3 different experiments are shown.

A



B

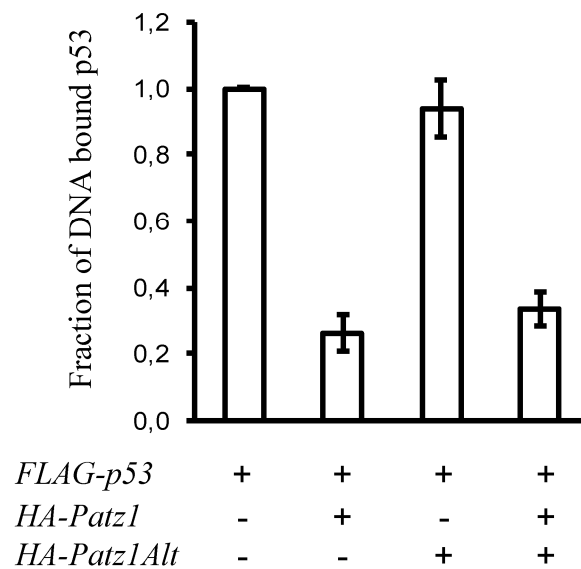
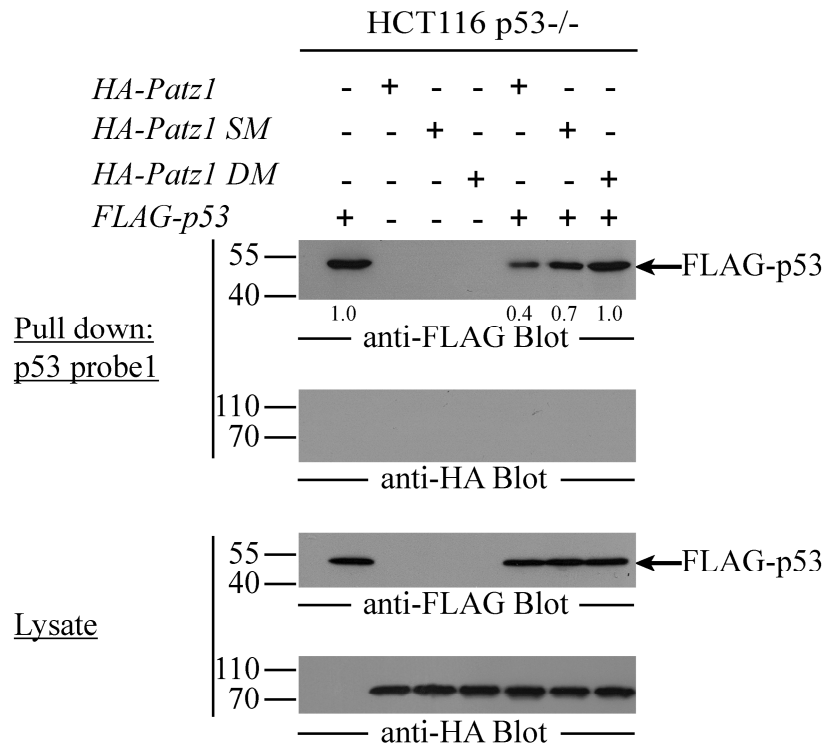


Figure 4.15 p53 – PATZ1 interaction inhibits p53 - DNA interaction. A) DNA pull down assay is performed with biotinylated DNA probes (probe 1; derived from the pG13 p53 reporter) and lysates from HCT116 p53^{-/-} cells transfected with the indicated plasmids B) Quantification of the amount of DNA bound p53 from 3 different experiments

4.13.2 PATZ1 Mutants Cannot Inhibit p53 – DNA Binding

In order to confirm that the inhibition of PATZ1 on p53 – DNA binding, we tested the ability of the PATZ1 site directed mutants that fail to interact with p53 to inhibit p53 DNA binding. In this experiment, we performed the DNA pull down assay by using overexpressed FLAG-p53 with or without single mutant PATZ1 SM (D521Y) or double mutant PATZ1 DM (D521Y/D527Y) in HCT116 p53^{-/-} cells. In figure 4.16A, we demonstrate that single mutant PATZ1 SM which has an impaired interaction with p53 could not prevent p53 DNA binding as effectively as wild type PATZ1 (lane 6) and double mutant PATZ1 DM which has no interaction with p53 has no inhibitory effect on the p53 – DNA interaction (lane 7). In figure 4.16B, the quantification of DNA bound p53 from 3 different experiments are shown. When immunoprecipitation results which show the interactions between p53 and PATZ1 and pull down results which show the effect of the interactions on p53 bound DNA are combined, it is clearly seen that there is an inverse correlation between p53 – PATZ1 and p53 – DNA interactions. The more p53 is bound to PATZ1, the less it binds to DNA. Therefore, we concluded that PATZ1 forms a complex with p53 which prevents p53 to bind to its specific DNA sequence.

A



B

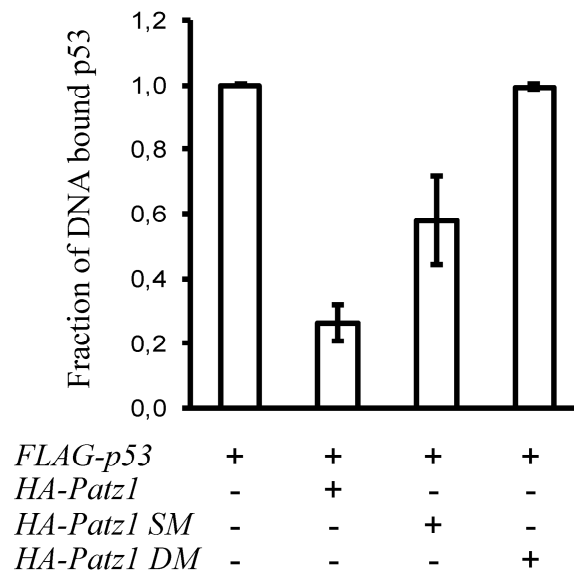


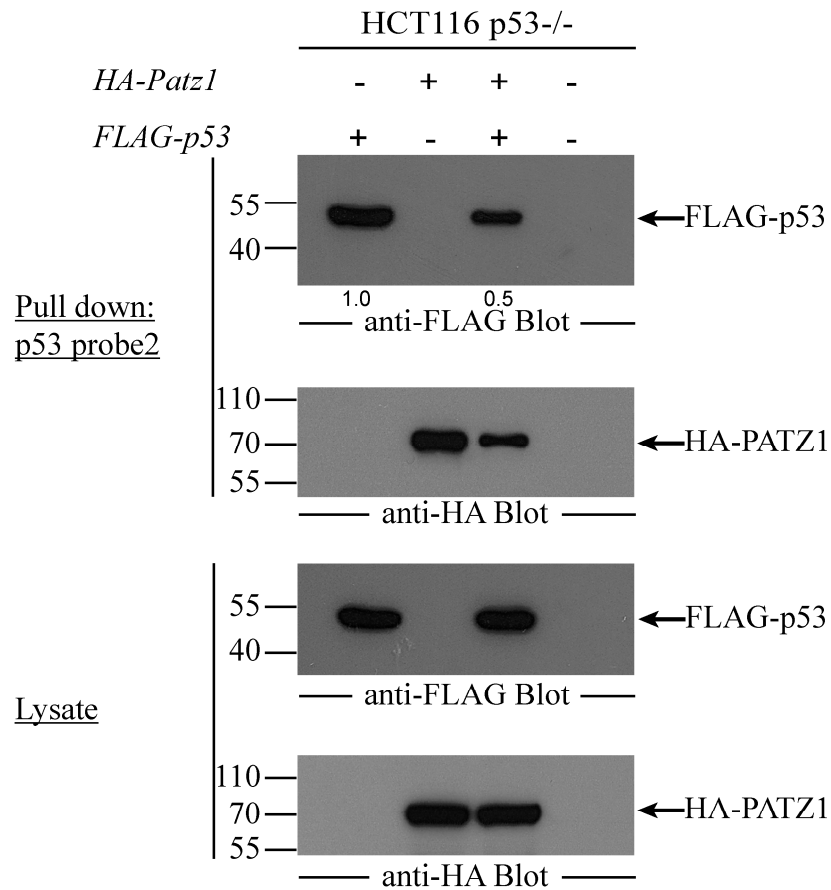
Figure 4.16 PATZ1 mutants that are incapable of interacting with p53 cannot prevent p53 – DNA interaction. A) DNA pull down assay is performed with biotinylated DNA probes (probe 1; derived from the pG13 p53 reporter) specific to the p53 protein and lysates from HCT116 p53^{-/-} cells transfected with the indicated plasmids B) Quantification of the amount of DNA bound p53 from 3 different experiments

4.14 The Inhibitory Effect of the p53 – PATZ1 Interaction on p53 – DNA Binding on Other p53 Targets

In order to determine if the ability of PATZ1 to inhibit p53 – DNA binding could be generalizable to other p53 consensus DNA binding sites, we repeated the DNA pull down assay with a different probe which is derived from the GADD45 gene promoter (probe 2). GADD45 is a known p53 responsive gene whose promoter has a specific p53 binding site. In this experiment, we again incubated the biotinylated probes (probe 2) with nuclear lysates from HCT116 p53^{-/-} cells transfected with FLAG-p53 in the presence or absence of HA-PATZ1 and captured the biotinylated beads with streptavidin magnetic beads. DNA pull down was followed by anti-FLAG or anti-HA western blots.

In figure 4.17A, we show that similar to the previous DNA pull down experiment, the amount of FLAG-p53 binding to DNA is decreased 50% in the presence of HA-PATZ1 (lane 3, top row) compared to the absence of HA-PATZ1 (lane1, top row). Interestingly, HA-PATZ1 could also bind to this DNA probe, as pulled down biotinylated DNA probes obtained from GADD45 promoter revealed HA-PATZ1 upon blotting with anti-HA-HRP antibody (second row). Moreover, DNA bound HA-PATZ1 was significantly decreased in the presence of FLAG-p53 (second row, lane 3) compared to samples only containing HA-PATZ1 (second row, lane 2). The lysates of the transfected cells show that FLAG-p53 (third row) and HA-PATZ1 and HA-PATZ1Alt (bottom row) were expressed at equal levels. In figure 4.17B, the quantification of the DNA bound p53 from 3 different experiments are shown.

A



B

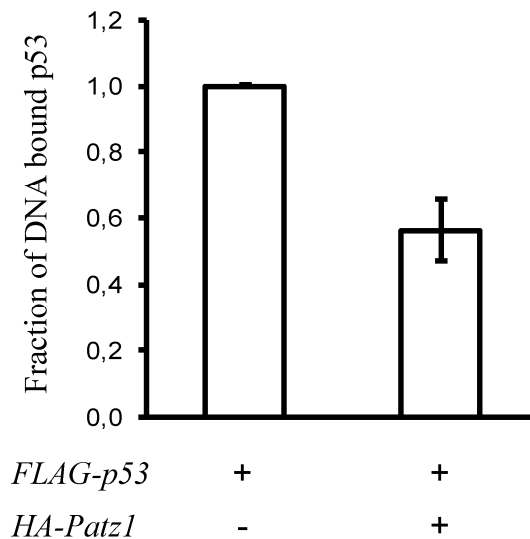


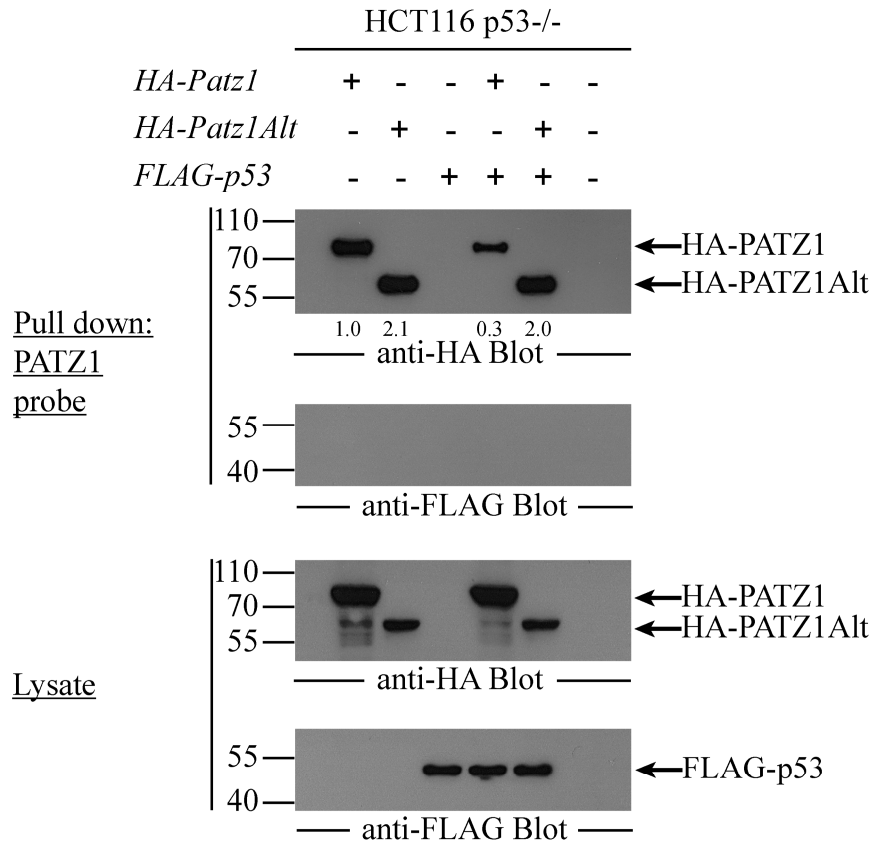
Figure 4.17 The inhibitory effect of PATZ1 in p53 – DNA interaction is valid for a different p53 binding consensus sequence. A) DNA pull down assay is performed with biotinylated DNA probes (probe 2; derived from the GADD45 promoter) specific to the p53 protein and lysates from HCT116 p53^{-/-} cells transfected with the indicated plasmids B) Quantification of the amount of DNA bound p53 from 3 different experiments

4.15 The p53 – PATZ1 Interaction Inhibits PATZ1 – DNA Binding

Up to this point, we checked the effect of the p53 – PATZ1 interaction on the p53 – DNA binding. PATZ1 is also a transcription factor like p53 and specifically binds to DNA. Therefore we next tested the effect of p53 on PATZ1 – DNA binding. In this experiment, we performed a DNA pull down assay with a double stranded biotinylated PATZ1 probe instead of a p53 probe. We incubated, these biotinylated ds DNA probes specific to PATZ1 with HA-PATZ1 or HA-PATZ1Alt overexpressing HCT116 p53^{-/-} nuclear cell lysates. Because PATZ1 and PATZ1Alt share exactly the same DNA binding domain, we expected these proteins to bind the probes with the same specificity. After incubation, the biotinylated probes were captured with streptavidin magnetic beads and anti-HA and anti-FLAG western blots were performed.

In the experiment depicted figure 4.18A, we found that the presence of p53 resulted in a 3 fold inhibition of PATZ1 – DNA binding (top row, lane 4) compared to the PATZ1 alone expressing samples (top row, lane 1). On the other hand, the presence of p53 did not have any significant changes in PATZ1Alt – DNA binding likely because PATZ1Alt and p53 do not interact in the absence of PATZ1 (top row lane 2 and 5). DNA pull down followed by anti-FLAG western blot revealed that FLAG-p53 did not bind to PATZ1 specific probes (second row). Lysates of transfected cells show that FLAG-p53 (third row) and HA-PATZ1 and HA-PATZ1Alt (bottom row) were expressed at equal levels in transfected cells. Surprisingly the amount of PATZ1Alt that can bind these probes in this *in vitro* binding reaction is roughly double of amount of PATZ1 that can bind the same probes. This indicates that the C-terminal domain of PATZ1 is inhibitory to DNA binding. In figure 4.18B, the quantification of DNA bound p53 from 3 different experiments are shown. As a result of this experiment, we concluded that the presence of p53 inhibits PATZ1 – DNA binding.

A



B

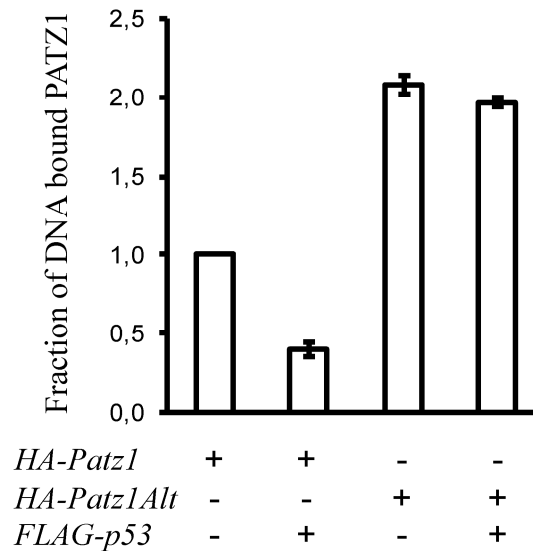


Figure 4.18 p53 – PATZ1 interaction inhibits PATZ1 - DNA interaction. A) DNA pull down assay is performed with biotinylated DNA probes specific to the PATZ1 protein and lysates from HCT116 p53^{-/-} cells transfected with the indicated plasmids B) Quantification of the amount of DNA bound PATZ1 from 3 different experiments

4.16 The Effect of the p53 – PATZ1 Interaction on Apoptosis

We wanted to find out if the interaction of p53 and PATZ1 would have an effect on apoptosis which is one of the outcomes of an activated p53 pathway. We hypothesized that if the p53-PATZ1 interaction has an inhibitory role on p53 function, the number of cells that undergo apoptosis as a result of DNA damage would vary compared to the normal cells. Therefore, we used HCT116WT cells stably infected with retroviruses encoding mock cDNA, PATZ1 or PATZ1Alt. Cells that stably express mock, PATZ1 or PATZ1Alt protein were either treated with 25mJ/cm² UV light or were left untreated. 24 hours after UV treatment, cells were stained with AnnexinV-FITC and SytoxRED prior to flow cytometry analysis. In this experiment, we identified live cells by forward scatter, side scatter and SytoxRED exclusion.

In this experiment SytoxRED only stained the dead cells, so that the alive cell population was SytoxRED negative. On the other hand, the apoptotic cells were stained with AnnexinV-FITC because this cell population is expected to express the ligand of AnnexinV on the cell surface due to the induction of apoptosis. Therefore, in order to determine the amount of the apoptotic cell population, we quantified the percentage of AnnexinV positive – SytoxRED negative cells falling in the Q3 electronic gate. In figure 4.19 we showed that after UV treatment, the percentage of apoptotic cells increased. Moreover, PATZ1 overexpressing HCT116WT cells were a higher percentage of apoptotic compared to either mock infected or PATZ1Alt overexpressing cells. Therefore, overexpression of PATZ1 affects the percentage of cells that become apoptotic after UV treatment likely by interfering with p53 function. A better inducer of apoptosis may exacerbate this difference between mock infected and PATZ1 overexpressing cells.

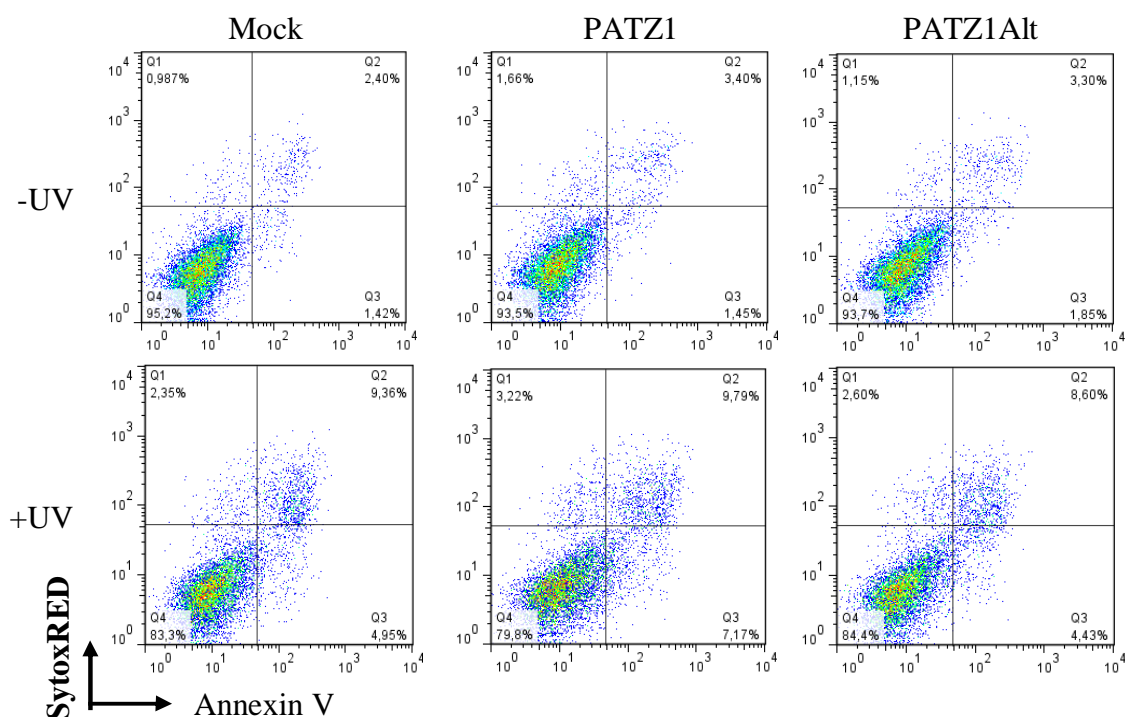


Figure 4.19 Flow cytometry analysis of stably PATZ1 or PATZ1Alt expressing HCT116 cells before and after DNA damage upon UV treatment. Mock cDNA, PATZ1 and PATZ1Alt overexpressing HCT116 cells are stained with Annexin-V and SytoxRED 24 hours after 25mJ/cm² UV treatment.

4.17 The Effect of the p53 – PATZ1 Interaction on Cellular Growth Rate

Another outcome of the activated p53 pathway is on cellular growth rate. Therefore, we decided to test the cell growth and dose response upon DNA damage induced by doxorubicin in stably PATZ1 overexpressing cells in the xCELLigence RCTA-DP system. In this system, cell growth was monitored in real time, and a cell index value was calculated every 15 minutes for 1 week. Doxorubicin was applied in the growth phase of the cells at different dilutions. In figure 4.20, we calculated the IC₅₀ values for doxorubicin's effect on HCT116 cells stably expressing PATZ1. IC₅₀ values were calculated from a 40 hour time window after doxorubicin treatment. Growth curves analysis and dose response curve analysis indicated that stably PATZ1 overexpressing HCT116 cells had 2 fold higher IC₅₀ values compared to control cells. This indicated that stably PATZ1 overexpressing cells were more resistant to doxorubicin compared to mock cDNA overexpressing cells.

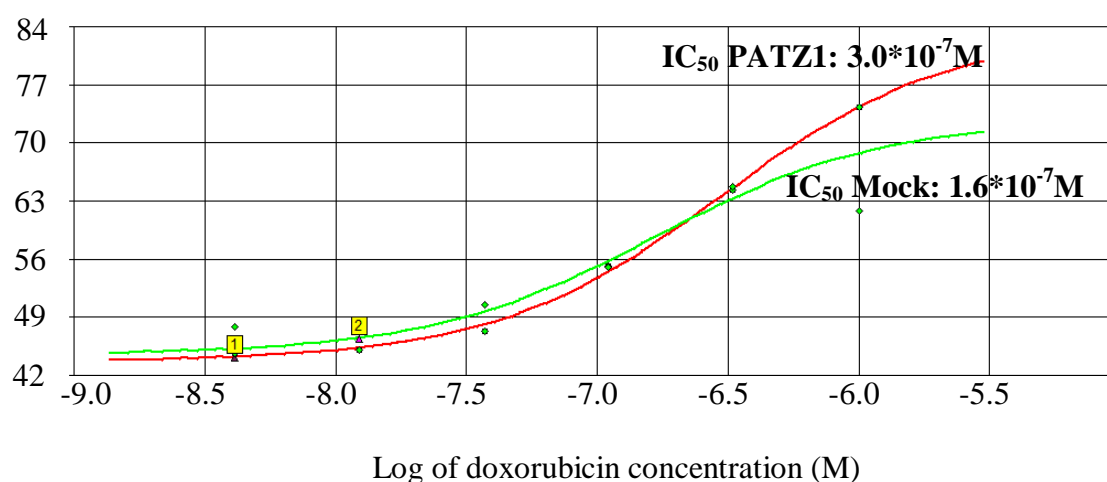


Figure 4.20 Dose response curve and IC₅₀ analysis of stably PATZ1 or mock cDNA overexpressing HCT116 cells after DNA damage induced by doxorubicin. Cell growth of mock cDNA and PATZ1 overexpressing cells was monitored in real time, and a cell index value was calculated every 15 minutes for 1 week in the xCELLigence RCTA-DP system upon DNA damage induced by doxorubicin. Dose response and IC₅₀ analysis are performed by RTCA 2.0 software.

5. DISCUSSION AND CONCLUSION

The tumor suppressor p53 is a stress responsive, sequence specific transcription factor which has roles in cell cycle arrest, senescence, apoptosis, autophagy, DNA repair and regulates metabolic pathways. More than 50% of human cancers have p53 mutations that allow cells to escape from death. In normal cells although p53 mRNA levels are high, the protein levels of p53 are kept low. This is due to the activity of interacting proteins such as MDM2 which ubiquitinates p53 and results in its proteasomal degradation. Upon cellular stress, such as DNA damage, p53 is posttranscriptionally modified and escapes from MDM2 mediated degradation which results in its accumulation. Posttranscriptionally modified p53 is active and begins its function as a transcription factor of genes related to cell cycle arrest, senescence and apoptosis. Like p53, the PATZ1 protein is also a transcription factor that specifically binds DNA through its C2H2 type zinc finger motifs. The PATZ1 transcription factor regulates important genes not only in B and T cell development, but also in embryonic stem cell development and differentiation, cell cycle and apoptosis. Moreover, the upregulation of PATZ1 mRNA levels is found to be correlated with colorectal, breast and testicular tumors¹⁴⁶⁻¹⁴⁸.

To identify the structure of the DNA binding domain of PATZ1, Jitka Eryilmaz, a post-doctoral fellow in the lab, performed homology modelling with known crystal structures in the PDB database. In figure 5.1, we show the homology model of PATZ1 interacting with double stranded DNA through its C2H2 type zinc finger domain in such a way that positively charged zinc fingers (shown in blue) are bound to the negatively charged double stranded DNA (shown in orange). Negatively charged residues in the structure (shown in red) tend to face away from DNA.

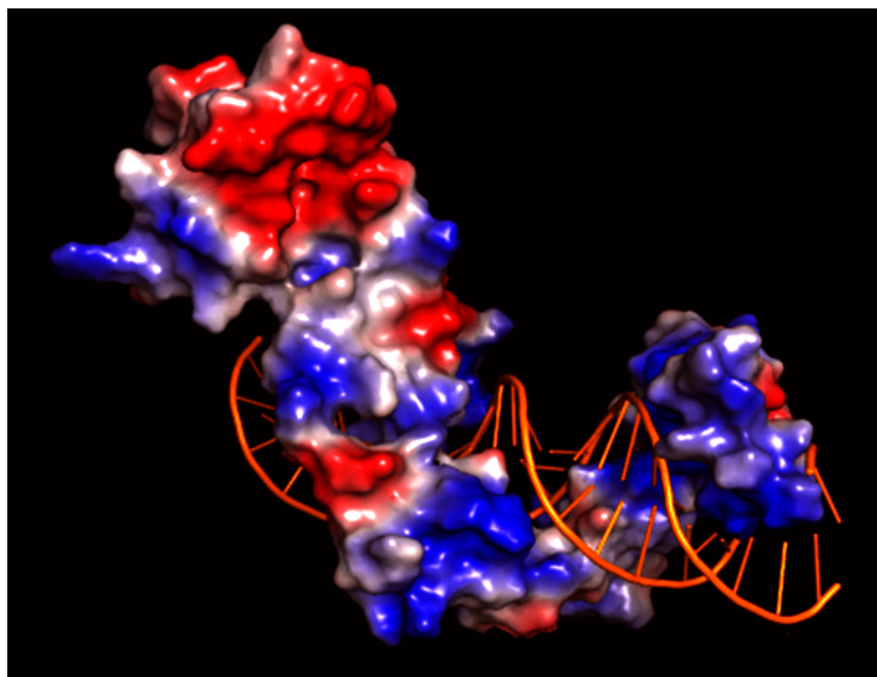


Figure 5.1 Homology model of PATZ1. In the shown homology model, PATZ1 is interacting with double stranded DNA through its C2H2 type zinc finger domain in such a way that positively charged zinc fingers (shown in blue) are bound to the negatively charged double stranded DNA (shown in orange). Negatively charged residues in the structure (shown in red) tend to face away from DNA.

We identified a pocket between the 6th and the 7th zinc finger motifs in the DNA binding domain of PATZ1 which is shown in figure 5.2. This putative pocket is located in a linker domain between zinc fingers 6 and 7 of the PATZ1 protein and is predicted to have a 9Å diameter. As seen from figure 5.2, this putative binding pocket is highly negatively charged and is enriched for amino acid such as aspartic acid and glutamic acid.

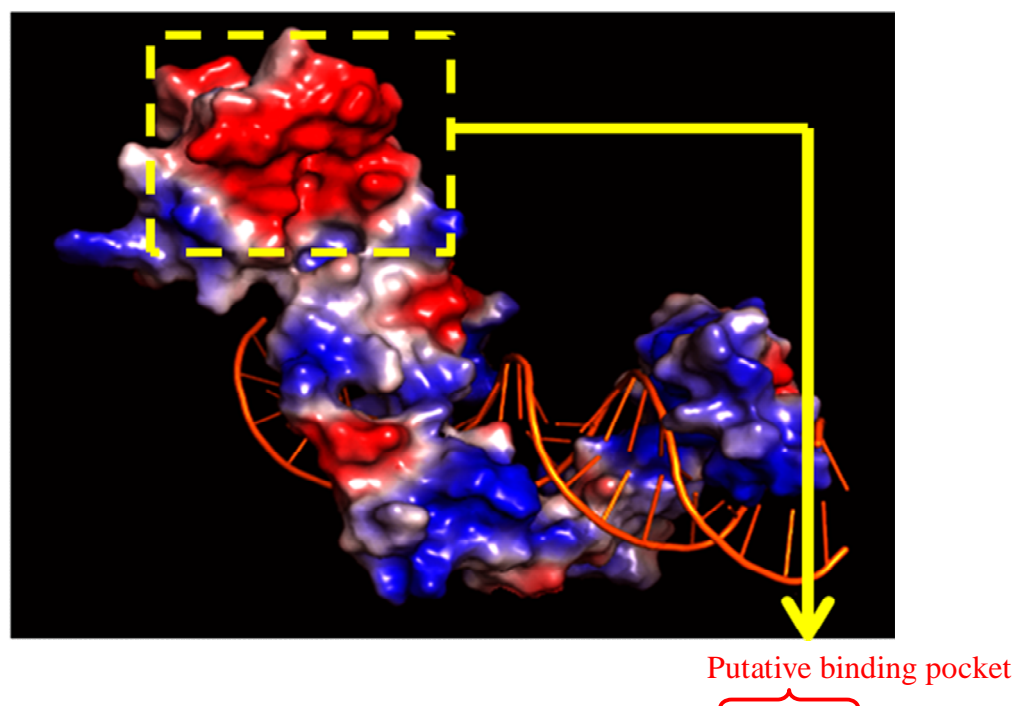


Figure 5.2 Identificaiton of the putative binding pocket between the 6th and 7th zinc finger motifs of PATZ1 in the homology model. This putative binding pocket is located in a linker domain between zinc fingers 6 and 7 of the PATZ1 protein and is predicted to have a 9Å diameter.

Because this region of the PATZ1 protein was necessary for interacting with p53 in *in vitro* binding assays, we performed *in silico* docking studies. We found that, petptide sequence which contains lysine 382 in the C terminal regulatory region of p53 perfectly fit the putative binding pocket of PATZ1.

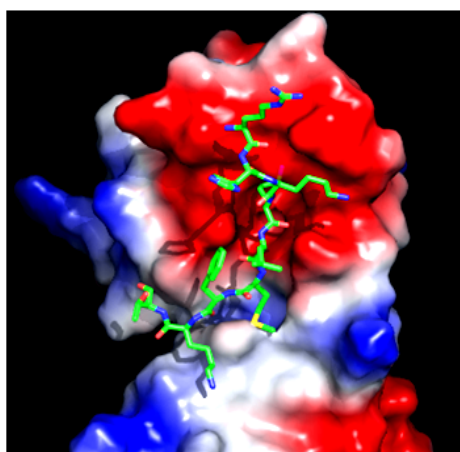


Figure 5.3 In silico docking study to find an interacting partner for PATZ1. Petptide (shoewn in green) sequence which contains lysine 382 in the C terminal regulatory region of p53 perfectly fit the putative binding pocket of PATZ1.

Therefore, computational based homology modeling agrees with immunoprecipitation experiments and shows that the C terminal tail of p53 binds to the negatively charged region of PATZ1. For this immunoprecipitation experiment, we overexpressed HA epitope tagged PATZ1 and FLAG epitope tagged p53 proteins in HCT116 p53^{-/-} cells. Here, we used p53 deficient cells to focus on the interaction of PATZ1 with transfected but not endogenous p53. As shown in figure 4.1, p53 bound PATZ1 but not PATZ1Alt.

The BTB/POZ domain is known to be used for protein – protein interactions of BTB/POZ containing zinc finger proteins. PATZ1 which is also a BTB/POZ containing zinc finger protein, interacts with p53. However, the alternative form that shares the same N terminal BTB/POZ domain does not interact with p53. Therefore, we conclude that unlike other protein – protein interactions, the p53 – PATZ1 interaction is not mediated by the BTB/POZ domain. In fact this interaction does not require the N terminal BTB/POZ domain because Myc epitope tagged truncations of the PATZ1 protein lacking the N terminal BTB domain continue to bind p53.

To test if residues in the putative pocket between the 6th and 7th zinc finger motifs of PATZ1 protein are important for p53 binding, we generated site directed mutants of the PATZ1 protein and tested its p53 binding ability. Specifically we mutated 521 and 527 aspartic acid which are negatively charged and bulky amino acids. We introduced a single mutation to the residue 521 and we generated a double mutant by introducing a second mutation to the residue 527 in addition to 521. We changed these negatively charged aspartic acids into tyrosines which are noncharged and as bulky as aspartic acids in order not to change the 3D conformation of the putative binding pocket. The single mutant PATZ1 had an impaired interaction with p53 whereas the double mutant PATZ1 lost the interaction completely. We conclude that the residues 521 and 527 in the binding pocket of PATZ1 are crucial for the p53 – PATZ1 interaction. A crystal structure of this region of the PATZ1 protein will be instrumental in defining it as a p53 binding motif. Homology searches showed that this region is not conserved among the other p53 binding proteins and that it is not similar in structure of sequence to other known p53 binding motifs such as the tudor domain of 53BP1 protein.

We predict that PATZ1 binds to the conserved RHK/RK sequence in the C terminal regulatory domain of p53. According to the docking studies the methylated form of p53K382 was a perfect candidate to be an interacting partner of the PATZ1 protein. In addition to p53, this conserved sequence is also present in the histone H4 protein. The region around methylated K20 of histone H4 is homologous to p53. Thus, we predict that histone H4 may also be an interacting partner of PATZ1. Moreover the methylation of histone H4 is also DNA damage mediated similar to the modification of p53. Like PATZ1, histones are localized in the nucleus and like p53 histone proteins play an important role in the DNA damage response.

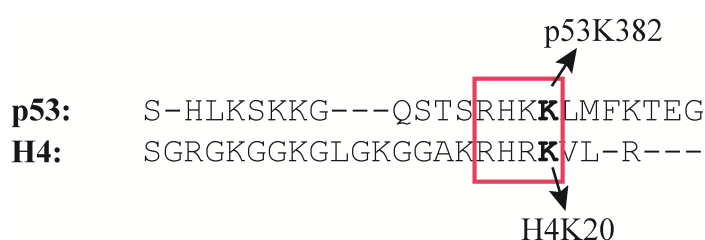


Figure 5.4 The conserved protein sequence that PATZ1 is predicted to bind. PATZ1 protein is expected to bind to the conserved ‘RHK/RK’ sequence of p53 and histone H4 as a result of the homology modeling.

We know that both p53 and PATZ1 are transcription factors that interact with each other. Therefore, this interaction may either be DNA dependent or independent. In order to understand if this interaction is DNA dependent or not, we repeated the p53 – PATZ1 interaction experiments in the presence of the DNA damaging agent, doxorubicin and the DNA intercalating ethidium bromide. Doxorubicin which is a genotoxic DNA damaging agent makes double strand breaks in the DNA and blocks MDM2 mediated p53 ubiquitination and the resulting proteosomal degradation²⁰. We overexpressed p53 and PATZ1 proteins and treated the cells with doxorubicin for 8 hours which is long enough to induce DNA damage and p53 accumulation. Compared to the p53 – PATZ1 interaction without doxorubicin treatment, there was no significant difference in the amount of PATZ1 that could bind p53. Therefore, we conclude that DNA damage does not affect the p53 – PATZ1 interaction. On the other hand, we wanted to see the effect of ethidium bromide which intercalates into DNA and is known to disrupt DNA dependent transcription factor interactions¹⁵⁴. Ethidium bromide treatment could not disrupt the interaction of p53 and PATZ1. Therefore, we conclude that this interaction is independent of DNA.

As we first detected the p53 – PATZ1 interaction under overexpression conditions, the overexpression of two proteins may result as an artifact of overexpression. Thus, we also demonstrated that endogenous p53 and PATZ1 proteins also interact. We confirmed the localization of these two proteins. p53 is known to be both in the cytoplasm and nucleus because it has both nuclear localization and export sequences. PATZ1 is predicted to be in the nucleus because it is a transcription factor, however we wanted to confirm if significant levels can be detected in the cytoplasm. Therefore, we performed cytoplasmic and nuclear fractionation during cell lysis. We performed western blot experiments with these lysates to identify the location of the p53 and PATZ1 proteins in HCT116 cells. We showed that p53 is both in the cytoplasm and nucleus as expected while PATZ1 is localized only to the nucleus. Therefore, we tested the endogenous p53 – PATZ1 interaction by immunoprecipitating nuclear fraction of the cell lysates.

p53 protein levels are very low in normal unstressed cells. Cells treated with doxorubicin dramatically increase the protein levels of p53. When we immunoprecipitated the endogenous p53 protein with an antibody that has an epitope on the N terminus of p53, endogenous PATZ1 protein interacted with p53 in both doxorubicin untreated and treated cells. Thus, even the minute amount of p53 in unstressed cells was enough to interact with PATZ1 protein. Upon doxorubicin treatment, p53 accumulated as expected. However, we were surprised to see that although doxorubicin treated cells have more p53, the amount of p53 that interacts with PATZ1 was same. This may be due to limiting amounts of PATZ1 protein. If nuclear levels of PATZ1 are lower than the levels of p53, then the interaction between these two proteins would be dependent on the PATZ1 protein levels. Then, regardless of the amount of p53 in doxorubicin treated or untreated cells, the amount of limiting PATZ1 that binds to this p53 would be the same. In order to test this hypothesis, we will perform an interaction assay with a fixed concentration of p53 but an increasing concentration of PATZ1. If our hypothesis is correct, we expect to see an increase in the amount of p53 bound PATZ1 as the levels of PATZ1 increase.

Surprisingly, there was an additional endogenous protein in p53 immunoprecipitates. The molecular weight of this protein indicated that it could either be the alternative splice variants of PATZ1, PATZ1Alt or PATZ1-003. PATZ1Alt could not bind to p53 in the overexpression experiments while the p53 binding ability of PATZ1-003 is not known. It is known that PATZ1 can form homodimers through its BTB/POZ domain¹²⁵. Therefore, we hypothesized that similar to homodimerization, PATZ1 may heterodimerize with its alternative splice form PATZ1Alt. If these two alternative isoforms are heterodimerizing, this heterodimer complex may interact with p53 through PATZ1. In order to test this hypothesis, we epitope tagged PATZ1 with Myc, PATZ1Alt with HA and p53 with FLAG and performed a triple immunoprecipitation experiment. We immunoprecipitated HA-PATZ1Alt and checked if there is Myc-PATZ1 in the precipitates and showed its presence with anti-Myc western blots. We also blotted these HA immunoprecipitates with anti-FLAG antibodies. These experiments demonstrate that PATZ1 and PATZ1Alt interact and that PATZ1Alt and p53 can interact only in the presence of PATZ1. Therefore, we concluded that p53 binds to PATZ1 but if there is PATZ1Alt around, PATZ1 can also heterodimerize with PATZ1Alt forming a p53-PATZ1-PATZ1Alt triple protein complex. Like other known interactions between BTB domain containing proteins, it was likely that the PATZ1 and PATZ1Alt interaction was mediated by the BTB domain. To identify the domain necessary for PATZ1 and PATZ1Alt heterodimerization, we overexpressed PATZ1Alt and the truncations of PATZ1 and repeated the immunoprecipitation experiment. We found that the loss of the BTB domain results in the loss of heterodimerization of the alternative splice variants. Therefore, we concluded that PATZ1 and PATZ1Alt heterodimerize through their identical N terminal BTB domains.

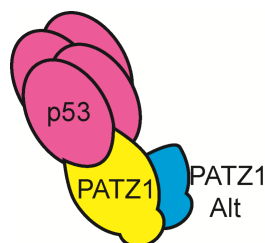


Figure 5.5 p53-PATZ1-PATZ1Alt complex. Schematic representation of the interaction of p53 (shown in pink) with the PATZ1 (shown in yellow) – PATZ1Alt (shown in blue) heterodimer.

Although we confirmed the interaction of p53 and PATZ1 in endogenous HCT116 cells, we wanted to repeat the same experiment with a different p53 antibody that sees a different epitope. In the previous endogenous immunoprecipitation experiment we used a p53 antibody that recognized an epitope in the N terminal part of p53. Next, we used a different p53 antibody that has an epitope on the C terminal part of the p53 protein. We immunoprecipitated endogenous p53 protein with the new antibody and confirmed the interaction again with anti-PATZ1 western blotting. Surprisingly, we found that PATZ1 could be immunoprecipitated even in the HCT116 p53^{-/-} cells. This was unexpected because this cell line is known to be p53 deficient and cannot express the p53 protein. In the lysates of these cells we detected a 47 kDa band which corresponds to the $\Delta 40$ p53 isoform of p53. Although the cell line is p53^{-/-}, it can express the $\Delta 40$ p53 isoform⁵³. The previous p53 antibody could not detect this alternative isoform because its epitope was in the N terminal part of p53 which is lacking in the $\Delta 40$ p53 isoform. With a new antibody that can detect p53 from the C terminus, we demonstrate that the $\Delta 40$ p53 isoform can also interact with PATZ1. This is expected because the $\Delta 40$ p53 isoform only lacks the N terminal first 40 amino acids. It has an intact C terminal domain exactly the same as p53. We think that PATZ1 interacts with p53 through its C terminal region from our homology modeling studies. Unlike p53, the $\Delta 40$ p53 protein level is not DNA damage responsive. Surprisingly, although the protein levels of $\Delta 40$ p53 isoform are not changed, its interaction with PATZ1 is seen only upon doxorubicin treatment. Therefore, we conclude that both p53 and $\Delta 40$ p53 can interact with PATZ1 but with different mechanisms. p53 binds to PATZ1 even in unstressed cells however, $\Delta 40$ p53 may need to be post transcriptionally modified upon DNA damage to interact with PATZ1.

We showed the interaction of p53 and PATZ1 proteins in both overexpression and endogenous conditions. Moreover we identified the required regions of the proteins for this interaction. Also, we tested the specificity of the p53 – PATZ1 interaction using mutant PATZ1 variants. There are other interacting partners of p53 such as MDM2 and MDM4 that can form heterodimers which is reminiscent of the PATZ1 and PATZ1Alt heterodimerization. The MDM2-p53 complex may also be able to interact with the PATZ1 and PATZ1Alt heterodimer. After the formation of the MDM2-p53-PATZ1-PATZ1Alt complex, MDM2 may ubiquitinate PATZ1 resulting in the proteosomal

degradation. Emre Deniz, another graduate student in our lab found that upon longer incubation with doxorubicin, PATZ1 levels fall in MEF and NIH3T3 cells. Therefore, further studies should try to identify any MDM2-PATZ1 interactions. If these two proteins are found in the same complex, then whether the degradation mechanism of PATZ1 is ubiquitination dependent should be tested. If indeed PATZ1 degradation is ubiquitin dependent, its ubiquitin ligase enzyme should be identified.

The start point for stress mediated functions of p53 after its activation through posttranslational modifications is the binding to the response elements of its target genes. Therefore, p53 – DNA binding is very important for p53 to act as a transcriptional activator or repressor. We wanted to find out if PATZ1 has an effect on the interaction between p53 and DNA. In order to understand this, we performed EMSA assays in which we used a biotinylated p53 probe consisting of the p53 binding consensus. We incubated FLAG-p53 overexpressed nuclear cell lysates with the biotinylated probe and later run the samples in non-denaturing polyacrylamide gels. In EMSA assays, the unbound free probe has a higher mobility than the protein bound probes. Therefore, if the protein binds to the probe, then in the gel we would detect a shift in the size of the probe. Addition of lysates containing PATZ1 to the reaction is expected to result in either a lower mobility complex resulting in a bigger shift or in the dissociation of the p53 – DNA complex resulting in a band similar to the unbound probe size. We observed a similar pattern in the probes incubated with FLAG-p53 alone or together with HA-PATZ1. This result may arise from the impurity of the lysates. In this assay, although we overexpress the p53 and PATZ1 proteins, we use complete nuclear lysates which contain many non-specific proteins that may interfere with protein – probe bindings. We performed DNA pull down assays in which biotinylated probes incubated with the protein of interest are pulled down with streptavidin beads and the associated proteins are identified by western blotting. We found that the presence of PATZ1 decreased the amount of p53 bound to probe almost 5 fold. PATZ1^{Alt} that does not interact with p53 did not affect p53 DNA binding, as expected. In further experiments we found that the single point mutant of PATZ1 that has an impaired interaction with p53 could not inhibit p53 DNA binding as much as the wild type PATZ1 protein. Moreover, a double mutant which cannot bind to p53 has no significant effect on p53 DNA binding. There was a direct correlation between the strength of the p53 – PATZ1 interaction and the inhibition of p53 – DNA binding: the stronger the

protein – protein interaction, the more inhibited was the p53 – DNA binding. Surprisingly, we found that PATZ1 also bound to same probes containing p53 binding site. Moreover, the amount of PATZ1 bound to the probe is decreased significantly in the presence of p53 compared to PATZ1 alone. This converse inhibition of PATZ1 DNA binding by p53 was also evident on other probes. Therefore, we concluded that p53 and PATZ1 form a complex that is incapable of binding to DNA. By inhibiting p53- DNA interaction, PATZ1 may result in a completely unfunctional p53 because the p53- DNA interaction is the first step in the activation or repression of the downstream elements. It has been shown that PATZ1 mRNA is upregulated in human colorectal, breast and testicular tumors^{146–148}. In those tumors, PATZ1 upregulation may inhibit the tumor suppressor p53 resulting in tumor formation. Cancer related mutations of p53 are generally in the conserved DNA binding domain of the protein^{97–99}. The peptide sequence that PATZ1 is predicted to bind is in the C terminal regulatory region which is conserved in mutant p53 proteins. Thus, cancer related mutant p53 may also bind to PATZ1. Moreover, it is known that mutant p53 forms heterotetramers with wild type p53 resulting in the dominant negative inactivation of wild type p53¹⁰⁸. We showed that the PATZ1-PATZ1Alt heterodimer can bind to p53. Similar to mutant p53, the PATZ1 homodimer or the PATZ1-PATZ1Alt heterodimer may form a multi-protein complex that inhibits p53 tetramerization resulting in the inhibition of p53 – DNA binding.

The interaction of a transcription factor and DNA is critical for its function. It has been reported that a single mutation in the zinc finger domain of another BTB/POZ zinc finger protein, Th-POK which is a master regulator of T helper lymphocyte lineage development, resulted in mice that are helper deficient (HD)^{155,156}. This naturally occurring mutation of residue 389 of Th-POK converts an arginine into glycine (R389G). When the sequences of the DNA binding domain of the members of this transcription factor family such as PATZ1, Bcl6, Bcl6b and ROG are aligned with Th-POK, it is evident that the arginine residue is conserved suggesting that it may be very important in DNA binding by all of these BTB/ZF transcription factors.




Figure 5.6 Conservation of the residue that is important for helper lineage commitment. Sequence alignment of the DNA binding domain of the members of BTB/ZF transcription factor family such as PATZ1, Bcl6, Bcl6b and ROG with Th-POK and conservation of R389 in Th-POK.

The arginine 389 residue in Th-POK corresponds to the arginine 403 in PATZ1. If a mutation in the DNA binding domain of PATZ1 at this residue interferes with DNA binding, it may be possible to understand general structural features necessary for BTB/ZF transcription factor DNA binding. Moreover, homology models of Th-POK and PATZ1 indicate that this residue is predicted to hold the 3rd and 4th zinc finger domains together. If the arginine 403 residue is important for PATZ1 structure, its mutation may cause conformational changes and decreased stability of the protein. Even if the protein would be stable, due to losing the direct interaction with DNA, this mutation may cause interfere with the ability of PATZ1 to bind to DNA as a transcription factor. Thus, the roles of PATZ1 in tumor formation may be blocked. Moreover, if the mutation of the arginine residue 403 results in a 3D conformational change, the p53 – PATZ1 interaction may be affected. If this interaction is impaired, then p53 would bind to DNA more efficiently. In order to understand this mutation in the DNA binding domain of PATZ1, we plan to repeat the interaction and pull down assays with mutant versions of PATZ1.

It has been reported that some gene specific transcription factors such as the ones that contain C2H2 type zinc finger motifs are inactivated during the G2/M transition of the cell cycle. This inactivation is due to the G2/M specific phosphorylation of SGEKP and SVGKP sequences in the linker domain between the zinc finger motifs¹⁵⁷. PATZ1 protein has also these two motifs in the linker regions between the 2nd – 3rd and 3rd – 4th zinc fingers. These potential phosphorylation sites may result in the inactivation of the protein through the blocked interaction with DNA upon G2/M transition dependent

phosphorylation. Therefore, in order to understand if these residues have a functional role on PATZ1, we plan to mutate these potential phosphorylation motifs. In addition to this, if these motifs may cause the inactivation of PATZ1 in the G2/M transition, the inhibition of p53 by PATZ1 would also be blocked resulting in the activation of p53 due to binding to its target DNA more efficiently. Mutation or complete deletion of this site, would block the G2/M transition dependent phosphorylation of PATZ1. Therefore, during the G2/M transition, PATZ1 would be still active and may inhibit p53 to functionally act as a tumor suppressor protein.



Figure 5.7 G2/M dependent phosphorylation motif in the linker domains of PATZ1. G2/M specific phosphorylation sequences, ‘SGEKP’ and ‘SVGKP’ are present in the linker domain between the 2nd – 3rd and 3rd – 4th zinc finger domains of the PATZ1 protein.

In unstressed conditions, p53 can be localized either to the cytoplasm or nucleus. Upon DNA damage, p53 is localized to the nucleus to act as a transcription factor. In order to test if the p53 interacting partner, PATZ1 has an effect on the translocation of p53 from the cytoplasm to the nucleus, we analyzed this translocation on the confocal microscope. We overexpressed GFP fused p53 proteins in HCT116 p53^{-/-} cells. With confocal microscopy, we visualized the p53-GFP protein mostly in the cytoplasm of the cells. Although, this was an overexpression situation, p53-GFP intensity was low. This may be due to the instability of the p53 protein in normal conditions. After DNA damage induction with doxorubicin, we clearly saw that p53-GFP fusion proteins translocated from the cytoplasm to the nucleus. Moreover, the intensity of p53-GFP increased upon DNA damage as expected. Next, we overexpressed PATZ1 protein in either nontreated or doxorubicin treated cells. However, there was not a significant change in the translocation of p53-GFP proteins. In this experiment, we could only visualize the p53 protein because it was fused to GFP. For further experiments, we plan to stain the HA-PATZ1 protein overexpression with HA-Rhodamine. This experiment would allow us to see the co-localization of the proteins. On the other hand, this experiment was performed with overexpressed proteins. For the further experiments, we plan to stain the endogenous p53 protein with an Alexa 488 conjugated antibody and the

PATZ1 protein with an Alexa 647 conjugated antibody. Therefore, we could detect both of the endogenous proteins stained with dyes with different excitation and emission wavelengths.

The main roles of p53 upon stress are to induce senescence, cell cycle arrest and apoptosis. In order to test if the p53 – PATZ1 interaction has a function on the induction of apoptosis, we used UV light to induce stress and apoptosis. Using flow cytometry, we analyzed the percentage of the cells that express Annexin-V receptor on their cell surface because apoptotic cells reverse their Annexin-V receptor from the inner part of the cell membrane to the cell surface. In this analysis we excluded the dead cells with SytoxRED staining. The percentage of the the alive (SytoxRED negative) and apoptotic (Annexin-V positive) cell population is approximately 2 fold higher in stably PATZ1 expressing HCT116 cells than in stably mock or PATZ1Alt expressing cells. From this experiment, we can conclude that PATZ1 may help p53 to function as an apoptosis inducer upon UV stress through interaction.

In addition to these, we wanted to analyze the real time growth of the stably PATZ1 overexpressing HCT116 cells upon doxorubicin treatment. We used different concentrations of doxorubicin to see the response on cellular growth. We measured the cell index numbers in the RTCA-DP system in every 15 minutes for a week. At the end of the experiment, we plotted a sigmoidal dose response curve for mock cDNA and PATZ1 overexpressing cells. Later, we calculated the inhibitory concentration necessary for inhibiting the 50% of the cells (IC_{50}). Stably PATZ1 overexpressing cells have a 2 fold higher IC_{50} value than mock cDNA expressing cells. In other words, PATZ1 overexpressing cells are more resistant to doxorubicin induced growth arrest and cell death. 2 fold concentration of doxorubicin is required to see the same death effect in the PATZ1 expressing cells which may indicate that PATZ1 inhibits the activity of p53 to induce cell death induced by doxorubicin. Although, we have found a different result in the FACS analysis, the stress inducers of the two experiments were different. Thus, the effect of PATZ1 on p53 function may be context dependent.

In light of our results showing the inhibition of p53 – DNA binding in the presence of PATZ1, we hypothesized that PATZ1 may have an inhibitory role on p53 to function as a transcriptional repressor. Therefore, we plan to see the functional activity of p53 in HCT116 cell lines that express PATZ1. In order to knock out PATZ1 in a cell line, we plan to use transcription activator like effector nucleases (TALENs). TALENs bind to the target sequence and introduce a double strand break in the DNA resulting in the activation of DNA repair mechanisms such as non-homologous end joining (NHEJ) and homologous recombination. Unless there is a rescue sequence homologous to the site of DNA break, the NHEJ mechanism is preferred, resulting in insertions or deletions in the DNA sequence^{158–161}. Nowadays, TALENs are commonly used for mutating genomic sequences in order to knock out the desired gene in the genome. For the knock out strategy of PATZ1, we also plan to design a forward and reverse TALEN targeting the first exon of the genomic sequence of PATZ1. In the spacer region of the forward and reverse TALENs, the nuclease of TALEN, FokI would form a homodimer and cut the DNA which would probably result in the destruction of the coding sequence through insertions or deletions. At the theoretical cut site of TALENs, there is an MboII restriction site. If there would be an insertion or deletion after TALEN activity, then the restriction site would be destroyed. Therefore, we would amplify the region with PCR, after genomic DNA isolation, and perform restriction digestion with MboII to perform an RFLP (restriction fragment length polymorphism) assay. If the DNA fragments are not cut, this means the restriction site is destroyed. Therefore, the DNA sequence in the exon is modified and coding sequence may be changed resulting in the stop of PATZ1 expression. The planned TALEN targets on the mouse Patz1 gene are shown in figure 5.8.

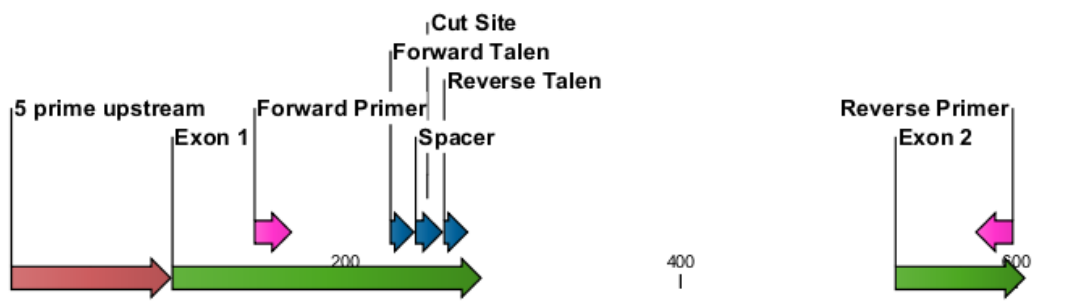


Figure 5.8 TALEN design for PATZ1 knock out cell lines. A forward and a reverse TALEN (shown in blue) targeting the first exon (shown in green) of the genomic sequence of PATZ1 are designed. After TALEN activity, the region is planned to be PCR amplified by forward and reverse primers (shown in pink) and mutation would be confirmed by RFLP assays and sequencing.

In addition to the results shown in this thesis, we also performed experiments to identify the downstream outcomes of the p53 – PATZ1 interaction. We performed luciferase assays with pG13, p21 and PUMA reporter plasmids. In all of the luciferase experiments, we saw a significant decrease in the transcriptional activity of p53 in the presence of PATZ1. Consistent with our pull down results, PATZ1 forms a complex with p53 and inhibits its binding to DNA, resulting in the inhibition of p53 dependent transcriptional activity. Moreover, we checked the mRNA levels of p53 target genes such as p21 and PUMA upon DNA damage induced by doxorubicin. PATZ1 overexpressing cells could increase their p21 and PUMA mRNA levels less than the control cells. This result demonstrated that PATZ1 overexpressing cells could repress p53 activity upon DNA damage. In addition to these, we performed RNA Sequencing in wild type and PATZ1^{-/-} mouse embryonic fibroblasts with or without DNA damage induced by doxorubicin. We analyzed the levels of p53 target genes and revealed that PATZ1 differentially regulates p53 target genes.

Considering all of our results, we prepared a model which explains the functional interaction of p53 and PATZ1. Both p53 and PATZ1 are transcription factors and have specific binding sites as represented in figure 5.9A. Overexpression of p53 or accumulation of p53 upon DNA damage results in the specific binding of p53 to its target DNA. Like p53, in the presence of PATZ1, we observe the specific interaction between its target DNA which is represented in figure 5.9B. However, when p53 and PATZ1 are together, they prefer to make a complex that is incapable of binding to DNA (figure 5.9C).

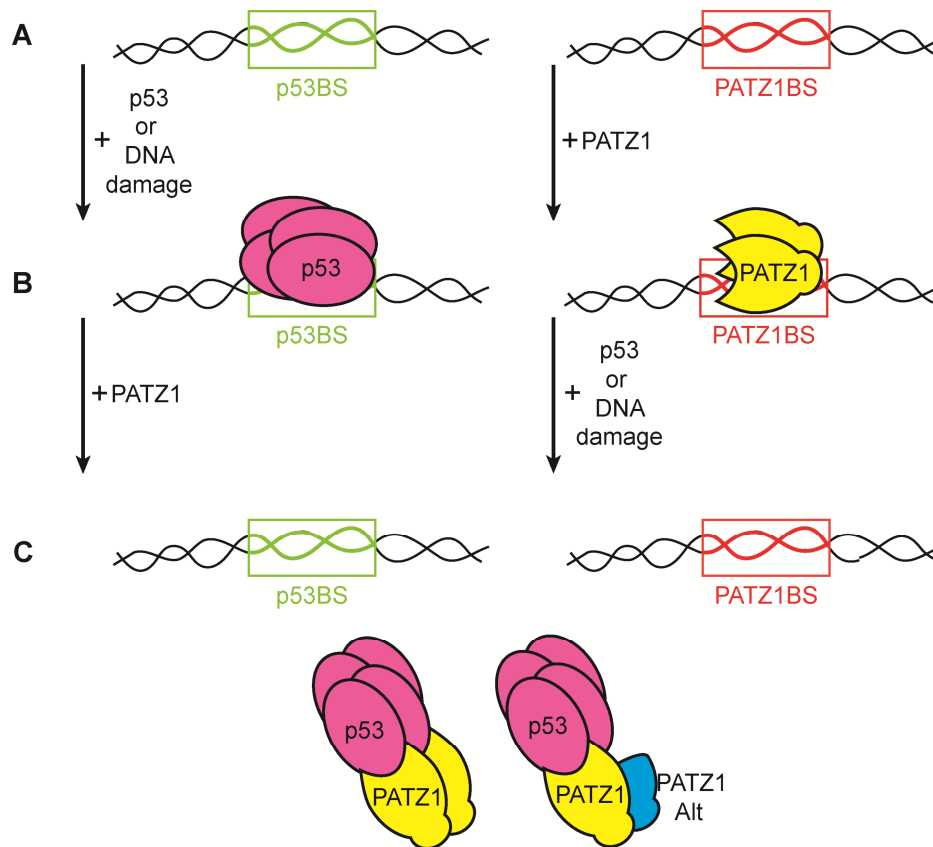


Figure 5.9 Model for functional interaction of p53 and PATZ1. Overexpression of p53 (shown in pink) or accumulation of p53 upon DNA damage results in the specific binding of p53 to its target DNA (shown in green). Like p53, in the presence of PATZ1 (shown in yellow), we observe the specific interaction between its target DNA (shown in red). However, when p53 and PATZ1 are together, they prefer to make a complex that is incapable of binding to DNA.

Neither p53 nor PATZ1 can bind to its target DNA, upon formation of the p53-PATZ1 complex as modeled in figure 4.18C. Because p53 and PATZ1 are both transcription factors, they can perform their transcriptional activation or suppression roles only by binding to DNA. Their interaction with DNA starts all the activation or repression of the target pathways. Therefore, the p53 – PATZ1 complex that is incapable of DNA binding, is very important in tumor suppression pathways. In conclusion, we demonstrated the interaction of p53 and PATZ1 and the effect of this interaction on DNA binding. p53 has many target genes which it can either activate or repress. p53 is mainly responsible for tumor suppression by inducing senescence, cell cycle and apoptosis. On the other hand, PATZ1 expression was shown to be induced in some cancer and tumor types. In addition to the literature that links not only p53 but also PATZ1 with cancer, our results also suggest that the formation of the p53 – PATZ1 complex may be critical for tumor formation and cancer.

REFERENCES

- 1 Levine AJ, Oren M. The first 30 years of p53: growing ever more complex. *Nat Rev Cancer* 2009; **9**: 749–758.
- 2 Vousden KH, Prives C. Blinded by the Light: The Growing Complexity of p53. *Cell* 2009; **137**: 413–431.
- 3 Bargonetti J, Friedman PN, Kern SE, Vogelstein B, Prives C. Wild-type but not mutant p53 immunopurified proteins bind to sequences adjacent to the SV40 origin of replication. *Cell* 1991; **65**: 1083–91.
- 4 MacCallum DE, Hupp TR, Midgley CA, Stuart D, Campbell SJ, Harper A *et al.* The p53 response to ionising radiation in adult and developing murine tissues. *Oncogene* 1996; **13**: 2575–87.
- 5 Honda R, Tanaka H, Yasuda H. Oncoprotein MDM2 is a ubiquitin ligase E3 for tumor suppressor p53. *FEBS Lett* 1997; **420**: 25–7.
- 6 Haupt Y, Maya R, Kazaz A, Oren M. Mdm2 promotes the rapid degradation of p53. *Nature* 1997; **387**: 296–9.
- 7 Kubbutat MH, Jones SN, Vousden KH. Regulation of p53 stability by Mdm2. *Nature* 1997; **387**: 299–303.
- 8 Honda R, Yasuda H. Activity of MDM2, a ubiquitin ligase, toward p53 or itself is dependent on the RING finger domain of the ligase. *Oncogene* 2000; **19**: 1473–6.
- 9 Li M, Brooks CL, Wu-Baer F, Chen D, Baer R, Gu W. Mono- versus polyubiquitination: differential control of p53 fate by Mdm2. *Science* 2003; **302**: 1972–5.
- 10 Grier JD, Xiong S, Elizondo-Fraire AC, Parant JM, Lozano G. Tissue-specific differences of p53 inhibition by Mdm2 and Mdm4. *Mol Cell Biol* 2006; **26**: 192–8.
- 11 Batta K, Kundu TK. Activation of p53 function by human transcriptional coactivator PC4: role of protein-protein interaction, DNA bending, and posttranslational modifications. *Mol Cell Biol* 2007; **27**: 7603–14.
- 12 Xirodimas DP, Saville MK, Bourdon J-C, Hay RT, Lane DP. Mdm2-mediated NEDD8 conjugation of p53 inhibits its transcriptional activity. *Cell* 2004; **118**: 83–97.
- 13 Shvarts A, Steegenga WT, Riteco N, van Laar T, Dekker P, Bazuine M *et al.* MDMX: a novel p53-binding protein with some functional properties of MDM2. *EMBO J* 1996; **15**: 5349–57.
- 14 Marine J-C, Francoz S, Maetens M, Wahl G, Toledo F, Lozano G. Keeping p53 in check: essential and synergistic functions of Mdm2 and Mdm4. *Cell Death Differ* 2006; **13**: 927–934.

- 15 Jackson MW, Berberich SJ. MdmX Protects p53 from Mdm2-Mediated Degradation. *Mol Cell Biol* 2000; **20**: 1001–1007.
- 16 Stad R, Little NA, Xirodimas DP, Frenk R, van der Eb AJ, Lane DP *et al.* Mdmx stabilizes p53 and Mdm2 via two distinct mechanisms. *EMBO Rep* 2001; **2**: 1029–34.
- 17 Linares LK, Hengstermann A, Ciechanover A, Müller S, Scheffner M. HdmX stimulates Hdm2-mediated ubiquitination and degradation of p53. *Proc Natl Acad Sci U S A* 2003; **100**: 12009–14.
- 18 Gu J, Kawai H, Nie L, Kitao H, Wiederschain D, Jochemsen AG *et al.* Mutual dependence of MDM2 and MDMX in their functional inactivation of p53. *J Biol Chem* 2002; **277**: 19251–4.
- 19 Findley HW. Targeting the MDM2 – p53 interaction as a therapeutic strategy for the treatment of cancer. 2015; : 49–58.
- 20 Riley MF, Lozano G. The Many Faces of MDM2 Binding Partners. *Genes Cancer* 2012; **3**: 226–39.
- 21 Ringshausen I, O’Shea CC, Finch AJ, Swigart LB, Evan GI. Mdm2 is critically and continuously required to suppress lethal p53 activity in vivo. *Cancer Cell* 2006; **10**: 501–14.
- 22 Dornan D, Wertz I, Shimizu H, Arnott D, Frantz GD, Dowd P *et al.* The ubiquitin ligase COP1 is a critical negative regulator of p53. *Nature* 2004; **429**: 86–92.
- 23 Leng RP, Lin Y, Ma W, Wu H, Lemmers B, Chung S *et al.* Pirh2, a p53-induced ubiquitin-protein ligase, promotes p53 degradation. *Cell* 2003; **112**: 779–91.
- 24 Chen D, Kon N, Li M, Zhang W, Qin J, Gu W. ARF-BP1/Mule is a critical mediator of the ARF tumor suppressor. *Cell* 2005; **121**: 1071–83.
- 25 Kruse J, Gu W. Review Modes of p53 Regulation. 2009; **2**: 609–622.
- 26 Shieh SY, Ikeda M, Taya Y, Prives C. DNA damage-induced phosphorylation of p53 alleviates inhibition by MDM2. *Cell* 1997; **91**: 325–34.
- 27 Kruse J-P, Gu W. SnapShot: p53 posttranslational modifications. *Cell* 2008; **133**: 930–30.e1.
- 28 Wang X, Taplick J, Geva N, Oren M. Inhibition of p53 degradation by Mdm2 acetylation. *FEBS Lett* 2004; **561**: 195–201.
- 29 Gu W, Roeder RG. Activation of p53 sequence-specific DNA binding by acetylation of the p53 C-terminal domain. *Cell* 1997; **90**: 595–606.
- 30 Rodriguez MS, Desterro JM, Lain S, Lane DP, Hay RT. Multiple C-terminal lysine residues target p53 for ubiquitin-proteasome-mediated degradation. *Mol Cell Biol* 2000; **20**: 8458–67.
- 31 Chuikov S, Kurash JK, Wilson JR, Xiao B, Justin N, Ivanov GS *et al.* Regulation of p53 activity through lysine methylation. *Nature* 2004; **432**: 353–60.

- 32 Shi X, Kachirskaja I, Yamaguchi H, West LE, Wen H, Wang EW *et al.* Modulation of p53 Function by SET8-Mediated Methylation at Lysine 382. *Mol Cell* 2007; **27**: 636–646.
- 33 Huang J, Perez-Burgos L, Placek BJ, Sengupta R, Richter M, Dorsey JA *et al.* Repression of p53 activity by Smyd2-mediated methylation. *Nature* 2006; **444**: 629–32.
- 34 Kitayner M, Rozenberg H, Kessler N, Rabinovich D, Shaulov L, Haran TE *et al.* Structural basis of DNA recognition by p53 tetramers. *Mol Cell* 2006; **22**: 741–53.
- 35 Cho Y, Gorina S, Jeffrey PD, Pavletich NP. Crystal structure of a p53 tumor suppressor-DNA complex: understanding tumorigenic mutations. *Science* 1994; **265**: 346–55.
- 36 el-Deiry WS, Kern SE, Pietenpol JA, Kinzler KW, Vogelstein B. Definition of a consensus binding site for p53. *Nat Genet* 1992; **1**: 45–9.
- 37 Beckerman R, Prives C. Transcriptional regulation by p53. *Cold Spring Harb Perspect Biol* 2010; **2**: a000935.
- 38 Contente A, Dittmer A, Koch MC, Roth J, Dobbelstein M. A polymorphic microsatellite that mediates induction of PIG3 by p53. *Nat Genet* 2002; **30**: 315–20.
- 39 Zheng X, Chen X. Aquaporin 3, a glycerol and water transporter, is regulated by p73 of the p53 family. *FEBS Lett* 2001; **489**: 4–7.
- 40 Johnson RA, Ince TA, Scotto KW. Transcriptional repression by p53 through direct binding to a novel DNA element. *J Biol Chem* 2001; **276**: 27716–20.
- 41 Bourdon J-C, Fernandes K, Murray-Zmijewski F, Liu G, Diot A, Xirodimas DP *et al.* p53 isoforms can regulate p53 transcriptional activity. *Genes Dev* 2005; **19**: 2122–37.
- 42 Riley T, Sontag E, Chen P, Levine A. Transcriptional control of human p53-regulated genes. *Nat Rev Mol Cell Biol* 2008; **9**: 402–412.
- 43 Vousden KH, Lu X. Live or let die: the cell's response to p53. *Nat Rev Cancer* 2002; **2**: 594–604.
- 44 el-Deiry WS. Regulation of p53 downstream genes. *Semin Cancer Biol* 1998; **8**: 345–57.
- 45 Kortlever RM, Higgins PJ, Bernards R. Plasminogen activator inhibitor-1 is a critical downstream target of p53 in the induction of replicative senescence. *Nat Cell Biol* 2006; **8**: 877–84.
- 46 Leal JFM, Fominaya J, Cascón A, Guijarro M V, Blanco-Aparicio C, Lleónart M *et al.* Cellular senescence bypass screen identifies new putative tumor suppressor genes. *Oncogene* 2008; **27**: 1961–70.
- 47 Baker SJ, Preisinger AC, Jessup JM, Paraskeva C, Markowitz S, Willson JK *et al.* p53 gene mutations occur in combination with 17p allelic deletions as late events in colorectal tumorigenesis. *Cancer Res* 1990; **50**: 7717–22.
- 48 Halevy O, Rodel J, Peled A, Oren M. Frequent p53 mutations in chemically induced murine fibrosarcoma. *Oncogene* 1991; **6**: 1593–600.

- 49 Eliyahu D, Goldfinger N, Pinhasi-Kimhi O, Shaulsky G, Skurnik Y, Arai N *et al.* Meth A fibrosarcoma cells express two transforming mutant p53 species. *Oncogene* 1988; **3**: 313–21.
- 50 Martins CP, Brown-Swigart L, Evan GI. Modeling the therapeutic efficacy of p53 restoration in tumors. *Cell* 2006; **127**: 1323–34.
- 51 Ventura A, Kirsch DG, McLaughlin ME, Tuveson DA, Grimm J, Lintault L *et al.* Restoration of p53 function leads to tumour regression in vivo. *Nature* 2007; **445**: 661–5.
- 52 Xue W, Zender L, Miething C, Dickins RA, Hernando E, Krizhanovsky V *et al.* Senescence and tumour clearance is triggered by p53 restoration in murine liver carcinomas. *Nature* 2007; **445**: 656–60.
- 53 Khoury MP, Bourdon J. The Isoforms of the p53 Protein. 2010; : 1–10.
- 54 Avery-Kiejda KA, Zhang XD, Adams LJ, Scott RJ, Vojtesek B, Lane DP *et al.* Small molecular weight variants of p53 are expressed in human melanoma cells and are induced by the DNA-damaging agent cisplatin. *Clin Cancer Res* 2008; **14**: 1659–68.
- 55 Fujita K, Mondal AM, Horikawa I, Nguyen GH, Kumamoto K, Sohn JJ *et al.* p53 isoforms Delta133p53 and p53beta are endogenous regulators of replicative cellular senescence. *Nat Cell Biol* 2009; **11**: 1135–42.
- 56 Keller DM, Zeng SX, Lu H. Interaction of p53 with cellular proteins. *Methods Mol Biol* 2003; **234**: 121–33.
- 57 Chen X, Farmer G, Zhu H, Prywes R, Prives C. Cooperative DNA binding of p53 with TFIID (TBP): a possible mechanism for transcriptional activation. *Genes Dev* 1993; **7**: 1837–49.
- 58 Horikoshi N, Usheva A, Chen J, Levine AJ, Weinmann R, Shenk T. Two domains of p53 interact with the TATA-binding protein, and the adenovirus 13S E1A protein disrupts the association, relieving p53-mediated transcriptional repression. *Mol Cell Biol* 1995; **15**: 227–34.
- 59 Lu H, Levine AJ. Human TAFII31 protein is a transcriptional coactivator of the p53 protein. *Proc Natl Acad Sci U S A* 1995; **92**: 5154–8.
- 60 Thut CJ, Chen JL, Klemm R, Tjian R. p53 transcriptional activation mediated by coactivators TAFII40 and TAFII60. *Science* 1995; **267**: 100–4.
- 61 Gu W, Shi XL, Roeder RG. Synergistic activation of transcription by CBP and p53. *Nature* 1997; **387**: 819–23.
- 62 Lill NL, Grossman SR, Ginsberg D, DeCaprio J, Livingston DM. Binding and modulation of p53 by p300/CBP coactivators. *Nature* 1997; **387**: 823–7.
- 63 Filhol O, Baudier J, Delphin C, Loue-Mackebach P, Chambaz EM, Cochet C. Casein kinase II and the tumor suppressor protein P53 associate in a molecular complex that is negatively regulated upon P53 phosphorylation. *J Biol Chem* 1992; **267**: 20577–83.

- 64 D'Orazi G, Cecchinelli B, Bruno T, Manni I, Higashimoto Y, Saito S *et al.* Homeodomain-interacting protein kinase-2 phosphorylates p53 at Ser 46 and mediates apoptosis. *Nat Cell Biol* 2002; **4**: 11–9.
- 65 Hofmann TG, Möller A, Sirma H, Zentgraf H, Taya Y, Dröge W *et al.* Regulation of p53 activity by its interaction with homeodomain-interacting protein kinase-2. *Nat Cell Biol* 2002; **4**: 1–10.
- 66 Fuchs SY, Adler V, Buschmann T, Yin Z, Wu X, Jones SN *et al.* JNK targets p53 ubiquitination and degradation in nonstressed cells. *Genes Dev* 1998; **12**: 2658–63.
- 67 Liu Y, Colosimo AL, Yang XJ, Liao D. Adenovirus E1B 55-kilodalton oncoprotein inhibits p53 acetylation by PCAF. *Mol Cell Biol* 2000; **20**: 5540–53.
- 68 Luo J, Su F, Chen D, Shiloh A, Gu W. Deacetylation of p53 modulates its effect on cell growth and apoptosis. *Nature* 2000; **408**: 377–81.
- 69 Murphy M, Ahn J, Walker KK, Hoffman WH, Evans RM, Levine AJ *et al.* Transcriptional repression by wild-type p53 utilizes histone deacetylases, mediated by interaction with mSin3a. *Genes Dev* 1999; **13**: 2490–501.
- 70 Luo J, Nikolaev AY, Imai S, Chen D, Su F, Shiloh A *et al.* Negative control of p53 by Sir2alpha promotes cell survival under stress. *Cell* 2001; **107**: 137–48.
- 71 Vaziri H, Dessain SK, Eaton EN, Imai S-I, Frye RA, Pandita TK *et al.* hSIR2/SIRT1 Functions as an NAD-Dependent p53 Deacetylase. *Cell* 2001; **107**: 149–159.
- 72 Zilfou JT, Hoffman WH, Sank M, George DL, Murphy M. The corepressor mSin3a interacts with the proline-rich domain of p53 and protects p53 from proteasome-mediated degradation. *Mol Cell Biol* 2001; **21**: 3974–85.
- 73 Oliner JD, Pietenpol JA, Thiagalingam S, Gyuris J, Kinzler KW, Vogelstein B. Oncoprotein MDM2 conceals the activation domain of tumour suppressor p53. *Nature* 1993; **362**: 857–60.
- 74 Li M, Chen D, Shiloh A, Luo J, Nikolaev AY, Qin J *et al.* Deubiquitination of p53 by HAUSP is an important pathway for p53 stabilization. *Nature* 2002; **416**: 648–53.
- 75 Huibregtse JM, Scheffner M, Howley PM. Cloning and expression of the cDNA for E6-AP, a protein that mediates the interaction of the human papillomavirus E6 oncoprotein with p53. *Mol Cell Biol* 1993; **13**: 775–84.
- 76 Iwabuchi K, Bartel PL, Li B, Marraccino R, Fields S. Two cellular proteins that bind to wild-type but not mutant p53. *Proc Natl Acad Sci U S A* 1994; **91**: 6098–102.
- 77 Brummelkamp TR, Fabius AWM, Mullenders J, Madiredjo M, Velds A, Kerkhoven RM *et al.* An shRNA barcode screen provides insight into cancer cell vulnerability to MDM2 inhibitors. *Nat Chem Biol* 2006; **2**: 202–6.
- 78 Bergamaschi D, Samuels Y, O'Neil NJ, Trigianti G, Crook T, Hsieh J-K *et al.* iASPP oncoprotein is a key inhibitor of p53 conserved from worm to human. *Nat Genet* 2003; **33**: 162–7.

- 79 Samuels-Lev Y, O'Connor DJ, Bergamaschi D, Trigianti G, Hsieh JK, Zhong S *et al.* ASPP proteins specifically stimulate the apoptotic function of p53. *Mol Cell* 2001; **8**: 781–94.
- 80 Waterman MJ, Stavridi ES, Waterman JL, Halazonetis TD. ATM-dependent activation of p53 involves dephosphorylation and association with 14-3-3 proteins. *Nat Genet* 1998; **19**: 175–8.
- 81 Jayaraman L, Moorthy NC, Murthy KG, Manley JL, Bustin M, Prives C. High mobility group protein-1 (HMG-1) is a unique activator of p53. *Genes Dev* 1998; **12**: 462–72.
- 82 Livesey KM, Kang R, Vernon P, Buchser W, Loughran P, Watkins SC *et al.* p53/HMGB1 complexes regulate autophagy and apoptosis. *Cancer Res* 2012; **72**: 1996–2005.
- 83 Das S, Raj L, Zhao B, Kimura Y, Bernstein A, Aaronson SA *et al.* Hsf1 determines cell survival upon genotoxic stress by modulating p53 transactivation. *Cell* 2007; **130**: 624–37.
- 84 Tian C, Xing G, Xie P, Lu K, Nie J, Wang J *et al.* KRAB-type zinc-finger protein Apak specifically regulates p53-dependent apoptosis. *Nat Cell Biol* 2009; **11**: 580–91.
- 85 Tanaka T, Ohkubo S, Tatsuno I, Prives C. hCAS/CSE1L associates with chromatin and regulates expression of select p53 target genes. *Cell* 2007; **130**: 638–50.
- 86 An WG, Kanekal M, Simon MC, Maltepe E, Blagosklonny M V, Neckers LM. Stabilization of wild-type p53 by hypoxia-inducible factor 1alpha. *Nature* 1998; **392**: 405–8.
- 87 Jayaraman L, Murthy KG, Zhu C, Curran T, Xanthoudakis S, Prives C. Identification of redox/repair protein Ref-1 as a potent activator of p53. *Genes Dev* 1997; **11**: 558–70.
- 88 Sarnow P, Ho YS, Williams J, Levine AJ. Adenovirus E1b-58kd tumor antigen and SV40 large tumor antigen are physically associated with the same 54 kd cellular protein in transformed cells. *Cell* 1982; **28**: 387–94.
- 89 Zantema A, Schrier PI, Davis-Olivier A, van Laar T, Vaessen RT, van der Eb AJ. Adenovirus serotype determines association and localization of the large E1B tumor antigen with cellular tumor antigen p53 in transformed cells. *Mol Cell Biol* 1985; **5**: 3084–91.
- 90 Szekely L, Selivanova G, Magnusson KP, Klein G, Wiman KG. EBNA-5, an Epstein-Barr virus-encoded nuclear antigen, binds to the retinoblastoma and p53 proteins. *Proc Natl Acad Sci U S A* 1993; **90**: 5455–9.
- 91 Feitelson MA, Zhu M, Duan LX, London WT. Hepatitis B x antigen and p53 are associated in vitro and in liver tissues from patients with primary hepatocellular carcinoma. *Oncogene* 1993; **8**: 1109–17.
- 92 Wang XW, Forrester K, Yeh H, Feitelson MA, Gu JR, Harris CC. Hepatitis B virus X protein inhibits p53 sequence-specific DNA binding, transcriptional activity, and association with transcription factor ERCC3. *Proc Natl Acad Sci U S A* 1994; **91**: 2230–4.

- 93 Crook T, Tidy JA, Vousden KH. Degradation of p53 can be targeted by HPV E6 sequences distinct from those required for p53 binding and trans-activation. *Cell* 1991; **67**: 547–56.
- 94 Werness BA, Levine AJ, Howley PM. Association of human papillomavirus types 16 and 18 E6 proteins with p53. *Science* 1990; **248**: 76–9.
- 95 LANE DP, CRAWFORD L V. T antigen is bound to a host protein in SY40-transformed cells. *Nature* 1979; **278**: 261–263.
- 96 Linzer DI, Levine AJ. Characterization of a 54K dalton cellular SV40 tumor antigen present in SV40-transformed cells and uninfected embryonal carcinoma cells. *Cell* 1979; **17**: 43–52.
- 97 Freed-Pastor W a, Prives C. Mutant p53: one name, many proteins. *Genes Dev* 2012; **26**: 1268–86.
- 98 Harris CC, Hollstein M. Clinical implications of the p53 tumor-suppressor gene. *N Engl J Med* 1993; **329**: 1318–27.
- 99 Petitjean A, Achatz MIW, Borresen-Dale AL, Hainaut P, Olivier M. TP53 mutations in human cancers: functional selection and impact on cancer prognosis and outcomes. *Oncogene* 2007; **26**: 2157–65.
- 100 Strano S, Dell’Orso S, Di Agostino S, Fontemaggi G, Sacchi A, Blandino G. Mutant p53: an oncogenic transcription factor. *Oncogene* 2007; **26**: 2212–9.
- 101 Brosh R, Rotter V. When mutants gain new powers: news from the mutant p53 field. *Nat Rev Cancer* 2009; **9**: 701–13.
- 102 Oren M, Rotter V. Mutant p53 gain-of-function in cancer. *Cold Spring Harb Perspect Biol* 2010; **2**: a001107.
- 103 Chan WM, Siu WY, Lau A, Poon RYC. How many mutant p53 molecules are needed to inactivate a tetramer? *Mol Cell Biol* 2004; **24**: 3536–51.
- 104 Song H, Hollstein M, Xu Y. p53 gain-of-function cancer mutants induce genetic instability by inactivating ATM. *Nat Cell Biol* 2007; **9**: 573–80.
- 105 Haupt S, di Agostino S, Mizrahi I, Alsheich-Bartok O, Voorhoeve M, Damalas A *et al.* Promyelocytic leukemia protein is required for gain of function by mutant p53. *Cancer Res* 2009; **69**: 4818–26.
- 106 Girardini JE, Napoli M, Piazza S, Rustighi A, Marotta C, Radaelli E *et al.* A Pin1/Mutant p53 Axis Promotes Aggressiveness in Breast Cancer. *Cancer Cell* 2011; **20**: 79–91.
- 107 Di Como CJ, Gaiddon C, Prives C. p73 function is inhibited by tumor-derived p53 mutants in mammalian cells. *Mol Cell Biol* 1999; **19**: 1438–49.
- 108 Gaiddon C, Lokshin M, Ahn J, Zhang T, Prives C. A subset of tumor-derived mutant forms of p53 down-regulate p63 and p73 through a direct interaction with the p53 core domain. *Mol Cell Biol* 2001; **21**: 1874–87.

- 109 Strano S, Munarriz E, Rossi M, Castagnoli L, Shaul Y, Sacchi A *et al.* Physical interaction with Yes-associated protein enhances p73 transcriptional activity. *J Biol Chem* 2001; **276**: 15164–73.
- 110 Adorno M, Cordenonsi M, Montagner M, Dupont S, Wong C, Hann B *et al.* A Mutant-p53/Smad complex opposes p63 to empower TGFbeta-induced metastasis. *Cell* 2009; **137**: 87–98.
- 111 Muller PAJ, Caswell PT, Doyle B, Iwanicki MP, Tan EH, Karim S *et al.* Mutant p53 drives invasion by promoting integrin recycling. *Cell* 2009; **139**: 1327–41.
- 112 Guo X, Keyes WM, Papazoglu C, Zuber J, Li W, Lowe SW *et al.* TAp63 induces senescence and suppresses tumorigenesis in vivo. *Nat Cell Biol* 2009; **11**: 1451–7.
- 113 Tomasini R, Tsuchihara K, Wilhelm M, Fujitani M, Rufini A, Cheung CC *et al.* TAp73 knockout shows genomic instability with infertility and tumor suppressor functions. *Genes Dev* 2008; **22**: 2677–91.
- 114 Weisz L, Oren M, Rotter V. Transcription regulation by mutant p53. *Oncogene* 2007; **26**: 2202–11.
- 115 Lin J, Teresky AK, Levine AJ. Two critical hydrophobic amino acids in the N-terminal domain of the p53 protein are required for the gain of function phenotypes of human p53 mutants. *Oncogene* 1995; **10**: 2387–90.
- 116 Frazier MW, He X, Wang J, Gu Z, Cleveland JL, Zambetti GP. Activation of c-myc gene expression by tumor-derived p53 mutants requires a discrete C-terminal domain. *Mol Cell Biol* 1998; **18**: 3735–43.
- 117 Matas D, Sigal A, Stambolsky P, Milyavsky M, Weisz L, Schwartz D *et al.* Integrity of the N-terminal transcription domain of p53 is required for mutant p53 interference with drug-induced apoptosis. *EMBO J* 2001; **20**: 4163–72.
- 118 Yan W, Chen X. Characterization of functional domains necessary for mutant p53 gain of function. *J Biol Chem* 2010; **285**: 14229–38.
- 119 Freed-Pastor WA, Mizuno H, Zhao X, Langerød A, Moon S-H, Rodriguez-Barrueco R *et al.* Mutant p53 disrupts mammary tissue architecture via the mevalonate pathway. *Cell* 2012; **148**: 244–58.
- 120 Yan W, Chen X. Identification of GRO1 as a critical determinant for mutant p53 gain of function. *J Biol Chem* 2009; **284**: 12178–87.
- 121 Bossi G, Marampon F, Maor-Aloni R, Zani B, Rotter V, Oren M *et al.* Conditional RNA interference in vivo to study mutant p53 oncogenic gain of function on tumor malignancy. *Cell Cycle* 2008; **7**: 1870–9.
- 122 Weisz L, Zalcenstein A, Stambolsky P, Cohen Y, Goldfinger N, Oren M *et al.* Transactivation of the EGR1 gene contributes to mutant p53 gain of function. *Cancer Res* 2004; **64**: 8318–27.
- 123 Chin K V, Ueda K, Pastan I, Gottesman MM. Modulation of activity of the promoter of the human MDR1 gene by Ras and p53. *Science* 1992; **255**: 459–62.

- 124 Scian MJ, Stagliano KER, Deb D, Ellis MA, Carchman EH, Das A *et al.* Tumor-derived p53 mutants induce oncogenesis by transactivating growth-promoting genes. *Oncogene* 2004; **23**: 4430–43.
- 125 Kobayashi A, Yamagiwa H, Hoshino H, Muto A, Sato K, Morita M *et al.* A Combinatorial Code for Gene Expression Generated by Transcription Factor Bach2 and MAZR (MAZ-Related Factor) through the BTB / POZ Domain. 2000; **20**: 1733–1746.
- 126 Sakaguchi S, Hombauer M, Bilic I, Naoe Y, Schebesta A, Taniuchi I *et al.* The zinc-finger protein MAZR is part of the transcription factor network that controls the CD4 versus CD8 lineage fate of double-positive thymocytes. *Nat Publ Gr* 2010; **11**: 442–448.
- 127 Costoya J a. Functional analysis of the role of POK transcriptional repressors. *Briefings Funct Genomics Proteomics* 2007; **6**: 8–18.
- 128 Fedele M, Benvenuto G, Pero R, Majello B, Battista S, Lembo F *et al.* A novel member of the BTB/POZ family, PATZ, associates with the RNF4 RING finger protein and acts as a transcriptional repressor. *J Biol Chem* 2000; **275**: 7894–7901.
- 129 Mastrangelo T, Modena P, Tornielli S, Bullrich F, Testi MA, Mezzelani A *et al.* SHORT REPORT A novel zinc ® nger gene is fused to EWS in small round cell tumor. 2000.
- 130 Stogios PJ, Downs GS, Jauhal JJS, Nandra SK, Privé GG. Sequence and structural analysis of BTB domain proteins. *Genome Biol* 2005; **6**: R82.
- 131 Reeves R. Molecular biology of HMGA proteins: hubs of nuclear function. *Gene* 2001; **277**: 63–81.
- 132 Pero R, Palmieri D, Angrisano T, Valentino T, Federico A, Franco R *et al.* POZ-, AT-hook-, and zinc finger-containing protein (PATZ) interacts with human oncogene B cell lymphoma 6 (BCL6) and is required for its negative autoregulation. *J Biol Chem* 2012; **287**: 18308–17.
- 133 Bilic I, Koesters C, Unger B, Sekimata M, Hertweck A, Maschek R *et al.* Negative regulation of CD8 expression via Cd8 enhancer – mediated recruitment of the zinc finger protein MAZR. 2006; **7**. doi:10.1038/ni1311.
- 134 OwJin Rong, MaHui, JeanAngela, GohZiyi, LeeYun Hwa, ChongYew Mei, SoongRichie, FuXin-Yuan, YangHenry and W. Patz1 Regulates Embryonic Stem Cell Identity. *Stem Cells Dev* 2014; **23**: 1062–1073.
- 135 Pero R, Lembo F, Palmieri EA, Vitiello C, Fedele M, Fusco A *et al.* PATZ attenuates the RNF4-mediated enhancement of androgen receptor-dependent transcription. *J Biol Chem* 2002; **277**: 3280–3285.
- 136 Cell M, Gene P, Morii E, Oboki K, Tatsuki R, Chem JB. GENES : STRUCTURE AND REGULATION : Interaction and Cooperation of mi Transcription Factor (MITF) and Factor (MAZR) for Transcription of Mouse Interaction and Cooperation of mi Transcription Factor (MITF) and Myc-associated Zinc-finger Protein-relate. 2002. doi:10.1074/jbc.M110392200.

- 137 Valentino T, Palmieri D, Vitiello M, Simeone A, Palma G, Arra C *et al.* Embryonic defects and growth alteration in mice with homozygous disruption of the Patz1 gene. *J Cell Physiol* 2013; **228**: 646–653.
- 138 Yoshikawa T, Piao Y, Zhong J, Matoba R, Carter MG, Wang Y *et al.* High-throughput screen for genes predominantly expressed in the {ICM} of mouse blastocysts by whole mount in situ hybridization. *Gene Expr Patterns* 2006; **6**: 213–224.
- 139 Nishiyama A, Xin L, Sharov AA, Thomas M, Mowrer G, Meyers E *et al.* Uncovering Early Response of Gene Regulatory Networks in {ESCs} by Systematic Induction of Transcription Factors. *Cell Stem Cell* 2009; **5**: 420–433.
- 140 Kim J, Chu J, Shen X, Wang J, Orkin SH. An Extended Transcriptional Network for Pluripotency of Embryonic Stem Cells. *Cell* 2008; **132**: 1049–1061.
- 141 Kitamura Y, Morii E, Jippo T, Ito A. Effect of {MITF} on mast cell differentiation. *Mol Immunol* 2002; **38**: 1173–1176.
- 142 Tshori S, Nechushtan H. Mast cell transcription factors—Regulators of cell fate and phenotype. *Biochim Biophys Acta - Mol Basis Dis* 2012; **1822**: 42–48.
- 143 Galli, Stephen J, Tsai Mindy , Piliponsky AM. The development of allergic inflammation Stephen. *Nature* 2008; **454**: 445–454.
- 144 Dawicki W, Marshall JS. New and emerging roles for mast cells in host defence. *Curr Opin Immunol* 2007; **19**: 31–38.
- 145 Cho JH, Kim MJ, Kim KJ, Kim J-R. POZ/BTB and AT-hook-containing zinc finger protein 1 (PATZ1) inhibits endothelial cell senescence through a p53 dependent pathway. *Cell Death Differ* 2012; **19**: 703–712.
- 146 Tian X, Sun D, Zhang Y, Zhao S, Xiong H, Fang J. Zinc finger protein 278 , a potential oncogene in human colorectal cancer. 2008; **40**: 289–296.
- 147 Yang WL, Ravatn R, Kudoh K, Alabanza L, Chin KV. Interaction of the regulatory subunit of the cAMP-dependent protein kinase with PATZ1 (ZNF278). *Biochem Biophys Res Commun* 2010; **391**: 1318–1323.
- 148 Fedele M, Franco R, Salvatore G, Paronetto MP, Barbagallo F, Pero R *et al.* PATZ1 gene has a critical role in the spermatogenesis and testicular tumours. 2008; : 39–47.
- 149 Burrow AA, Williams LE, Pierce LCT, Wang Y. Over half of breakpoints in gene pairs involved in cancer-specific recurrent translocations are mapped to human chromosomal fragile sites. 2009; **11**: 1–11.
- 150 Tritz R, Mueller BM, Hickey MJ, Lin AH, German G, Hadwiger P *et al.* siRNA Down-regulation of the PATZ1 Gene in Human Glioma Cells Increases Their Sensitivity to Apoptotic Stimuli. *Cancer Ther* 2008; **6**: 865–876.
- 151 Esposito F, Boscia F, Franco R, Tornincasa M, Fusco A, Kitazawa S *et al.* Down-regulation of oestrogen receptor- β associates with transcriptional co-regulator PATZ1 delocalization in human testicular seminomas. 2011; : 110–120.

- 152 Valentino T, Palmieri D, Vitiello M, Pierantoni GM, Fusco a, Fedele M. PATZ1 interacts with p53 and regulates expression of p53-target genes enhancing apoptosis or cell survival based on the cellular context. *Cell Death Dis* 2013; **4**: e963.
- 153 McKinney K, Prives C. Efficient Specific DNA Binding by p53 Requires both Its Central and C-Terminal Domains as Revealed by Studies with High-Mobility Group 1 Protein. *Mol Cell Biol* 2002; **22**: 6797–6808.
- 154 Lai JS, Herr W. Ethidium bromide provides a simple tool for identifying genuine DNA-independent protein associations. *ProcNatAcadSciUSA* 1992; **89**: 6958–6962.
- 155 Bilic I, Ellmeier W. The role of BTB domain-containing zinc finger proteins in T cell development and function. *Immunol Lett* 2007; **108**: 1–9.
- 156 He X, He X, Dave VP, Zhang Y, Hua X, Nicolas E *et al.* The zinc finger transcription factor Th-POK regulates CD4 versus CD8 T-cell lineage commitment. *Nature* 2005; **433**: 826–33.
- 157 Dovat S, Ronni T, Russell D, Ferrini R, Cobb BS, Smale ST. A common mechanism for mitotic inactivation of C2H2 zinc finger DNA-binding domains. *Genes Dev* 2002; **16**: 2985–90.
- 158 Christian M, Cermak T, Doyle EL, Schmidt C, Zhang F, Hummel A *et al.* Targeting DNA double-strand breaks with TAL effector nucleases. *Genetics* 2010; **186**: 757–61.
- 159 Miller JC, Tan S, Qiao G, Barlow K a, Wang J, Xia DF *et al.* A TALE nuclease architecture for efficient genome editing. *Nat Biotechnol* 2011; **29**: 143–8.
- 160 Bogdanove AJ, Voytas DF. TAL effectors: customizable proteins for DNA targeting. *Science* 2011; **333**: 1843–6.
- 161 Mussolino C, Cathomen T. On target? Tracing zinc-finger-nuclease specificity. *Nat Methods* 2011; **8**: 725–6.

APPENDIX

APPENDIX A: Chemicals Used In The Study

Chemicals and Media Components	Supplier Company
Acetic Acid	Merck, Germany
Acid Washed Glass Beads	Sigma, Germany
Acrylamide/Bis-acrylamide	Sigma, Germany
Agarose	peQLab, Germany
Anti c-Myc Antibody	Roche, Germany
Anti-GFP Antibody	Roche, Germany
Anti-HA Affinity Matrix	Roche, Germany
Anti-Myc Peroxidase	Roche, Germany
Ammonium Persulfate	Sigma, Germany
Ammonium Sulfate	Sigma, Germany
Ampicillin Sodium Salt	CellGro, USA
Bacto Agar	BD, USA
Bacto Tryptone	BD, USA
Boric Acid	Molekula, UK
Bradford Reagent	Sigma, Germany
Bromophenol Blue	Sigma, Germany
Chloramphenicol	Gibco, USA
D-Glucose	Sigma, Germany
Distilled water	Milipore, France
DMEM	PAN, Germany
DMSO	Sigma, Germany
DNA Gel Loading Solution, 5X	Quality Biological, Inc, USA
DPBS	CellGro, USA
EDTA	Applichem, Germany

Chemicals and Media Components	Supplier Company
Ethanol	Riedel-de Haen, Germany
Ethidium Bromide	Sigma, Germany
Fetal Bovine Serum (FBS)	Biological Industries, Israel
Glycerol Anhydrous	Applichem, Germany
Glycine	Applichem, Germany
HBSS	CellGro, USA
HEPES	Applichem, Germany
Hydrochloric Acid	Merck, Germany
Isopropanol	Riedel-de Haén, Germany
Kanamycin Sulfate	Gibco, USA
LB Agar	BD, USA
LB Broth	BD, USA
L-Glutamine	Hyclone, USA
Liquid nitrogen	Karbogaz, Turkey
Magnesium Chloride	Promega, USA
2-Mercaptoethanol	Sigma, Germany
Methanol	Riedel-de Haen, Germany
Monoclonal Anti-HA Antibody	Sigma, Germany
Penicillin-Streptomycin	Sigma, Germany
Phenol-Chloroform-Isoamylalcohol	Amersco, USA
PIPES	Sigma, Germany
Potassium Acetate	Merck, Germany
Potassium Chloride	Fluka, Germany
Potassium Hydroxide	Merck, Germany
Protease Tablets (EDTA-free)	Roche, Germany
ProtG Sepharose	Amersco, USA
RNase A	Roche, Germany
SDS Pure	Applichem, Germany

Chemicals and Media Components	Supplier Company
Skim Milk Powder	Fluka, Germany
Sodium Azide	Amresco, USA
Sodium Chloride	Applichem, Germany
TEMED	Applichem, Germany
Tris Buffer Grade	Amresco, USA
Tris Hydrochloride	Amresco, USA
Triton X100	Promega, USA
Tween20	Sigma, Germany
SuperSignal West Pico Chemiluminescent Substrate	Thermo Scientific, USA

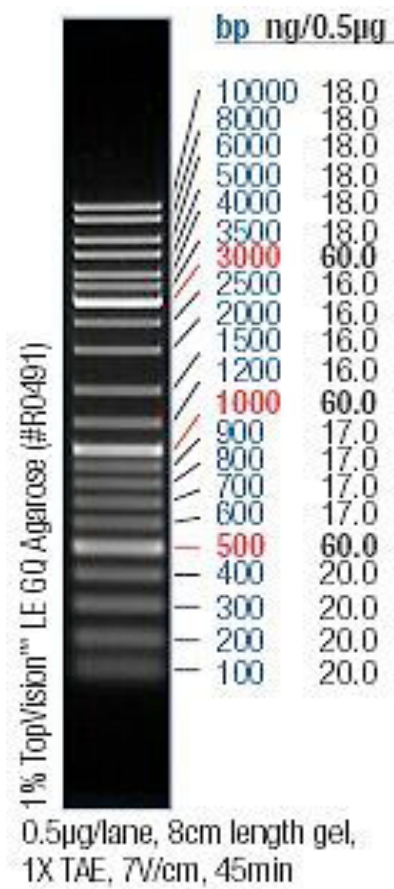
APPENDIX B: Equipment Used In The Study

Equipment	Company
Autoclave	Hirayama, Hiclave HV-110, Japan
Balance	Sartorius, BP221S, Germany
	Schimidzu, Libror EB-3200 HU, Japan
Cell Counter	Cole Parmer, USA
Centrifuge	Eppendorf, 5415D, Germany
	Hitachi, Sorvall RC5C Plus, USA
CO ₂ Incubator	Binder, Germany
Deepfreeze	-80°C, Forma, Thermo Electron Corp., USA
	-20°C, Bosch, Turkey
Distilled Water	Millipore, Elix-S, France
Electrophoresis Apparatus	Biogen Inc., USA
	Biorad Inc., USA
Electroporation Cuvettes	Eppendorf, Germany
Electroporator	BTX-ECM630, Division of Genetronics, Inc, USA
Filter Membranes	Millipore, USA
Flow Cytometer	BDFACSCanto, USA
Gel Documentation	Biorad, UV-Transilluminator 2000, USA
Heater	Thermomixer Comfort, Eppendorf, Germany
Hematocytometer	Hausser Scientific, Blue Bell Pa., USA
Ice Machine	Scotsman Inc., AF20, USA
Incubator	Memmert, Modell 300, Germany
	Memmert, Modell 600, Germany
Laminar Flow	Kendro Lab. Prod., Heraeus, HeraSafe HS12, Germany
Liquid Nitrogen Tank	Taylor-Wharton, 3000RS, USA
Magnetic Stirrer	VELP Scientifica, ARE Heating Magnetic Stirrer, Italy
Microliter Pipettes	Gilson, Pipetman, France
	Eppendorf, Germany

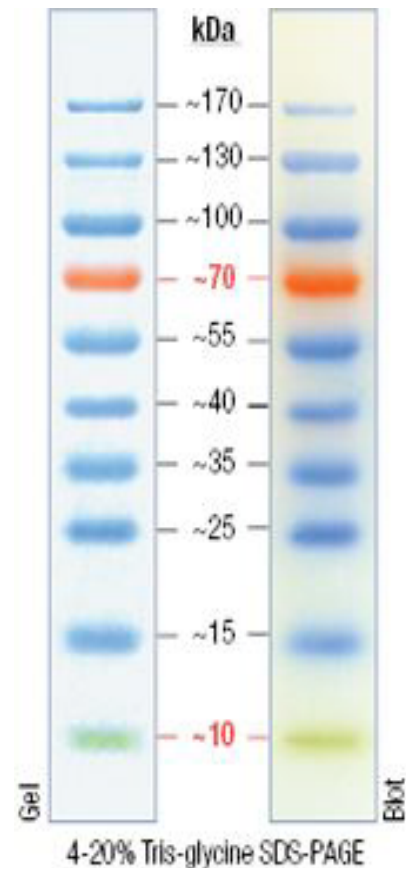
Microscope	Olympus CK40,Japan Olympus CH20,Japan Olympus IX70,Japan Zeiss Confocal LSM710, German
Microwave Oven	Bosch,Turkey
pH meter	WTW, pH540 GLP MultiCal, Germany
Power Supply	Biorad, PowerPac 300, USA
Refrigerator	Bosch,Turkey
Shaker Incubator	New Brunswick Sci., Innova 4330, USA
Spectrophotometer	Schimadzu, UV-1208, Japan Schimadzu, UV-3150, Japan
Thermocycler	Eppendorf, Mastercycler Gradient, Germany
Vortex	Velp Scientifica,Italy

APPENDIX C: DNA and Protein Molecular Weight Marker

Gene Ruler™ DNA Ladder Mix
Fermentas, Germany



Page Ruler™ Prestained Protein
Ladder Fermentas, Germany



APPENDIX D: Plasmids Used In This Project

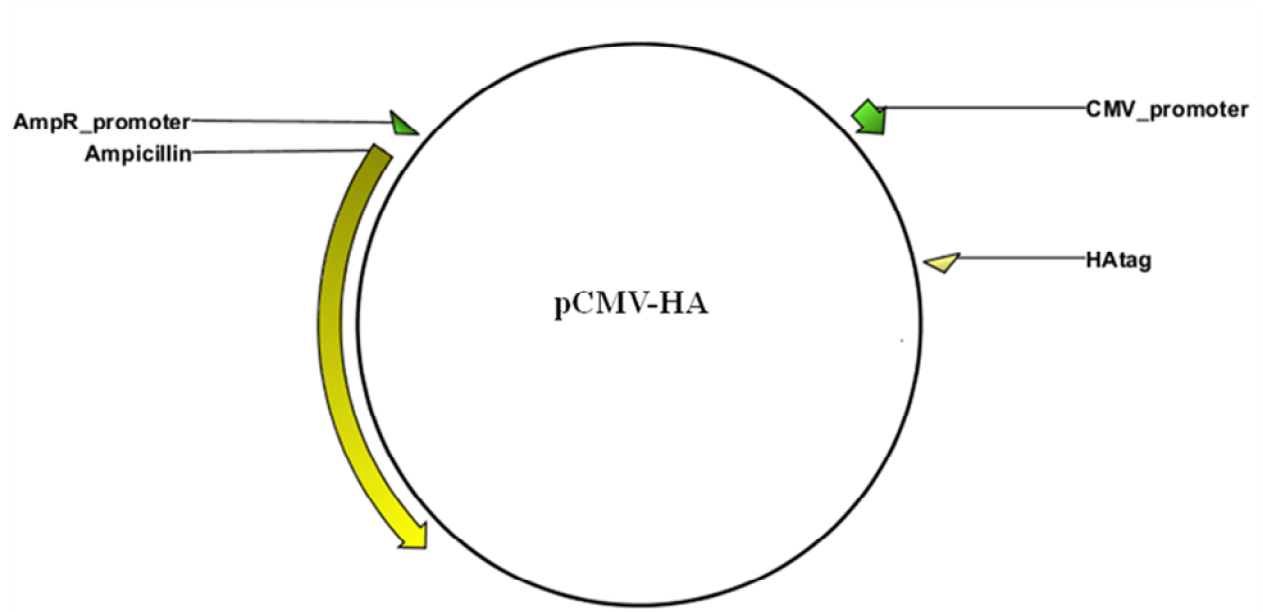


Figure D.1 Map of pCMV-HA plasmid

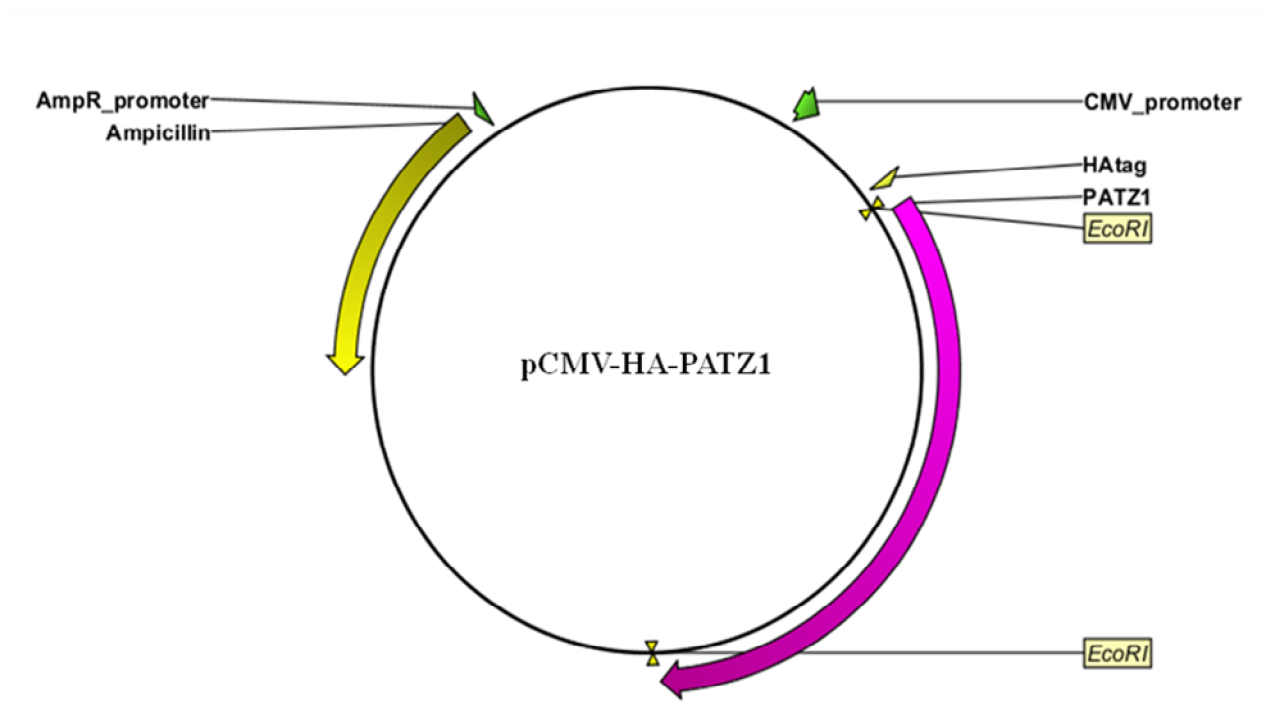


Figure D.2 Map of pCMV-HA-PATZ1 plasmid

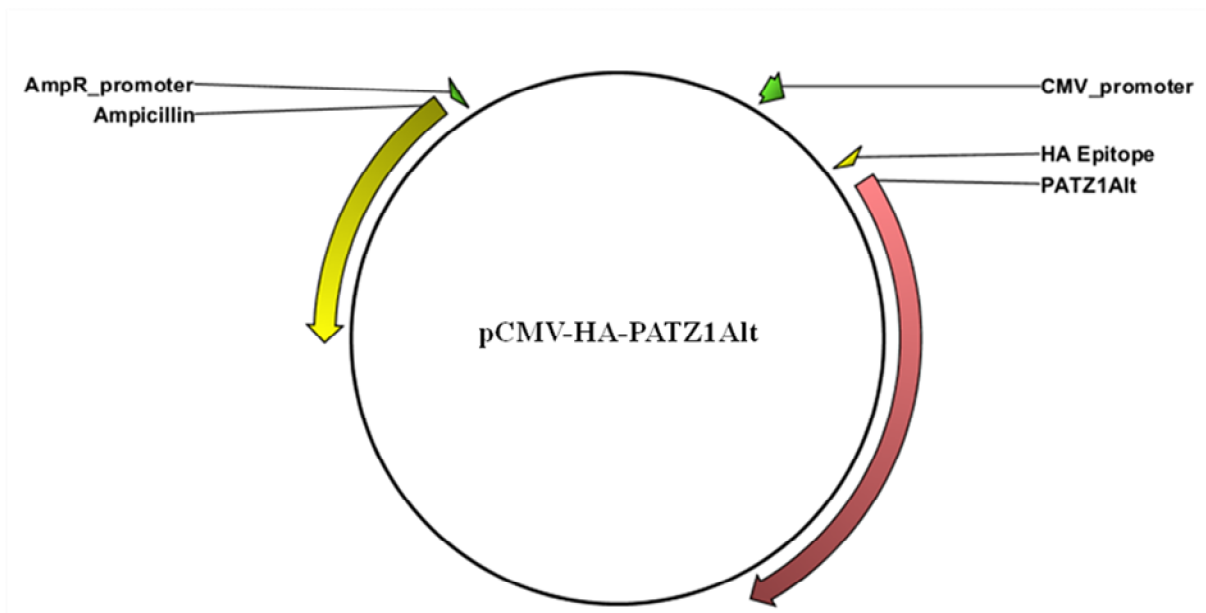


Figure D.3 Map of pCMV-HA-PATZ1Alt plasmid

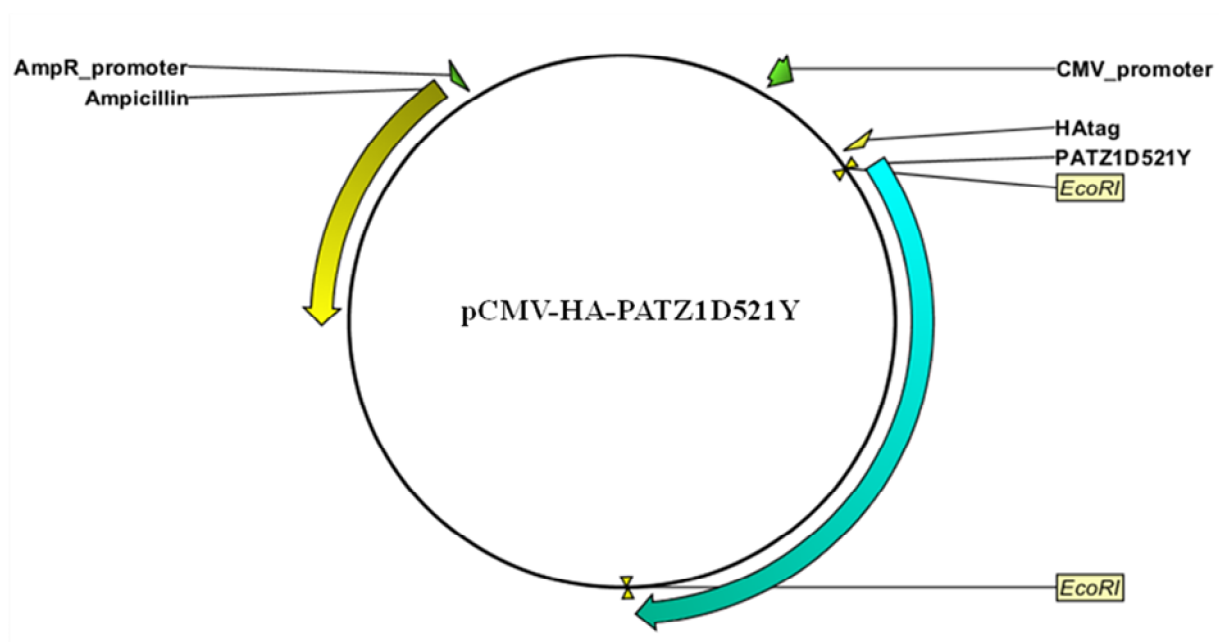


Figure D.4 Map of pCMV-HA-PATZ1D521Y plasmid

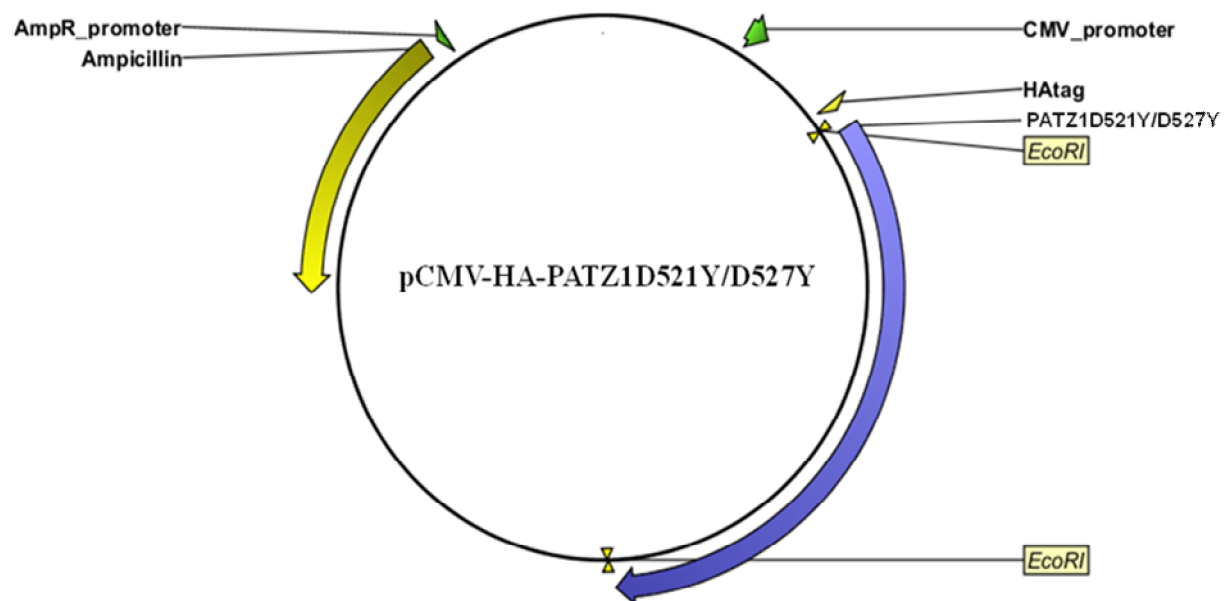


Figure D.5 Map of pCMV-HA-PATZ1D521Y/D527Y plasmid

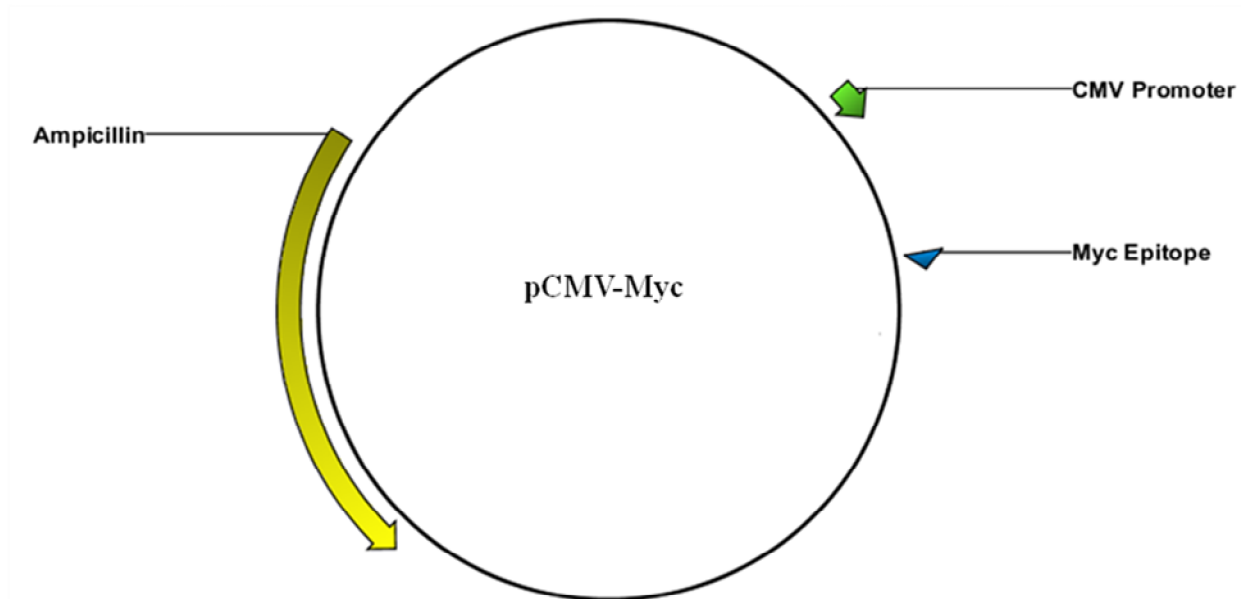


Figure D.6 Map of pCMV-Myc plasmid

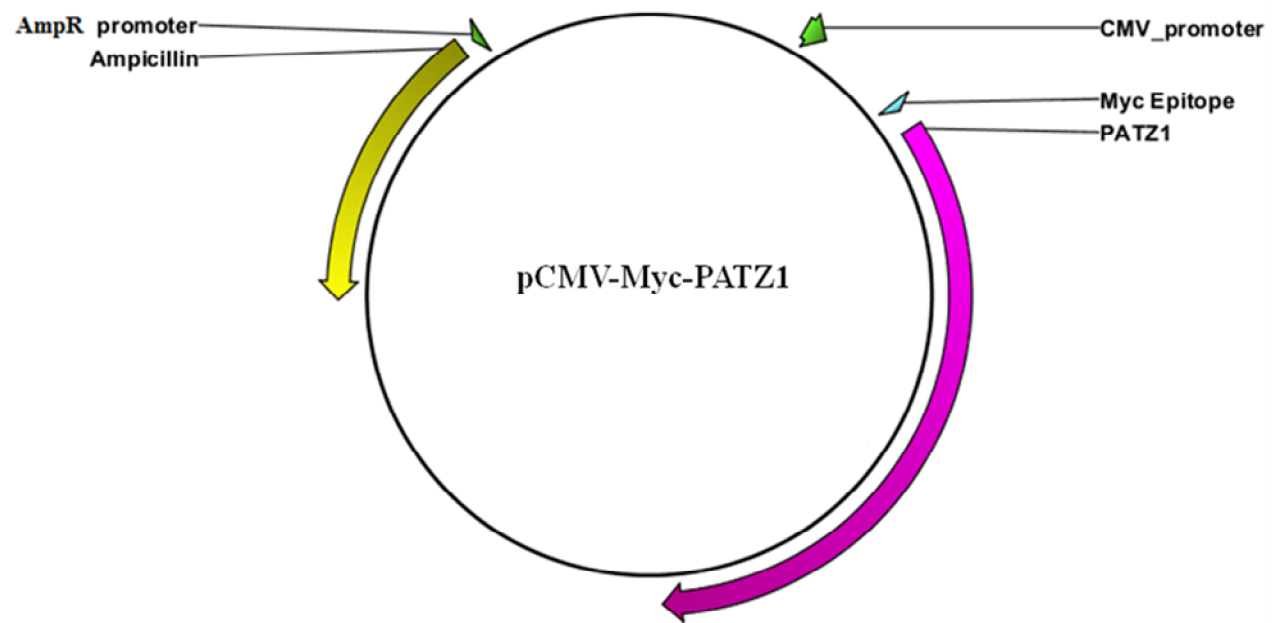


Figure D.7 Map of pCMV-Myc-PATZ1 plasmid

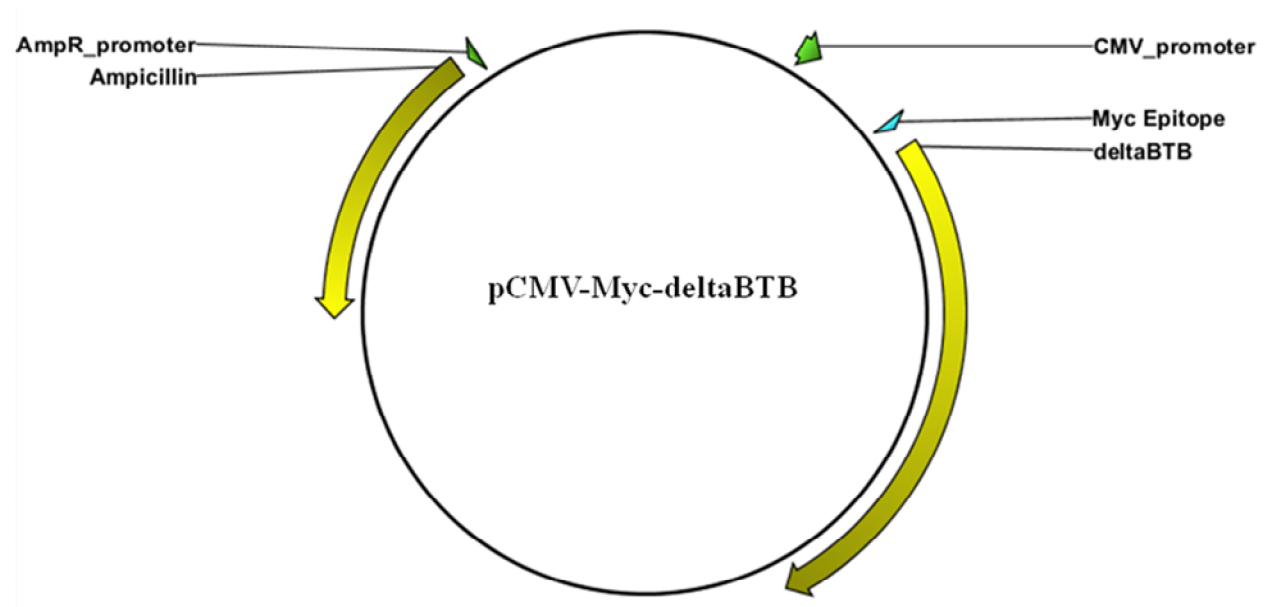


Figure D.8Map of pCMV-Myc-deltaBTB plasmid

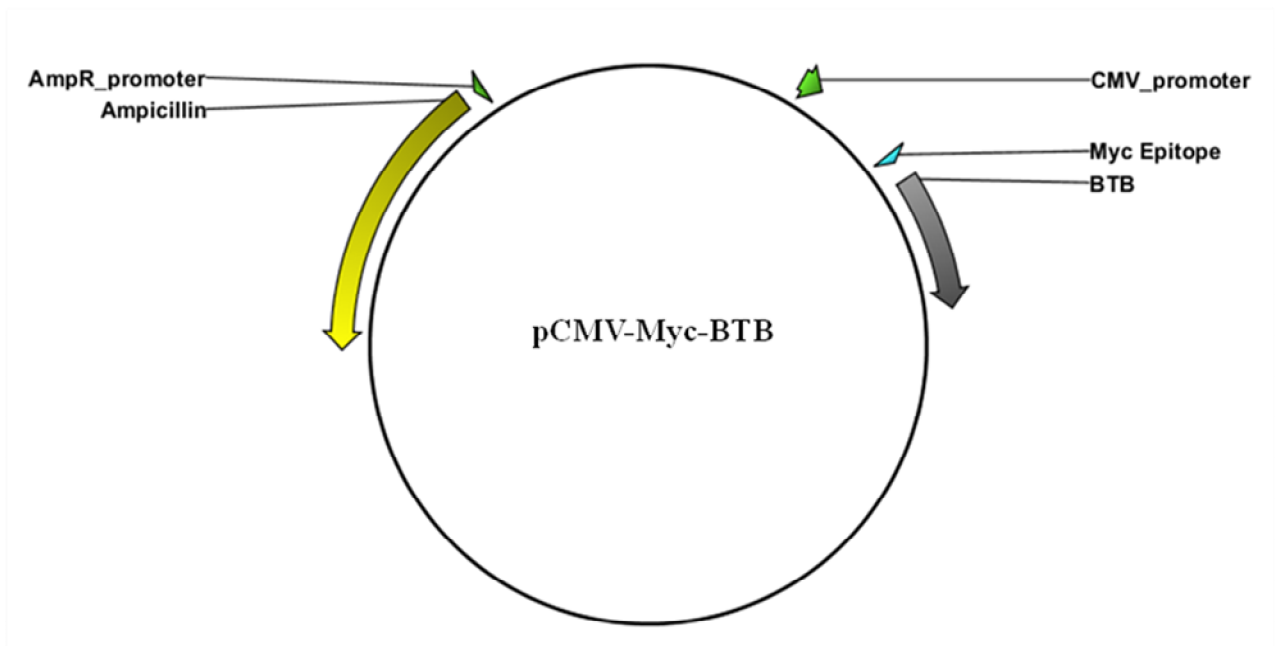


Figure D.9 Map of pCMV-Myc-BTB plasmid

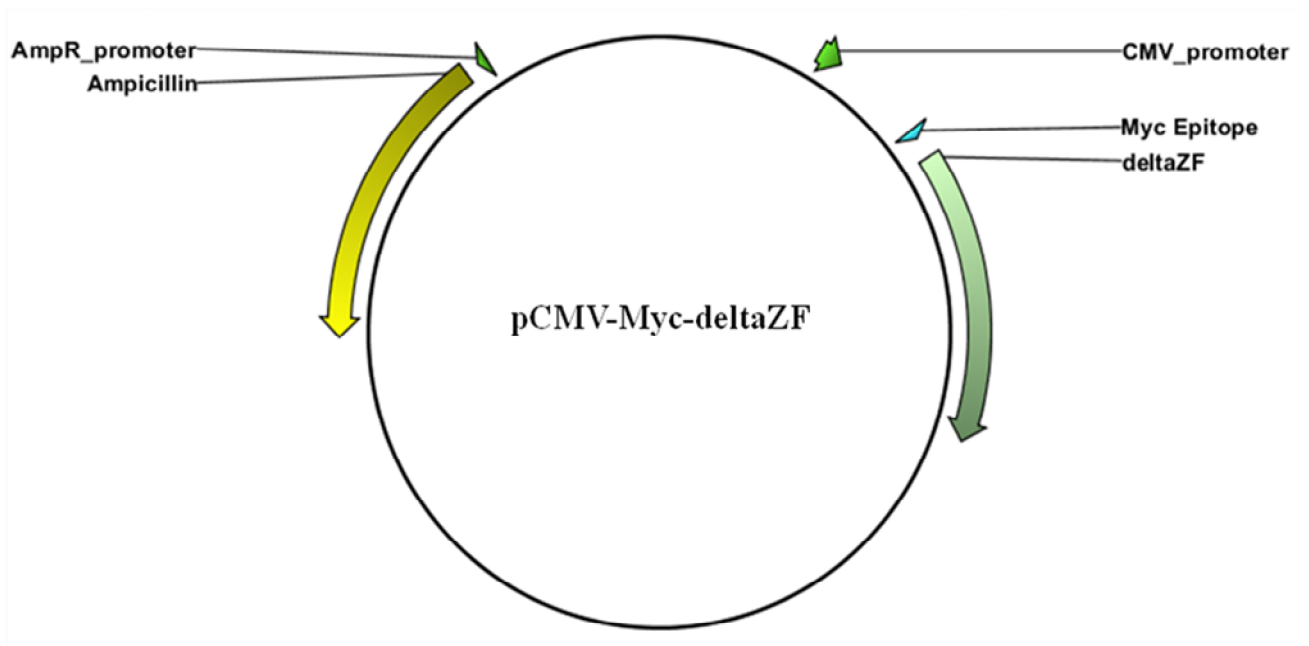


Figure D.10 Map of pCMV-Myc-deltaZF plasmid

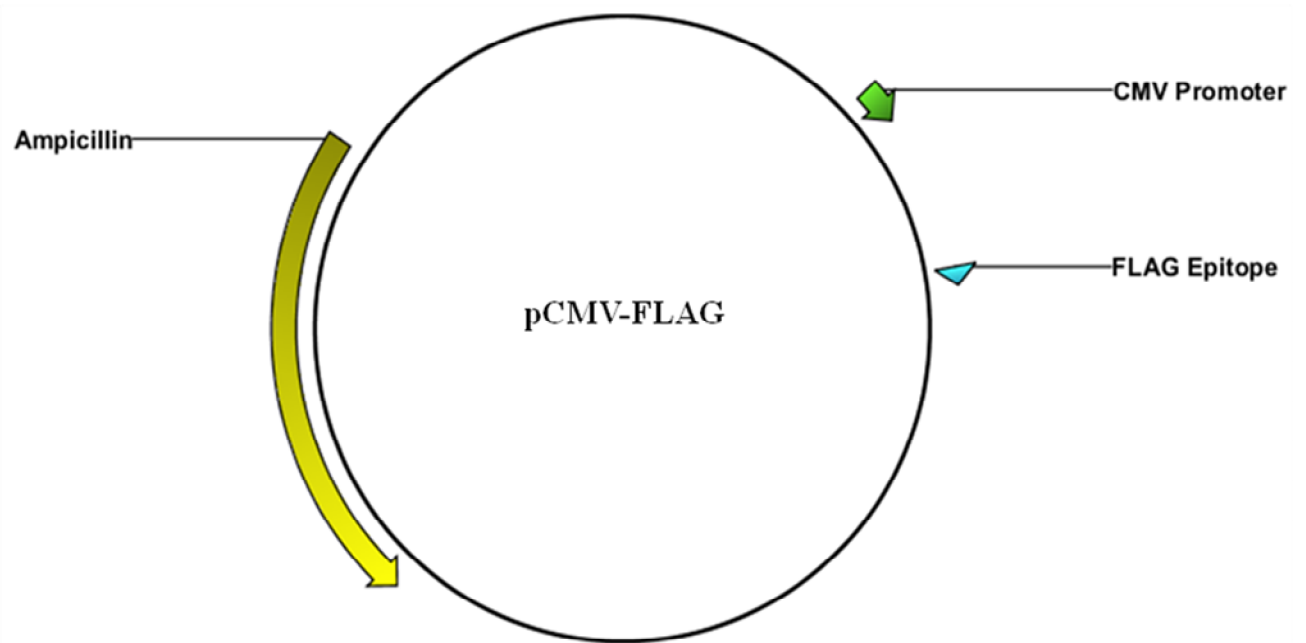


Figure D.11 Map of pCMV-FLAG plasmid

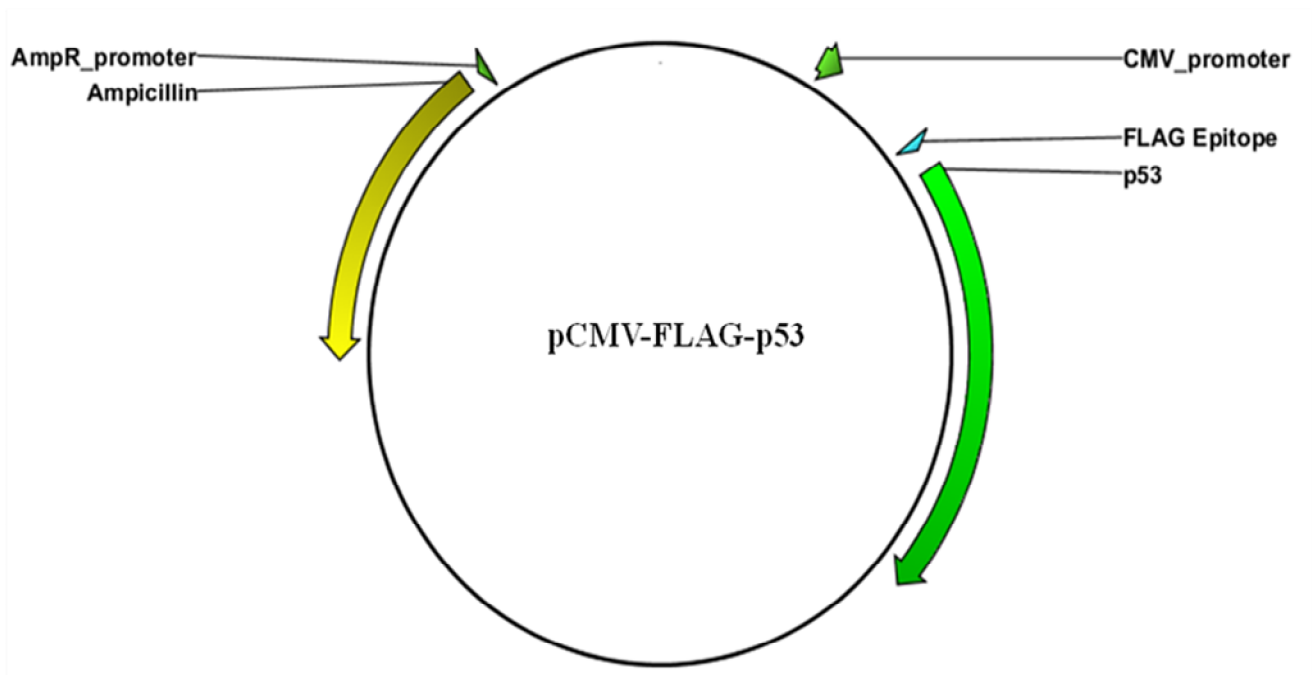


Figure D.12 Map of pCMV-FLAG-p53 plasmid

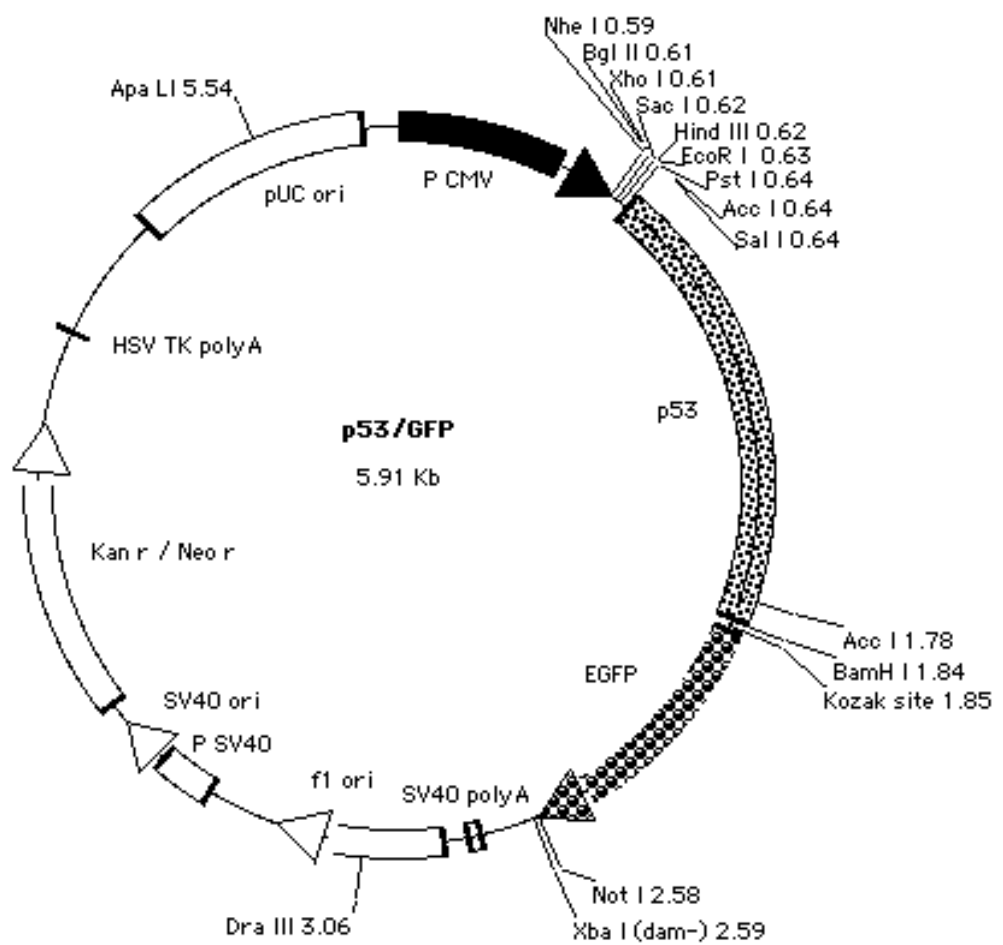


Figure D.13 Map of p53-GFP plasmid